

Transcription Factors *Emx2* and *Foxb1* Reveal Aspects of Neuronal Migration in the Forebrain

Von der Naturwissenschaftlichen Fakultät
der Gottfried Wilhelm Leibniz Universität Hannover
zur Erlangung des Grades eines

DOKTORS DER NATURWISSENSCHAFTEN

Dr. rer. nat.-

genehmigte Dissertation

von

MSc Tianyu Zhao

geboren am 03.Juli 1976 in Yingkou, P.R.China

2009

Referent: Prof. Dr. Herbert Hildebrandt
Medizinische Hochschule Hannover

Korreferent: Prof. Dr. Gregor Eichele
Max-Planck Institut für Biophysikalische Chemie, Göttingen

Tag der Promotion: 19.12.2008

CONTENTS

ABSTRACT	-1-
ZUSAMMENFASSUNG	-2-
ABBREAVIATION	-3-
INTRODUCTION	-4-
Transcription factors: a general introduction.....	-4-
Classification of transcription factors.....	-5-
Homeobox transcription factor <i>Emx2</i>	-5-
Emx2 function in developing Hippocampus.....	-6-
Radial glial cells.....	-9-
Emx2 and Cajal-Retzius cells.....	-10-
Emx2 and cortical angiogenesis.....	-11-
Transcription factors and cell lineage study.....	-13-
General background of lineage tracing.....	-14-
Z/AP and Rosa26 mouse line.....	-15-
Transcription factor Foxb1 and fork head gene family.....	-16-
Hypothalamus development and transcription factor Foxb1.....	-19-
MATERIALS AND METHODS	- 21-
Animal handling and breeding.....	-21-
Alkaline phosphatase staining.....	-21-
Apoptosis (TUNEL).....	-22-
Beta galactosidase staining on mouse brain.....	-23-
BrdU injection and detection.....	-24-
Genotyping.....	-24-
Table of primer.....	-25-
Immunohistochemistry.....	-26-
Table of antibodies.....	-27-
In Situ Hybridization.....	-28-
RNA Probe generation.....	-28-
Sample preparation.....	-30-
Robotic ISH procedure in summary.....	-28-
Morphometry.....	-32-
Nissl staining.....	-33-
Statistics.....	-33-
Southern Blot.....	-34-
Whole mount in situ hybridization.....	-34-
RESULTS	-37-
Chapter 1.....	-37-
Publication #1: Emx2 in the developing fissure region.....	-37-
Chapter 2.....	-52-
Publication #2: Cajal-Retzius neurons that produce Vascular Endothelial Growth Factor have a role in cortical Angiogenesis.....	-52-
Chapter 3.....	-84-
Publication #3:Foxb1-driven Cre expression in somites and the neuroepithelium of diencephalon, brainstem, and spinal cord.....	-84-
Chapter 4.....	-86-
Publication#4: Genetic mapping of Foxb1-cell lineage shows migration from caudal diencephalons to telencephalon and lateral hypothalamus.....	-86-

DISCUSSION	-139-
Emx2 in cortical development.....	-139-
The lineage study of transcription factor through driven Cre recombinase activity provide a new orientation to understand embryonic development beyond the expression.....	-141-
Tangential migration is an communication between transcription factors.....	-142-
Lineage studies require precise Cre recombinase activity and fast responding reporters.....	-143-
REFERENCES	-144-
PUBLICATIONS	-151-
CURRICULUM VITAE	-152-
KNOWLEDGEMENTS	-153-
ERKÄRUNG	-154-

ABSTRACT

The mammalian nervous system is an amazingly complex and highly ordered structure and is responsible for cognitive functions like memory and intelligence. Its embryonic development is under tight control by a hierarchy of transcription factors and the corresponding downstream genes. I have dedicated part of my PhD work to investigate the function of a key transcription factor, *Emx2*. Together with molecular regulation, events at the cellular level are also very important for brain development. Novel techniques for tracing the lineage and migration of specific cell populations are advancing our understanding of the emergence of brain architecture. Part of my PhD work consisted in making and using genetic tools to analyze the migration of young neurons in the developing brain.

Transcription factor *Emx2* is expressed in developing forebrain progenitors and controls the development of the cortex. During cortical genesis, reelin-secreting Cajal-Retzius cells (CR cells) are essential for correct cortical plate lamination. In mice deficient in *Emx2*, the CR cell population disappears from the cortical marginal zone abnormally early, which results in impaired cortical development. In the first part of the thesis, I will focus on the development of a special cortical region named hippocampus. I will show that most CR cells of the hippocampal formation, fated to occupy the outer marginal zone of the Dentate Gyrus of the hippocampus, fail to be generated in the *Emx2* mutant. The radial glial scaffolding of the fissure region was abolished. I also identified a special subpopulation of CR cells characterized by a specific combination of markers, whose development is independent of *Emx2*. Further studies demonstrated that the CR cells have an influence on cortical angiogenesis through the secretion of VEGF-A (Vascular endothelial growth factor A).

In the second part of this work, I knocked in the cDNA for Cre recombinase after the *Foxb1* regulatory sequences. In this way, I generated a "genetic neuroanatomy" tool, i.e. a novel mouse mutant line, the *Foxb1-Cre* line. Developmental transcription factor *Foxb1* has a very restricted pattern in the developing neural tube with a rostral boundary between the caudal and rostral diencephalon. Therefore, by crossing these mice with marker mouse lines like Z/AP and ROSA26R, I have been able to trace the *Foxb1* cell lineage during brain development. One of my unexpected findings is a large, longitudinally oriented migration stream apparently originated in the thalamic region and following an axonal bundle to end in the anterior portion of the lateral hypothalamic area. With this new tool I also uncovered novel diencephalon to telencephalon migrations.

Keywords: angiogenesis, Cajal-Retzius cells, *Emx2*, *Foxb1*, hypothalamus, reelin, tangential migration, thalamus, vegfa

Zusammenfassung

Das Nervensystem des Säugetiers ist eine erstaunlich komplexe und sehr organisierte Struktur und ist verantwortlich für kognitive Funktionen wie Erinnerung und Intelligenz. Seine embryonale Entwicklung wird gesteuert von einer Hierarchie von Transkriptionsfaktoren und den entsprechenden untergeordneten Genen. Ein Teil meiner Doktorarbeit beschäftigt sich mit der Untersuchung der Funktion des Transkriptionsfaktors *Emx2*. Ereignisse auf zelluärer Ebene zusammen mit molekularer Regulation sind ebenso wichtig für die Gehirnentwicklung. Neue Techniken, die es ermöglichen, die Migration und die Abstammung von spezifischen Zellpopulationen zu verfolgen, erweitern unser Wissen über die Entstehung der Gehirn-architektur. Teil meiner Doktorarbeit beinhaltet die Erzeugung und den Einsatz von genetischen Methoden, um die Migration von jungen Neuronen in dem sich entwickelnden Gehirn zu untersuchen.

Der Transkriptionsfaktor *Emx2* wird in Vorläuferzellen im sich entwickelnden Vorderhirn exprimiert und kontrolliert die Entwicklung des Kortex. Während der Entstehung des Kortex sind Reelin-sekretierende Cajal-Retzius Zellen (CR Zellen) erforderlich für die richtige Schichtenbildung in der kortikalen Platte. In *Emx2* defizienten Mäusen verschwinden die CR Zellpopulationen zu früh von der kortikalen marginalen Zone, wodurch es zur Beeinträchtigung der kortikalen Entwicklung kommt. In dem ersten Teil meiner Arbeit wird die Entwicklung des Hippokampus untersucht. Ich werde zeigen, dass die Mehrzahl der CR Zellen der hippocampalen Formation, die sich in der äusseren marginalen Zone des Gyrus Dentatus des Hippokampus befinden, in der *Emx2* Mutante nicht gebildet wird. Das Gerüst aus radialen Glia der Fissurregion wird nicht ausgebildet. Ich konnte ebenfalls mit einer Kombination von Markern eine spezielle Subpopulation von CR Zellen charakterisieren, deren Entwicklung unabhängig von *Emx2* ist. Weitere Untersuchungen ergaben, dass die CR Zellen einen Einfluss auf die kortikale Angiogenese durch die Sekretion von VEGF-A (Vascular endothelial growth factor A) haben.

In dem zweiten Teil dieser Arbeit beschreibe ich wie ich die cDNA der Cre Rekombinase hinter die *Foxb1* regulatorischen Sequenzen eingefügt habe. Auf diese Weise habe ich ein "genetisches neuroanatomisches Werkzeug" bzw. eine neue Mauslinie erzeugt, die *Foxb1*-Cre Linie. *Foxb1* hat ein sehr begrenztes Expressionsmuster in sich entwickelnden Gehirn mit einer rostralen Grenze zwischen dem kaudalen und rostralen Dienzephalon. Durch die Kreuzung dieser Mäuse mit den Mauslinien *Z/AP* und *ROSA26R* konnte ich die Abstammung und Migration von *Foxb1* positiven Zellen untersuchen. Ein unerwartetes Ergebnis ist die Beobachtung eines longitudinal orientierten Migrationsstromes von Zellen aus dem Thalamus ein Axonenbündel folgend bis zur lateralen hypothalamischen Region. Mit dieser Methode konnte ich eine neue Migration vom Dienzephalon zum Telenzephalon nachweisen.

Schlagwörter: Angiogenese, Cajal-Retzius Zellen, *Emx2*, *Foxb1*, Hypothalamus, Reelin, Tangentiale Migration, Thalamus, vegfa

Abbreviations

AP	alkaline phosphatase
BMP	bone morphogenetic protein
bp	base Pair
Brdu	bromodeoxyuridine
cDNA	complementary DNA
Cpe	choroid plexus epithelium
CR cell	Cajal-Retzius cell
DAB	3, 3'-diaminobenzidine
ddH ₂ O	double distilled H ₂ O
DEPC	diethylpyrocarbonate
Dig	digoxin
DNA	deoxyribonucleic acid
DGCL	dentate granule cell layer
E	embryonic day
ES cell	embryonic stem cell
EtOH	ethanol
FCS	fetal calf serum
GFAP	glial fibrillary acidic protein
h	hour
hPLAP	human placenta alkaline phosphatase
ISH	in situ hybridization
Kb	kilo base pair
KO	knock out
M	mole
MBO	mammillary body
MeOH	methanol
MGE	medium ganglionic eminence
min	minute
mM	milimole
μM	micromole
μg	microgram
μl	micro liter
OCT	optimal freezing medium
PBS	Phosphate Buffered Saline
PCR	Polymerase Chain Reaction
pM	pico mole
RNA	ribonucleic acid
U	unit
UV	ultra violets
V	volt
VMH	ventral medial hypothalamus
VEGF	vascular endothelium growth factor

INTRODUCTION

The objective of genetics as a scientific discipline is to find out how genes regulate the development and function of living organisms. The mammalian nervous system possesses amazing complexity and highly ordered structure and is responsible for cognitive functions like memory and intelligence. The study of its development is a fascinating subject, to which nowadays major scientific efforts are dedicated. The correct development of the brain depends on the stepwise and hierarchical expression of certain genes which encode "transcription factors". These factors are proteins able to bind the DNA and activate or repress the expression of other genes. The study of brain development is to a high degree the analysis of the control of gene expression by transcription factors.

Transcription factors: a general introduction

A transcription factor is a protein that binds to a specific DNA region through a "DNA binding domain" in order to regulate the expression of a gene. Transcription factors often work together with other proteins (forming a complex) to allow or prevent certain DNA sequences from being transcribed into RNA. The expression of genes encoding transcription factor proteins is itself controlled by other transcription factors. The

transcription factor cascade can be activated by stimuli coming from inside or outside the cell.

Classification of transcription factors

There are approximately 2600 potential transcription factors (i.e. proteins with DNA binding motif) in the human genome, representing about the 8% of the total transcripts (Babu et al., 2004). From the point of view of their functions, they can be classified as:

- 1) General transcription factors (the basic factors that allow transcription to occur)
- 2) Cell cycle controllers (to determine how large a cell will be and when it will divide into two daughter cells)
- 3) External or internal signaling sensors (to response to environmental change or alterations from other cascade and make the cell adapt to new living conditions)
- 4) Finally, the transcription factors that we will deal with in this PhD thesis - developmental regulators expressed at certain developmental stages and in certain anatomical regions to guide the proper cell differentiation by activating or repressing the expression of downstream genes.

Transcription factors can also be classified by the structure of their DNA binding domains, such as helix-turn-helix, homeodomain, paired domain, winged helix domain, etc.

Homeobox transcription factor *Emx2*

The mouse *Emx* family of transcription factors has two members, *Emx1* and *Emx2*. Both are, from the point of view of their function, developmental regulators. From the point of view of the structure of the DNA binding domain that they encode they are homeobox genes. This means that the proteins *Emx1* and *Emx2* possess a

homeodomain as their DNA binding domain. *Emx1* and *2* are homologous to a gene of the fruit fly *Drosophila melanogaster* called *ems* (*empty spiracles*). This gene is responsible for the development of the fly brain (Boncinelli et al., 1994; Simeone et al., 1992). *Emx* genes have been identified not only in mice but also in humans, birds (*Gallus gallus*), amphibians (like the toad *Xenopus laevis* and the salamander *Ambystoma maculatum*) and fishes (like the zebrafish *Danio rerio*) (Cecchi and Boncinelli, 2000). The two mouse *Emx* genes have a similar expression pattern during development, that is, they are expressed in the same brain structures at the same time. However, mice artificially engineered to carry no *Emx2* genes (i.e., knockout or null mutant mice) show a much more severe abnormal phenotype than knockout mice for *Emx1* (Bishop et al., 2002; Muzio and Mallamaci, 2003), indicating that the *Emx2* protein can substitute for *Emx1* if this is missing, but *Emx1* cannot substitute for *Emx2*.

The expression of transcription factor gene *Emx2* must be regulated by other transcription factors which bind to one of several regulatory regions of the *Emx2* gene DNA. To date, the only known transcription factor regulating *Emx2* expression is *Gli3* (Theil et al., 1999). After *Emx2* is activated, it must regulate the expression of other genes, but none of these "*Emx2* targets" has been discovered yet.

Emx2 is expressed beginning at the three somite stage in the mouse forebrain primordium and it can also be detected in the neuroepithelium during cortical development (Simeone et al., 1992). In the cortex, *Emx2* is expressed in a medial-caudal to lateral-rostral gradient which has key roles in cortical patterning (Bishop et al., 2000; Bishop et al., 2002). The *Emx2* null mutants die at birth and show abnormally reduced cortex and hippocampus (Pellegrini et al., 1996). This hippocampal alteration will be the focus of part of the present PhD work.

***Emx2* function in developing Hippocampus**

Anatomically, the telencephalon consists of basal ganglia and pallium. The pallium is mostly formed by a multi-layered structure named cortex. The cortex is heterogeneous because of its many functional specializations and the different phylogenetic age of its

different parts. The “Neocortex”, mostly referred as cortex, is the latest evolutionary acquisition of the vertebrate brain while the “Paleocortex” and “Archicortex” are considered ancient. The Neocortex is the seat of higher cognitive functions like intelligence and perception, while the Paleocortex has mostly olfactory functions.

The Archicortex is also called Hippocampus (seahorse), because the first anatomists, centuries ago, thought that this part of the brain looked like a seahorse (convoluted and covered by protuberances). The Hippocampus is responsible for the generation of new memories and their storage (Bird and Burgess, 2008; Teyler and DiScenna, 1985). It has been shown long time ago to be one of the most important parts affected in human brains affected by Alzheimer’s Disease (Ball, 1977). For this reason, the hippocampus is one of most studied brain structures, and several thousands of scientific publications contain the keywords "Hippocampus" and "Alzheimer disease". Damage to the hippocampus leads not only to difficulty to create new memories, but also to problems in recalling old ones.

Emx2 has an early, very high level expression during neurogenesis in the hippocampal primordium, and it might control hippocampal growth and specification (Pellegrini et al., 1996; Tole et al., 2000; Zhao et al., 2006). In the *Emx2* null mutant mouse, a certain part of the Hippocampus, the so called "Dentate Gyrus", is completely missing (Pellegrini et al., 1996; Yoshida et al., 1997).

The Dentate Gyrus is a peculiar, very specialized part of the Hippocampus. Its histology (cellular composition), anatomy (connections) and development have been described in detail (Altman and Bayer, 1990a; Altman and Bayer, 1990b; Amaral and Witter, 1995; Soriano et al., 1989a; Soriano et al., 1989b). It is formed by three layers of cells, namely, marginal layer, granule cell layer and polymorph layer. The most important and characteristic one is the granule cell layer which has a peculiar V shape (see Fig. 1). The dentate neuroepithelium is a small area in the vicinity of the “fimbria”, a large axonal bundle formed by the prolongations of hippocampal neurons (pyramidal cells) born in the days before the dentate starts to develop. The stem cells that give rise to the dentate have the unique characteristic that they produce progenitor cells able to migrate themselves out of the neuroepithelium and move in the direction

of the settling place, while still dividing (see Fig. 1). In that way, along the dentate migratory pathway one can find progenitors as well as young migrating neurons (Schlessinger et al., 1975; Zhao et al., 2006). *Emx2* expression can be detected in the developing Dentate Gyrus as well as in the adult. Surprisingly, the adult Dentate Gyrus is a major source of neurons (a phenomenon called "adult neurogenesis") (Hong et al., 2007; Kuhn et al., 1996; Yoshida et al., 1997).

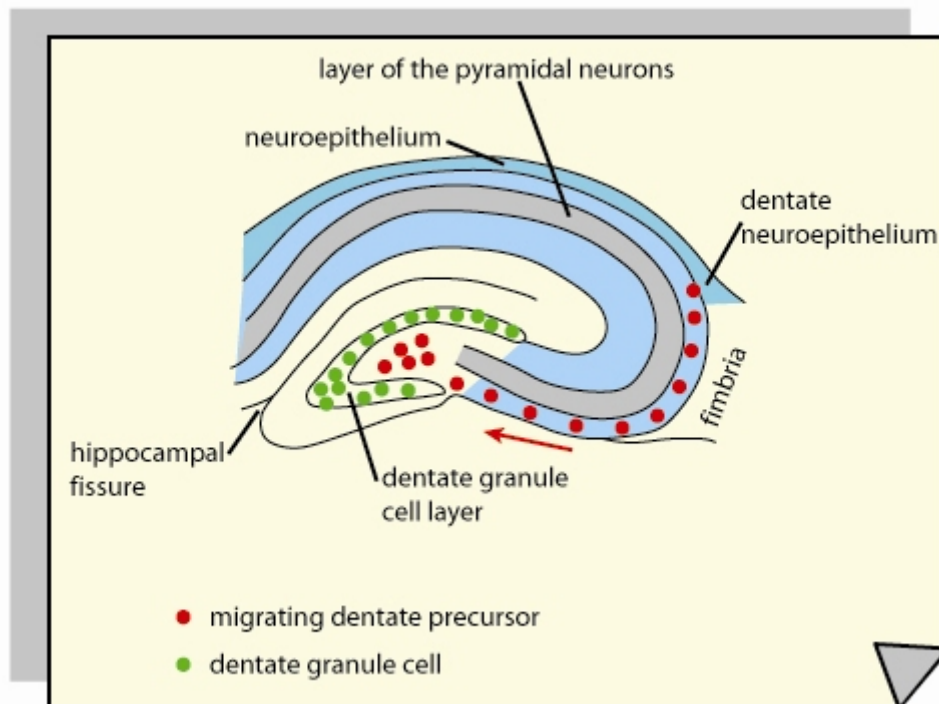


Figure 1. Schematic showing the development of Dentate Gyrus granule layer.

Neurons and precursors (red dots) born from dentate neuroepithelium migrate along radial glial scaffolding towards Dentate Gyrus region (green dots). As they migrate, precursors can also divide, originating a new precursor and a neuron, both of which keep migrating towards the Dentate Gyrus.

Radial glial cells

To migrate in an orderly fashion, progenitors and young neurons need a substrate that supports their migratory movements and that leads to the target (in this case, the

presumptive Dentate Gyrus). This substrate is the “radial glial scaffolding” (green in Fig. 2). The radial glial scaffolding is formed by the very long cellular processes of radial glial cells whose bodies reside in the neuroepithelium. Radial glia cells are actually not unique to the Dentate Gyrus (unlike the migrating precursors), but found everywhere in the developing brain. They extend their fibers towards the pial surface (outer brain surface) crossing the entire cerebral wall from the ventricular surface, resulting in the formation of a dense scaffold. In the cortex, the radial glial cells persist throughout the entire period of neurogenesis. They act as progenitor cells generating various cell types including neurons. At the end of neurogenesis, the radial glial cells stop dividing and mostly trans-differentiate into astrocytes (Gaiano et al., 2000; Heins et al., 2002).

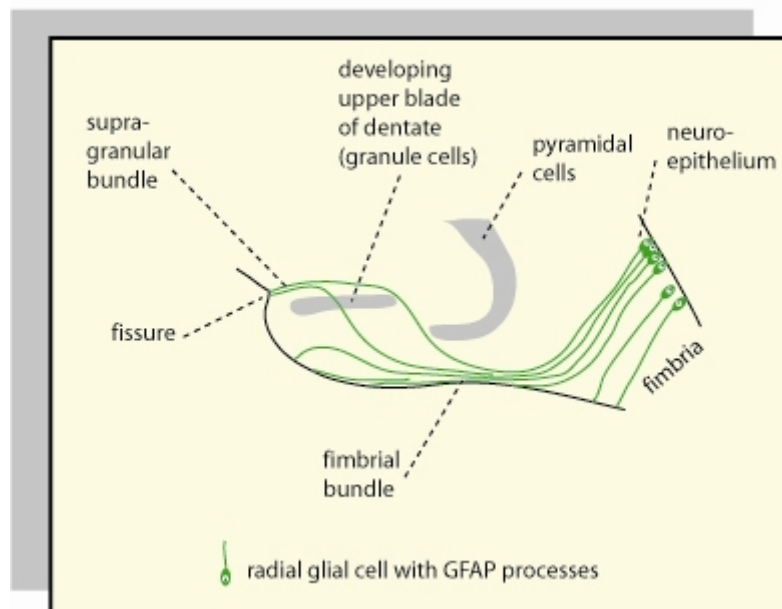


Figure 2. Schematic showing of DGCL glial scaffolding.

***Emx2* and Cajal-Retzius cells**

Cajal-Retzius (CR) cells are special neurons located in the periphery of the developing cortex. They are characterized by the secretion of reelin, a protein required for the orderly development of the layers of the cortex. Reelin is a large glycoprotein

that acts as a signal in the marginal zone to regulate the migration of cortical neurons (D'Arcangelo et al., 1995).

A very interesting feature of cortical development is the migration of neurons from the ventricular region (inner side of the brain) to the pial surface (outer side of the brain). After migration, cortical neurons accumulate forming a dense cell layer called cortical plate. Birthdating studies have shown that neurons within the cortical plate are arranged in inside-out manner (Angevine and Sidman, 1961; Gleeson and Walsh, 2000). This means that, in normal developing cortex, the newest neurons always migrate through the old neurons to settle ever more peripherally: in this way, the cortical neurons generated first are always located more deeply than the ones generated later. In the so-called reeler mouse mutant, which lacks the protein reelin, the cortical plate is disorganized and, as a consequence, the cortical layers form defectively and are mixed, not respecting the "inside-out" anymore (Gonzalez et al., 1997). The reeler mice show an impaired motor coordination, tremors and ataxia.

CR cells, the reelin-secreting neurons, express also *Calretinin* (*Calb2*) and *Emx2*. In the *Emx2* null mutant, the CR cells are lost by the late embryonic period (Mallamaci et al., 2000). The CR cells are born between embryonic day (E) 10.5 and E13.5 in a very restricted part of the pallium named "cortical hem".

The cortical hem is a transient neuroepithelial region located in the posterior and medial pallium, intercalated between the hippocampus and the choroid plexus. Genes of the *Wnt* family, encoding powerful signalling proteins, are abundantly expressed in the cortical hem (Fig.3).

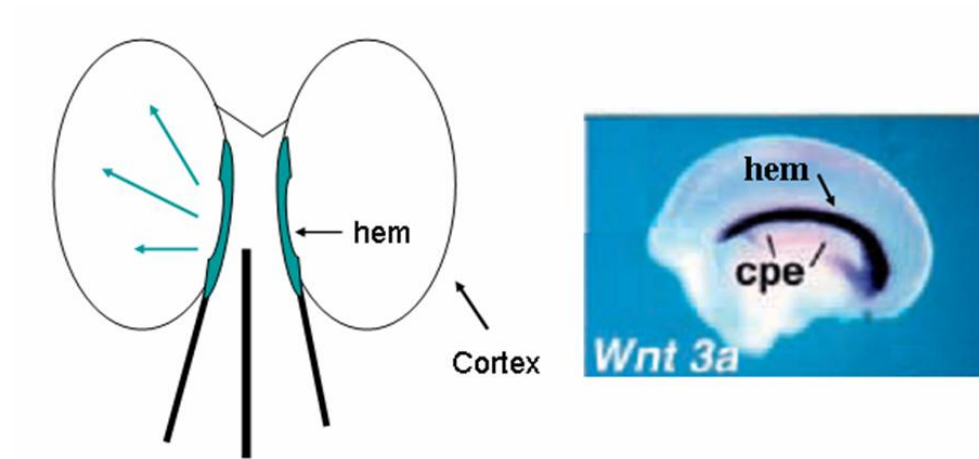


Figure 3. Schematic representation of the cortical hem and its cell migration pathway.

The position of the cortical hem is illustrated by *wnt3a* in situ from medial view of telencephalic hemisphere at E12.5 (Grove et al., 1998) (right). Cells generated from cortical hem (green region) follow the migratory pathway indicated by the green arrows (left).

Emx2 and cortical angiogenesis

Emx2 is expressed in the developing cortical area from early embryonic days. It plays an important role in cortical patterning and growth. The most obvious defect in mutant mice is the retarded cortical growth: the cortical area is much smaller than in the wild type mouse (Pellegrini et al., 1996).

Angiogenesis (blood vessel formation) has a very close relation with growth by supplying the necessary nutrition to the growing tissues. The formation of the vascular system begins very early in development and is under elaborate control. It consists of a complex process of remodeling and refining the initial pattern with proliferation and sprouting of new vessels from existing ones (Risau, 1997)

The mechanism of angiogenesis is under heavy investigation because of its blooming medical potential. Several pathways (VEGF, angioprotein/Tie, Ephrin/Eph receptor, TGF-beta, PDGF and Delta/Nortch) have been illustrated by different groups in the

last 2 decades (Rossant and Howard, 2002). Among them, the vascular endothelial growth factor (VEGF) and its receptors play perhaps the most important role in angiogenesis.

VEGF family has 4 different genes (A-D) coding for a group of glycoproteins, and VEGFa has 5 isoforms in human and 3 isoforms in mouse, called Vegfa-120,-164, and -188 (classified by the amino acid length of the corresponding protein) (Ferrara and Davis-Smyth, 1997). Isoforms 120 and 164 are the most abundant. Vegfa-164 is the most powerful of the three. Mice deficient in VEGF present early embryonic lethality even if heterozygous (Carmeliet et al., 1996; Ferrara et al., 1996).

VEGFA is expressed in the neuroepithelium, where *Emx2* is present, as well as in a pial area named perineural vascular plexus (Breier et al., 1992; Carmeliet et al., 1996). VEGFA shares receptors (Neuropilin 1 and 2) (Chen et al., 1997) with *Sema3a*, an important axonal guidance factor, which suggests more complicated roles of VEGFA in cortical development.

Transcription factors and cell lineage study

After being born from the neuroepithelium, the new neurons journey toward their final location. Cell birth and cell migration are the major processes during brain development. Defects in neuronal migration can lead to diseases such as mental retardation, epilepsy, and severe learning disabilities (Marin and Rubenstein, 2003). The forebrain contains neurons originated in several different regions. Neurons from different regions of the neuroepithelium could contribute different properties to the final region of the brain where they end up (Stern and Fraser, 2001). The complexity of forebrain architecture reflects the complex migratory movements required during development. Understanding these elaborate processes is therefore essential to discerning the mechanisms underlying its normal and pathological development (Caqueret et al., 2005).

Although technical breakthroughs in microscopy made "live" observation and 4D reconstruction of cell migration in the worm *C. elegans* become true more than 10 years ago (Thomas et al., 1996), the lacking of comprehensive tools still makes "live" observation and complete mapping of developmental migration in the mammalian brain a mission impossible. The novel discipline called "genetic neuroanatomy" provides a partial solution. It uses mouse genetic tools (mouse mutant lines and mouse reporter lines) and is based on the very specific and restricted expression of many transcription factors, which makes them ideal markers of specific neuronal populations.

Part of my PhD work falls under the label of "genetic neuroanatomy", since it consisted in the creation of a mouse mutant line very useful to study neuronal migration in the developing diencephalon.

General background of lineage tracing

Embryonic development is a process combining a vast amount of cell proliferation and migration events. To understand this process, ideally we would need a description of the fate of every cell in the embryonic brain primordium. Efforts in this direction have been made since the early days of the 20th century and various methods to map cell fate have been developed: direct observation, vital dyes, retrovirus-induced marker expression and, lately, DNA recombination.

For the spontaneous DNA recombination method, two transgenic mouse lines are generated: one carries a reporter gene (beta galactosidase or alkaline phosphatase) blocked by a stop codon delimited by *loxP* sites, and the other expresses the enzyme "Cre recombinase" under the control of a promoter that controls the expression of a gene of interest (Song et al., 1996; Zinyk et al., 1998). When the two lines are crossed, mice are obtained which carry at the same time reporter genes flanked by *loxP* sites and Cre recombinase which will be activated in the cells expressing the gene of interest. In the cells expressing such gene, Cre recombinase will be produced, and it will recombine the *loxP* sites, in this way deleting the stop codon and allowing expression of the reporter gene. This provides us with a "lineage marker". Because the recombination of *loxP* sites is irreversible and inheritable, every cell that expresses the gene of interest will become (through Cre recombinase expression and Cre-mediated activation of the reporter gene) permanently labeled. If other cells are born from this one, they will also permanently express the reporter gene: the whole family or "lineage" will be made visible by reporter expression.

Z/AP and Rosa26 mouse line

One gene can be expressed in different parts of body at different time points. Very often, the loss of function mutation disrupts the gene function at early development in

such a way that the embryo dies, depriving us of the opportunity to see how the mutation would affect later development or even adult function.

In the early 1980s, it was discovered that a DNA recombinase, named *Cre*, from P1 bacteriophage could specifically catalyze recombination between two sequences 34 base-pair long (*loxP* sites) with high efficiency (Sternberg and Hamilton, 1981; Sternberg et al., 1981). The *loxP* site is a palindromic sequence (i.e. it is symmetric and reads the same left-to-right or right-to-left) except for an 8-base pair long asymmetric core sequence which gives the *loxP* site directionality. If there are *loxP* sites with the same orientation on one DNA strand, the enzyme Cre recombinase will delete the DNA sequence that separates both *loxP* sites, and will "glue" together the ends so that the DNA molecule will be intact after the deletion (recombination) (see Fig. 4 left).

After the discovery of Cre-mediated recombination, it was immediately obvious that it could be used as a tool for targeted deletion of specific DNA sequences, in this way generating targeted mutations. It is enough to flank the target gene with *loxP* sites in embryonic stem cells (ES cell) and introduce Cre at a special time and place to achieve an interruption of gene function.

To use this handy tool as a cell lineage marker, special "reporter mouse lines", like ROSA26R and Z/AP, have been generated. In ROSA26R mice, the DNA sequence between the two *loxP* sites encodes an in frame stop codon and a polyA tail. Additionally, a beta-galactosidase sequence was placed right after the 2nd *loxP* site (see Fig. 4 middle). This modified sequence was cloned into a constitutively active site (ROSA 26 locus) of the mouse genome. Normally, the beta-galactosidase is silent because the stop codon ends transcription before it reaches the beta-galactosidase reporter gene. After introducing Cre recombinase, the stop codon is eliminated and subsequently the beta-galactosidase reporter gene is activated and the enzyme beta-galactosidase starts to accumulate in the cell body. The enzymatic activity of beta galactosidase can be easily detected and in this way it marks the territory where the Cre recombinase is expressed (Soriano, 1999).

For the Z/AP reporter mouse, the design is similar, but the reporter gene encodes the enzyme "human placental alkaline phosphatase" (hPLAP) (see Fig. 4), which can be detected after Cre recombinase expression (Lobe et al., 1999).

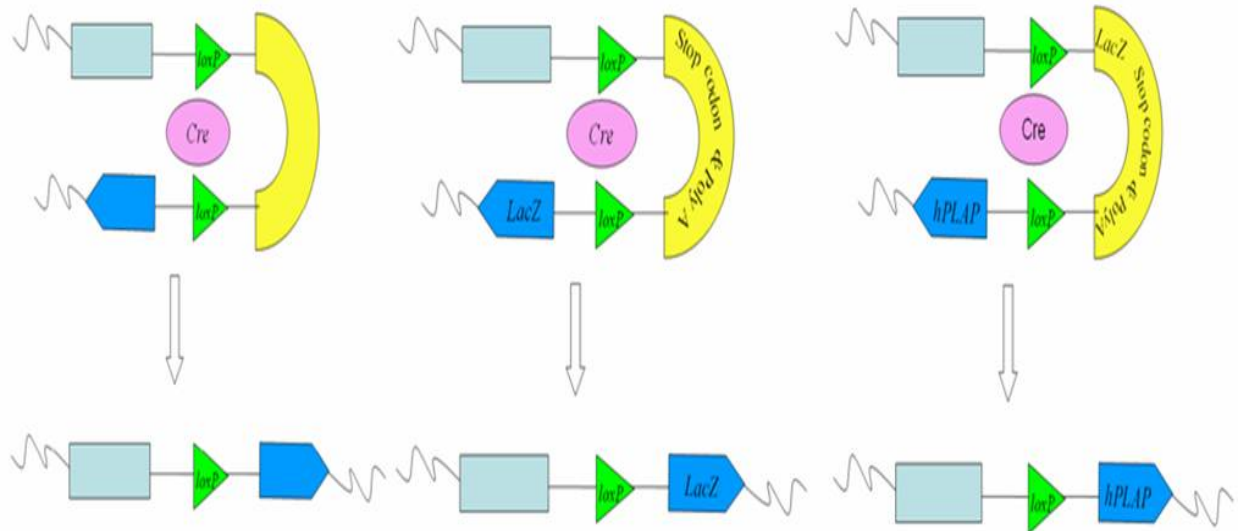


Figure 4. Schematic showing of Cre recombinase mediated DNA recombination eliminates the sequence between 2 *loxP* sites (left). Under this principle, Rosa26 (middle) and Z/AP (right) marker mouse line were generated.

Transcription factor *Foxb1* and fork head gene family

Forkhead box (or "Fox") genes were discovered in the fruit fly *Drosophila melanogaster*. The forkhead gene family contains 17 gene subclasses (A to Q) and more than 100 members, according to the amino acid sequence of their conserved forkhead domain. Despite this highly conserved forkhead domain, other functional domains are highly variable which allow different regulation and binding activity. As the result, the proteins of different Fox family members have significant variation in function and regulation which makes this protein family important in many biological processes. To date, Fox proteins are known to be involved in metabolism,

development, differentiation, proliferation, apoptosis, migration, invasion and longevity (Myatt and Lam, 2007).

The forkhead domain is a DNA sequence encoding a subgroup of the winged-helix class of protein which has DNA binding properties (see Fig. 5).

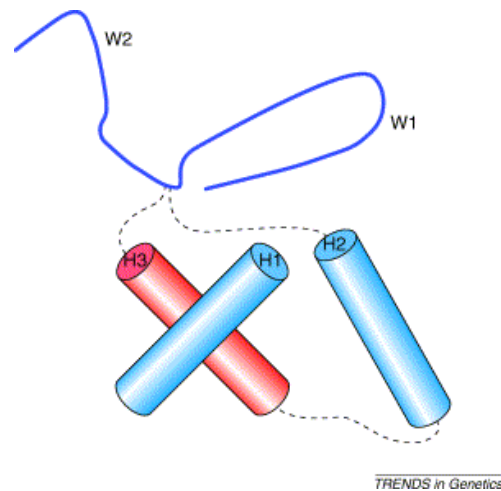


Figure 5. The three-dimensional structure of the forkhead domain derived from X-ray crystallography data for forkhead protein. The α helices (H1–H3) and two wings (W1–2) are shown. The recognition helix H3 (red) lies in the major groove of DNA (Lehmann et al., 2003).

Fox proteins can both activate or repress gene expression through the recruitment of co-factors or repressors. Deregulation of Fox protein activity or expression results in changes in both direct and indirect target genes. Although *Fox* genes have very important roles in the development of many organs, the manner in which they regulate their downstream gene networks is still not clear.

Foxb1, also known as *Mf3* and *Fhk5*, is a developmental transcription factor belonging to the forkhead family. In the mouse, the earliest *Foxb1* mRNA could be detected on embryonic day 7.5 at the primitive streak region (Wehr et al., 1997). As the embryo develops, *Foxb1* expression is mostly restricted to the floor plate, the ventral spinal cord, hindbrain, midbrain, and mammillary body region of the hypothalamus (Alvarez-Bolado et al., 2000a) (see Fig.6). Between E10.5 and E12.5, *Foxb1* shows transient expression in the dorsal thalamus and this expression marks

the most rostral boundary of *Foxb1* expression (Zhao et al., 2007). After birth, *Foxb1* expression is maintained in the mesencephalon and mammillary body (Zhao et al., 2007). Early studies of *Foxb1* mutant mice have demonstrated that *Foxb1* is a key developmental regulator of the development of the caudal midbrain and hypothalamus (Alvarez-Bolado et al., 2000a; Wehr et al., 1997).

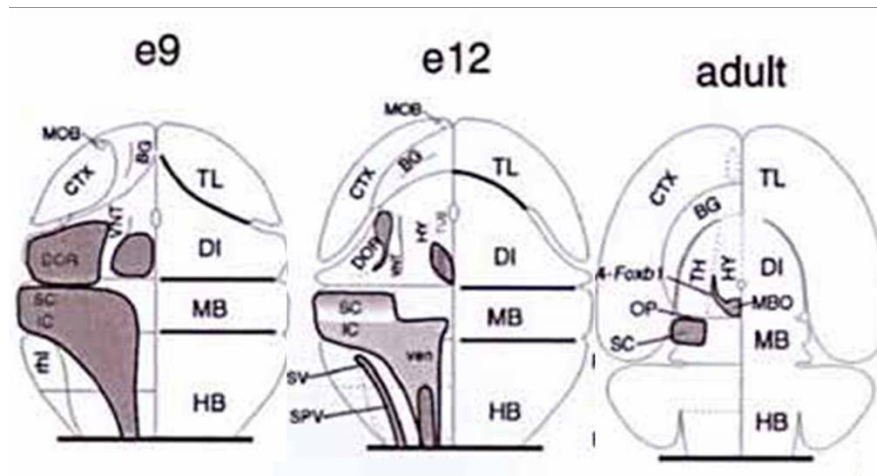


Figure 6. Flat map of *Foxb1* expression in the brain. The schematic drawing shows the developmental distribution of *Foxb1* expression on E9.0, E12.0 and adult. At early stages of development, *Foxb1* was abundant in the diencephalon, middle brain and hindbrain. The expression reduced dramatically after E12.5 in the forebrain part and later in the adulthood, the *foxb1* expression can only be found in superior colliculus and mammillary body (Alvarez-Bolado et al., 2000a). BG: basal ganglia, CTX: cortex, DI: diencephalon, DOR: dorsal thalamus, HB: hindbrain, HY: hypothalamus, IC, inferior colliculus, MB: middle brain, MBO: mammillary body, MOB: main olfactory bulb, OP: olivary pretectal nucleus, SC: superior colliculus, , SPV: spinal nucleus of the trigeminal, Th: thalamus, TL: telencephalon, VNT: ventral thalamus (prethalamus).

Foxb1 null mutant mice are born alive but show growth retardation. Those which arrive to adulthood show a defect in body weight and size. Other defects can be found in the inferior and superior colliculi, and female mice are not able to nurture and wean their pups properly (Wehr et al., 1997). This is probably due to the fact that *Foxb1*^{-/-} female mice have don't complete the mammary gland development (Kloetzli et al., 2001).

Hypothalamus development and transcription factor *Foxb1*

The hypothalamus occupies the ventral half of the diencephalon on both sides of the third ventricle and lies immediately above the pituitary gland. It is an important interface between the endocrine and autonomic systems and is essential for survival and reproduction. The hypothalamus fulfills these functions by regulating a wide range of processes such as blood pressure, body temperature, energy balance and motivated behaviors.

After intensive study of physiological and clinical aspects, researchers are starting to focus on hypothalamus development. Previous work has illustrated how early morphogens like *sonic hedgehog* (*Shh*) and BMPs induced the cell fate (Shimamura and Rubenstein, 1997) and how a genetic regulation network (i.e. *Sim1*, *OTP*, *ARNT2*) patterned the entire region (Michaud et al., 1998; Wang and Lufkin, 2000). However, little is known about the actual process of building the hypothalamic tissue in all its complexity (i.e. hypothalamic histogenesis).

Brain development consists of at least two major processes: one is neuron production and the other is neuron migration. Hypothalamic neurons originate in the neuroepithelium lining the third ventricle. After being born, a hypothalamic neuron must follow an either radial or tangential pathway of migration to its destination or final settling place. How this process is regulated by genes to create the very complex pattern of neuronal nuclei that characterizes the hypothalamus is not well understood.

Foxb1 expression in hypothalamus is restricted to the mammillary region. In *Foxb1* null mutant mice, the mammillary body develops but shows an immature mammillothalamic tract (Alvarez-Bolado et al., 2000b). however, following by dramatic size reduction at postnatal day 4 (P4) with a detectable large scale apoptosis the mammillary body disappears totally by P7 (Alvarez-Bolado et al., 2000b).

The mammillary body is a substantial component of Papez circuits (Papez, 1995) which is one of the most important circuits of the emotional limbic system. The lack of mammillary body in mice provokes behavioral alterations like deficit in spatial working memory (Radyushkin et al., 2005).

MATERIALS AND METHODS

Animal handling and breeding

All experiments with animals were carried out in accordance with the European Communities Council Directive of 24 November 1986 (86/609/EEC) and under the authorization Az 32.22/Vo (Ordnungsamt der Stadt Göttingen).

The *Foxb1*, *Emx2*, *Rosa26* and Z/AP mouse line are kept in C57BL/6 background as well as the wild type mouse used in the thesis.

Animals with the appropriate genotypes were mated overnight and the females inspected for vaginal plug on the following morning; noon of the "plug day" was considered embryonic day 0.5 (E0.5). Pregnant female mice were first anaesthetized with CO₂ and then killed by cervical dislocation.

Alkaline phosphatase staining

Preparation: Take the embryo out and wash in cold PBS

Fixation: Embryonic brains were fixed in ice cold 4% paraformaldehyde depending on their age

<E11.5 or E11.5 30min

E12.5 30min then cut in the middle 30min

>13.5 1h then cut into 150µm thick sections in an agarose block. Fix again for 30min on ice.

Rinse in PBS 3 times for 20-30 min at room temperature (3x10min, shaking)

Heat inhibition

Heat inactive the endogenous AP by heat up to 72°C in water bath for 30min

Rinse again with PBS at room temperature.

Staining

Rinse with AP buffer (100mM Tris-Cl, PH 9.5, 100mM NaCl, 10mM MgCl₂) for 10min before stain with color solution (250μl NBT +187.5μl BCIP per 50ml AP buffer) at 4°C over night or at room temperature until the appropriate color appeared.

Postreaction fixation

Fix with 4% paraformalhyde for 1h at 4°C.

Apoptosis (TUNEL)

The Apoptag kit (Chemicon) was used on formaldehyde-fixed, paraffin-embedded samples following the instructions of the manufacturer.

Beta galactosidase staining on mouse brain

Preparation

Take the embryo out and wash it with cold PBS

Fixation

Embryos were fixed depending on their ages

E10.5 and earlier than E10.5 30 min

E11.5 40 min

E12.5 50min

E13.5 30 min then cut in the middle 30min

With the FixA solution (see the table)

FixA	25 ml	50 ml	100 ml
37% Formaldehyd (FA)	0.675	1.35	2.7
25% Glutaraldehyd	0.2	0.4	0.8
10% NP40 (Sigma)	0.05	0.1	0.2
10XPBS	2.5	5.0	10
dH2O	21.575	43.15	86.3

For animals older than E13.5, fix with 4% paraformaldehyde for 1h at 4°C. After washing with PBS, put into a low melting point agarose block and section with a vibraslicer into 150µm thick sections.

Fix the sections again 30min with FixA on ice.

Staining:

Tissues are then washed 2 times each for 10min with PBS at RT before staining with the X-Gal solution (see the table)

X-Gal solution	10ml	25ml	50ml
1xPBS	9.35	23.375	45.25
X-Gal (40mg/ml in Dimethylformamid)	0.25	0.625	1.25
K3Fe(CN)6 200mM	0.25	0.625	1.25
K3Fe(CN)6 200mM	0.25	0.625	1.25
MgCl2 100mM	0.2	0.5	1.0

Staining lasted a few hours to overnight until the appropriate color appeared.

Postreaction fixation

Fix with 4% paraformalhyde for 1h at 4°C.

Brdu injection and detection

Pregnant female mice were intraperitoneally injected with Brdu (RPN201, Amersham Biosciences, Buckinghamshire, England) (50µg/g of body weight) at 12:00, 15:00, 18:00h on the appropriate pregnancy date. Embryos were collected then fixed in 4% paraformaldehyde before embedded in paraffin. After sectioning, an anti Brdu antibody was used for detection.

Genotyping

Genotyping was performed from the direct lysate from animal tails or yolk sack.

Lyse the tail in 200µl PBDN buffer with 0.2 mg/ml Proteinase K.

Shaking at 55°C for 2-3 h or until the tail disappear then heat up to 85°C for 1h.

Spin down 1 min to pellet the hair (do not use the hair at all)

Take 1µl liquid directly for a 20µl PCR

An universal PCR mixture recipe is used in all the genotyping:

1000 µl total volume

100 µl 10x buffer w/o MgCl₂

10µl dNTP20mM

45µl MgCl₂ 50mM

3.3µl primer 1 (100pM)

3.3µl primer 2(100pM)

3.3µl primer 3(100pM), if applicable

7 µl polymerase 5u/µl

831.4µl H₂O

All the PCR reaction is running under a similar 30-cycle program with different annealing temperature. The complete polymerase kit is from Genecraft.

Table of primers

Gene detected	Primer	Primer Sequence
Foxb1cre	1	CAC TGG GAT GGC GGG CAA CGT CTG
	2	CAT CGC TAG GGA GTA CAA GAT GCC
	3	CTC GGC ATG GAC GAG CTG TAC AAG
Lrp6	1	CAG GCA TGT AGC CCT TGG AG
	2	ACT AAC AGC CCT GCA CTG CC
	3	GTA GAG TTC CCA GGA GGA GCC
Gbx2	1	TCT CGG AAC CCC AAG ATT GTC GCT
	2	TGG ATG TCC ACA TCT AGG AGG TGC
	3	CAC GAG ACT AGT GAG ACG TGC TAC
Emx2	1	GAA CGA CAC AAG TCC CGA GAG TTT C
	2	CTC ATA TTG CCC TAA CAA AGC TGA GC
	3	CAC GAG ACT AGT GAG ACG TGC TAC
ZAP	1	GGA AGT CAG TGG GAG TGG TAA C
	2	GTC TCG GTG GAT CTC GTA TTT C
Rosa 26	1	CGT CAC ACT ACG TCT GAA CGT CG
	2	CAG ACG ATT CAT TGG CAC CAT GC

Immunohistochemistry

Immunohistochemistry works were performed on either formaldehyde-fixed, paraffin-embedded samples or on Direct frozen samples.

Preparation:

For paraffin embedded section: Re-hydrate the section through Xylol, 100% EtOH, 90% EtOH, 70% EtOH, and 50% EtOH.

For Frozen sections, fix for 25min with 4% paraformaldehyde at room temperature

Antigen retrieval

Treat the section in 97°C Dako antigen retrieval solution for 20 min

Or boiling in Citrate buffer 3 times each 5min depends on antibody in use.

Bleaching (only with DAB detection)

Bleach the section with 3% H₂O₂ in Water for 15min at Room temperature

Pre-incubation

Pre-block the section with PBS + 10% FCS+0.1% Tween20 for 1h at room temperature.

First antibody application

Dilute first antibody into appropriate dilution with PBS+10%FCS+0.1 % Tween20 then incubate over night at 4°C

Secondary antibody detection

For florescent detection: apply appropriate Alexa flour antibody with 1/500 dilution with PBS. Incubate for 1h at room temperature in darkness. The experiments finished after intensive washing.

For DAB detection: apply appropriate biotinlated secondary antibody and incubate for 1h at room temperature

Amplification (only with DAB antibody)

Dilute extravidin 1/100 in PBS+10%FCS and incubate 1h at room temperature.

Detection (only with DAB antibody)

Drop the mixture of DAB (0.05%) and H₂O₂ (1%) onto the section wait for 2 min. the experiments finished after intensive washing.

Table of antibodies

Antibody Name	Company	Working Dilution	Host Species	Antigen Retrieval Method
anti-calretinin	Swant	1/500	Rabbit	Citrate buffer
anti-GFAP	DAKO	1/100	Rabbit	Citrate buffer
anti-2h3	DSHB	1/4	Mouse	Citrate buffer
anti-Calbindin	Chemicon	1/100	Rabbit	Not nessary
anti-beta gal	Abcam	1/100	Rabbit t	Dako solution
anti-beta gal	Abcam	1/100	Chicken	Dako solution
anti-Ki67	BD bioscience	1/20	Mouse	Citrate buffer
anti-OrexinA	R&D system	1/20	Mouse	Dako solution
anti MCH	Phoenix Phama.	1/100	Rabbit	Dako solution
anti-Brdu	DAKO	1/100	Mouse	Citrate buffer
anti-nestin	Chemicon	1/100	Mouse	not nessary
anti-GAD67&65	Abcam	1/100	Rabbit	Dako solution

In Situ Hybridization

The robotic in situ hybridization was performed according to newly developed high throughput non radioactive ISH with a Tecan platform (Herzig et al., 2001; Yaylaoglu et al., 2005). Because of the robust RNase activity and instability of RNA molecule, all glassware and metal tools used have to be autoclaved and properly covered from condemnation. The solutions in this procedure have to be made up from ddH₂O or DEPC treated ddH₂O.

RNA Probe generation

Design a gene specific oligonucleotide using a primer selection program (primer3). For primer synthesis, attach T7 promoter sequence (GCGTAATACGACTCACTATAGGG) to 5' terminal of the forward primer and the SP6 sequence (GCGATTTAGGTGACACTATAG) to the 3' terminal of reverse sequence in order to allow RNA polymerase to bind.

-PCR template amplification

Different primer has different annealing temperature. To avoid this, I used a touch-down PCR program for universal amplification. The E14.5 mouse cDNA was used as amplification template.

Step	Temp (°C)	Time	GO to	Cycles	Gradient
1	94	2 min			
2	94	20 sec			
3	65	30 sec			-0.5°C
4	72	5 min	2	10	
5	94	20 sec			
6	60	30 sec			
7	72	5 min	5	29	
8	72	15 min			
9	8	forever			

Run the PCR product on an agarose separation gel. Cut the band of desirable size for DNA extraction. If the product is not enough, a second round amplification with T7 and Sp6 primer should be performed.

-RNA probe synthesis

RNA probes are synthesised according to the following formula:

	Concentration	Volume
H2O (DEPC)		add up to 20µl
5xRNA synthesis buffer		4µl
10X Dig. labeled rNTP mixutre		2µl
Rnase inhibitor	40U/µl	1µl
polymerase	50U/µl	1µl
template		500ng

The reaction last 150 min at 37°C then stopped by adding 1µl following mixture

H ₂ O (DEPC)	16,4 µl
MgCl ₂ (0,3 M)	1,6 µl
DNase (10 U/µl)	2,0 µl

The reaction last for another 20 min at 37°C then we precipitate the mixture of cold (-20°C) 72 µl NH₄Ac (4M, autoclaved) and 470 µl EtOH (100%).

The quality of RNA probe is controlled by RNA analyzer.

Sample preparation

-Embryo embedding

Dissect the embryos out from pregnant female at the proper age and wash in ice-cold PBS.

Penetrate with optimal freezing medium (OCT) on ice in a pitredish for 10min

Embed the embryo with an appropriate orientation in an OCT containing embedding chamber.

Freeze the embryo by putting this copper bottomed embedding chamber onto an aluminum surface which cooled down to -70°C

The quick frozen block can be kept in -80°C for an undefined time.

-Sectioning and pretreatment

Section the frozen block in a Leica cryostat (CM3050S) into 20µm thick and plate them in order onto a Super Frost Plus microscopy slide.

The tissues on slide then were fixed with 4% paraformaldehyde for 25min followed with two times 5 min acetlzation (0.25% acetic anhydride, 0.1M triethanolamine, PH8.0)

The slides then washed with PBS, 0.9% NaCl and passing a serious of EtOH solutions before air dried.

The sections are ready for an immediately ISH assay or can be kept at -20°C for later.

Robotic ISH procedure in summary

cycles	T (min)	volume	Reagent	l. class	container	temperature
5	5 min.	300	H2O2 in MeOH	ethanol	325	24° C
7	5 min.	300	PBS (1)	water	1000	24° C
2	5 min.	300	0.2M HCl	water	200	24° C
4	5 min.	300	PBS (2)	water	1000	24° C
1	5 min.	400	PK buffer	water	200	24° C
2	10 min.	300	Proteinase K in PK buffer	water	200	24° C
7	5 min.	300	PBS (3)	water	1000	24° C
2	10 min.	300	4% PFA (1)	water	200	24° C
7	5 min.	300	PBS (4)	water	1000	24° C
2	15min	300	hyb-mix (1)	hyb-mix	200	24° C
1	15 min.		heat up to 64° C	hyb-mix	-	64° C
1	330 min	300	probe hybridization	probe	300	64° C
5	5 min.	300	5 x SSC	water o/n	450	62° C
5	10 min.	350	formamide I	water o/n	450	62° C
5	12 min.	350	formamide II	water o/n	450	62° C
3	8 min.	300	0.1 x SSC (1)	water o/n	450	62° C
1	8 min.	300	0.1 x SSC (2)	water o/n	450	24° C
4	5 min.	300	NTE (1)	water o/n	1000	24° C
6	5 min.	300	20 mM iodoacetamide (1)	water o/n	325	24° C
4	5 min.	300	NTE (2)	water o/n	1000	24° C
2	5 min.	300	TNT (1)	water o/n	1000	24° C
6	5 min	300	4% sheep serum (1)	water o/n	325	24° C
4	5 min.	200	TNT (2)	water o/n	1000	24° C
2	10 min.	300	TNB blocking buffer	water o/n	325	24° C
2	5 min.	200	TNT (3)	water o/n	1000	24° C
2	5 min.	300	maleate wash buffer (1)	water o/n	1000	24° C
2	10 min.	350	blocking reagent	water o/n	200	24° C
2	5 min.	300	maleate wash buffer (2)	water o/n	1000	24° C
2	5 min.	250	TNT (4)	water o/n	1000	24° C
3	5 min.	350	TMN	water o/n	325	24° C
4	5 min.	200	TNT (2)	water o/n	1000	24° C
4	10 min.	300	TNB blocking buffer	water o/n	325	24° C
2	30 min	350	antiDIG-POD	water o/n	200	24° C
6	5 min.	200	TNT (3)	water o/n	1000	24° C
1	25 min	250	tyramide-biotin	-		24° C
6	5 min.	250	maleate wash buffer (1)	water	1000	24° C
2	20 min	350	Neutravidin	water	200	24° C

Materials and Methods

6	5 min.	250	maleate wash buffer (2)	water	1000	24° C
4	5 min.	250	TNT (4)	water	1000	24° C
2	5 min.	400	TMN	water	325	24° C
3	10 min	350	BCIP/NBT	water	200	24° C
3	x	400	System liquid (1)	System liquid		24° C
1	x	300	NTE (3)	water	1000	24° C
1	10 min.	200	4% PFA (2)	water	200	24° C
3	x	400	System liquid (2)	System liquid		24° C

Morphometry

Morphometrical analysis of cortical vascularization was carried out on histological slides with 25 micrometer thick sections from embryonic mouse brains (E12.5, E15.5 or E18.5) labeled by non-isotopic *in situ* hybridization with probes against endothelial-specific marker gene *Col4a1*. Then we used Cell-F software (Olympus SIS, Münster, Germany) to measure the labeled surface area and expressed the result as a percentage of the total area in upper (MZ plus CPL) vs. lower cortical layers. The sections were taken along the sagittal plane to ensure that the cortical slice they contained was in a homogeneous developmental stage. Transverse sections would have included a developmental gradient from more mature (lateral) to less mature (medial). The slides were digitally photographed at a resolution of 1.6 micrometer/pixel using a microscope with a motorized scanning stage and a digital camera (Leica Microsystems GmbH, Wetzlar, Germany), and saved as tiff files. Eight sections from each of three embryos for every age and genotype were chosen for analysis. For consistency, all sections selected for morphometrical evaluation were taken from a medio-lateral level that included the olfactory bulb. Besides, sections in this level are the most perpendicular to the cortical layers (i.e., they do not cut tangentially or sidewise through the layers). A parallel series of Nissl-stained sections was used to determine the limits of “upper” and “lower” layers.

Nissl staining

Preparation of 0.1% Cresyl violet solution

Add Cresyl echt violet (or cresyl violet acetate) 0.1 g into 100ml distilled water, mix well.
Add 300 μ l glacial acetic acid into every 100ml 0.1% Cresyl violet solution just before use and filter.

Staining procedure

Prepare the section as described (see the preparation of immunocytochemistry).
Insufficient deparafinization will cause uneven staining.

Immerse the sections into 0.1% Cresyl violet solution for 5min at room temperature

Rinse quickly in distilled water for 1min

Differentiate and clarified in 70% EtOH plus 0.1% glacial acetic acid for 2 min check under the microscope

Wash in 90% EtOH for 2min

Wash again for 2 times 5min in 100% EtOH.

Clear in xylol for 2 times 5mins

Mount with permanent mounting medium such as Eukit

Statistics

Statistical analyses were carried out with GraphPad Prism 4 (GraphPad Software Inc., San Diego, USA). Details can be found in the figure legends.

Southern Blot

Digest 10 µg genomic DNA in TE buffer with proper NEB enzyme over night at 37°C

Load the substance on a 0.7% gel and run for over night at the proper voltage (1V per cm)

Photograph gel picture under the UV light

Denature the gel with 0.25M HCl for 10 min

Denature again with 0.4M NaOH for 20min

Prepare Hybond+ membrane as the same size of the gel with orientation mark and assemble the transfer chamber (from bottom: gel, Hybond membrane, blotting paper, paper towel, glass plate and weight) and leave it over night.

Put the membrane into hybridization bottle with the DNA binding side in.

Wash 2 times with hybridization buffer as room temperature

Add proper volume of hybridization buffer and rotate the probe at 65°C for 1h

Synthesis the radio active probe and measure the probe concentration

Add proper amount of probe into the hybridization tube and hybridize over night

Remove the hybridization buffer and wash with 5xSSC for 3 times 5 min

Wash again with 2xSSC 3 times 10min

Wash finally with 0.1x SSC 3 time 10min

Wrap the membrane and expose on film in a cassette at -80°C over night

Whole mount in situ hybridization

Preparation

Dissect embryos out in ice-cold PBS

Fix in 4% paraformaldehyde, shaking are 4°C overnight.

Wash with ice-cold PBT (PBS+0.1% Tween20) twice

Embryos could be used directly

Or in alterative:

Pass through a 25%, 50% 75% MeOH in PBT until 100% MeOH

Embryos can be stored in -20°C until use

Rehydrate by taking embryos through this MeOH/PBT series in reverse

The first day

Bleach with 6% H₂O₂ in PBT for 1 hour at room temperature

Wash 3 times each 5 min in PBT at room temperature

Treat embryo with 10µg/ml proteinase K in PBT at room temperature 4 to 8 mins

Wash with 2mg/ml glycine in PBT 2 times each 10min at room temperature

Wash with PBT 3 times each 5 mins

Fix again with 4% paraformaldehyde plus 0.2% Glutaraldehyde in PBT for 20 min at room temperature

Wash again with PBT 3 times 5 min

Rinse with Prehyb (50% Formamide, 5XSSC PH4.5, 1% SDS, 50µg/ml yeast tRNA, 50µg/ml Heparin) at 70°C for 1 hour then add probe into the tube and incubate over night

The second day

Remove the probe and wash 3 times each 30min with prewarmed Solution I (50% Formamide, 5XSSC PH4.5, 1% SDS)

Wash 3 times with TNT (10mM TrisCl PH 7.5, 0.5M NaCl, 0.1% Tween20) at room temperature

Treat with 100µg/ml RNase in TNT for 1h at room temperature

Wash with TNT:Solution II I (50% Formamide, 2XSSC PH4.5, 0.2% SDS)

(1:1) 5 min at room temperature

Wash 3 times each 30 min with Solution II at 65 °C

Wash with MAB (100mM Maleic acid, 150mM NaCl, 2mM levamisole, 0.1% Tween20) 3 times each 5 min

Preblock embryos in 10% sheep serum in MAB/2% blocking reagent for 2 hour at room temperature

Remove the block reagent and add AB mix (anti-Dig Alkaline Phosphatase in MAB/Block with 1% sheep serum) shake at 4°C over night

The third day

Remove the antibody and wash the whole day with MAB

The fourth day

Wash 3 times each 10 mins with NTMT (100mM TrisCl PH 9.5, 50mM MgCl₂, 100mM NaCl, 0.1% Tween20, 2mM Levamisole)

Incubate in BM purple Solution at room temperature until desirable color appears.

Post-fix with 4% paraformaldehyde for 1h at room temperature

RESULTS

Chapter 1

Publication #1: *Emx2* in the developing fissure region

Tianyu Zhao, Nadine Kraemer, Judit Oldekamp, Murat Cankaya, Nora Szabo, Sabine Conrad, Thomas Skutella and Gonzalo Alvarez-Bolado
European Journal of Neuroscience 13: 2895-2907 (2006)

Emx2 in the developing hippocampal fissure region

Tianyu Zhao,¹ Nadine Kraemer,² Judit Oldekamp,^{1,*} Murat Çankaya,^{1,3} Nora Szabó,¹ Sabine Conrad,⁴ Thomas Skutella^{4,†} and Gonzalo Alvarez-Bolado^{1,†}

¹Max Planck Institute of Experimental Endocrinology, 30625 Hannover, Germany

²Neuroscience Research Center, Charité Central Campus, 10117 Berlin, Germany

³Atatürk University, School of Arts and Sciences, Department of Chemistry, 25240 Erzurum, Turkey

⁴Tübingen University School of Medicine, Anatomical Institute, Department Tissue Engineering, 72074 Tübingen, Germany

Keywords: Cajal-Retzius cell, dentate gyrus, *Pax6*, radial glia, reelin

Abstract

Mice deficient in transcription factor gene *Emx2* show developmental alterations in the hippocampal dentate gyrus. *Emx2*, however, is also expressed in the region around the developing hippocampal fissure. The developing fissure contains a radial glial scaffolding, and is surrounded by the outer marginal zone and the dentate marginal zone, which become specifically colonized by neurons and differentiate into stratum lacunosum-moleculare and molecular layer of the dentate, respectively. In this study we show that the *Emx2* mutant lacks the glial scaffolding of the fissure and has an outer marginal zone (precursor of the stratum lacunosum-moleculare), as well as a dentate marginal zone severely reduced in size while most of the *reelin* (*Reln*)-expressing cells that should occupy it fail to be generated. We have also identified a subpopulation of hippocampal *Reln*-expressing cells of the marginal zone, probably born in the hem, expressing a specific combination of markers, and for which *Emx2* is not essentially required. Additionally, we show differential mutant phenotypes of both *Emx2* and *Pax6* in neocortical vs. hippocampal *Reln*-expressing cells, indicating differential development of both subpopulations.

Introduction

Although it is known that the hippocampus of mice deficient in transcription factor *Emx2* lacks the granule cell layer of the dentate gyrus (Pellegrini *et al.*, 1996; Yoshida *et al.*, 1997), defects in other hippocampal subdivisions have to our knowledge been unnoticed. We have reported observations suggesting that the morphogenesis of the hippocampal fissure could also be affected (Oldekamp *et al.*, 2004). The marginal zone in close contact with the developing fissure (outer marginal zone or OMZ) is crucially important for hippocampal development, because it gives rise to a specific layer of the CA (Cornu Ammonis) region (the stratum lacunosum-moleculare) (Soriano *et al.*, 1994). Therefore, investigating its development in the *Emx2* mutant could contribute to the understanding of the still unknown function of this gene. Although in adult brains the hippocampal fissure could be considered ‘a virtual line’ (Sievers *et al.*, 1992), in the embryonic brain it is certainly a real space occupied by specific glial cells and their processes, as well as by blood vessels (Rickmann *et al.*, 1987; Sievers *et al.*, 1992). During development, the region around the hippocampal fissure could be considered as consisting of a central radial glial scaffolding (Rickmann *et al.*, 1987; Sievers *et al.*, 1992) and two apposed marginal zones – the OMZ and the dentate gyrus marginal zone (DMZ). These are surrounded by the inner marginal zone (IMZ). The OMZ, DMZ and IMZ arise as specializations of the

telencephalic marginal zone, and each of them is colonized by specific neuronal populations and differentiates into a peculiar hippocampal layer, respectively, stratum radiatum, stratum lacunosum-moleculare and molecular layer of dentate gyrus (Soriano *et al.*, 1994). Each of these layers has specialized cytoarchitecture, connectivity and functions (Amaral & Witter, 1995). In this work we will use the name ‘developing hippocampal fissure region’ to refer to the OMZ + DMZ. The developing hippocampal fissure region contains abundant *reelin* (*Reln*)-expressing neurons, some of which, like in the neocortical marginal zone, are called Cajal-Retzius cells (Soriano *et al.*, 1994; Soriano & Del Rio, 2005). Here we show that, in the developing *Emx2*^{-/-} hippocampal fissure region, the radial glial scaffolding is absent, the OMZ and DMZ are atrophic and *Reln*-expressing cells are missing, except a specific subpopulation. We have characterized this subpopulation by determining the expression or lack thereof of eight additional marginal zone markers. Finally, we compared the *Emx2*^{-/-} region of the hippocampal fissure with that of *Small eye* mice, lacking transcription factor gene *Pax6* (Hill *et al.*, 1991; Walther & Gruss, 1991), a functional antagonist of *Emx2* in neocortical development (Bishop *et al.*, 2000, 2002; Muzio *et al.*, 2002a,b; Muzio & Mallamaci, 2003). The differential phenotypes of *Emx2* as well as *Pax6* on both subpopulations are evidence of differential development of neocortical vs. fissural *Reln*-expressing cells of the marginal zone.

Correspondence: Dr G. Alvarez-Bolado, as above.

E-mail: gonzalo.alvarez-bolado@mpihaan.mpg.de

*Present address: Max Planck Institute of Psychiatry, Department Molecular Neurogenetic, 80804 Munich, Germany.

†T.S. and G.A.-B. contributed equally to this work.

Received 12 October 2005, revised 1 February 2006, accepted 20 March 2006

Materials and methods

Animals

Emx2^{+/-} female mice of C57Bl6 genetic background (Pellegrini *et al.*, 1996) were mated overnight with *Emx2*^{+/-} males and inspected for vaginal plug at 09.00 h on the following day; noon of this day was

considered embryonic day 0.5 (E0.5). Pregnant females were lightly anaesthetized with isoflurane vapours (IsoFlo-vet from Schering-Plough, New Jersey, USA), then killed by cervical dislocation. All adult animals used in this study were anaesthetized with isoflurane and killed by cervical dislocation. All embryos used were decapitated. Embryos were collected, polymerase chain reaction-genotyped (Savaskan *et al.*, 2002), and further processed. *Small eye* (Pax6-deficient) mutant mice in the C56BL/6J × DBA/2J background were similarly used. Adult animals were always manipulated under light anaesthesia with isoflurane vapors.

Experiments were carried out in accordance with the guidelines of the European Communities Council Directive of 24 November 1986 (86/609/EEC). The study was approved by the Service of Animal Protection of Lower Saxony.

BrdU injections

Pregnant mice from heterozygous crossings were intraperitoneally injected with BrdU (RPN201, Amersham Biosciences, Buckinghamshire, England) (50 µg/g of body weight), at 12.00, 15.00 and 18.00 h (Takahashi *et al.*, 1993) on the appropriate pregnancy date (either at E10.5, E11.5, E12.5, E13.5 or E14.5). Embryos were collected at E12.5 and E14.5 (for E10.5 injections) or E18.5. Reelin-BrdU double-labelling studies were carried out on two *Emx2*^{-/-} and two wild-type brains per injection age.

Immunohistochemistry

Embryos were fixed in 4% formaldehyde, embedded in paraffin and sectioned at 20 µm. Primary antibodies used: anti-nestin MAB353 (which is actually antibody 'Rat-401'; Hockfield & McKay, 1985) 1 : 5 and anti-reelin MAB5366 1 : 250 (both from Chemicon, Temecula, California, USA), anti-BrdU M0744 1 : 100 and anti-glial fibrillary acidic protein (GFAP) Z0334 1 : 1000 (both from Dakocytomation, Glostrup, Denmark), and anti-Ki-67 1 : 20 (BD Biosciences, Erembodegen, Belgium). We used biotinylated second antibodies, extravidin 1 : 100 and diaminobenzidine (both from Sigma, Saint Louis, Missouri, USA), or 'Alexa' fluorescent second antibodies (Molecular Probes, Portland, Oregon, USA). Heat-induced epitope retrieval was carried out in citrate buffer 0.1 M, with the help of a microwave oven. Two homozygous and two wild-type embryos were used per age.

Apoptosis detection (TUNEL)

The Apoptag kit (Chemicon) was used on formaldehyde-fixed, paraffin-embedded samples following the instructions of the manufacturer.

In situ hybridization

In situ detection of mRNAs with digoxigenin-labelled antisense riboprobes was performed on 20-µm cryostat sections, as described (Wilkinson & Nieto, 1993). We added an amplification step (tyramide), resulting in up to 100-fold increase in sensitivity (Adams, 1992; Yang *et al.*, 1999). We used a GenePaint platform (Tecan Group, Maennedorf, Switzerland) so that prehybridization, hybridization, post-hybridization and detection were carried out automatically (Herzig *et al.*, 2001). *In situ* hybridization was carried out on two wild-type and two homozygous brains (*Emx2* or *Pax6*) for every age. For Fig. 10, quantification was carried out by

densitometric analysis of digital photography files with NIH-Image software (in the public domain). We measured average density per surface unit on identical square fields tightly fitting the hippocampal fissure region on four sections of each genotype at E18.5. 'Relative abundance values' were calculated by considering the highest value of each experiment as 100%. All sections compared had been automatically treated for *in situ* hybridization (see above) in the course of the same experiment.

Results

The Emx2^{-/-} hippocampal fissure region lacks radial glial scaffolding

In the *Emx2*^{-/-} dentate gyrus the radial glial marker protein GFAP is very decreased, suggesting alterations of the glial scaffolding (Oldekamp *et al.*, 2004). Here we wanted to investigate in detail the state of the radial glial fibres in the dentate of this mutant. Detection of nestin, an intermediate filament specifically expressed in radial glial cells (Hockfield & McKay, 1985), has been used to label the radial glia in cortex and hippocampus in foetal brains (Super *et al.*, 2000; Alcantara *et al.*, 2006). The anti-nestin antibody showed that in wild-type, the dentate migratory pathway at E18.5 was wide and formed by abundant fibres. Its two portions, radial and tangential, could be easily identified. The tangential portion ran parallel to the pia and abutted the tertiary matrix (Fig. 1A and C). In the mutant, however, the nestin-positive migratory pathway starting in the dentate neuroepithelium was abnormally sparse and short (Fig. 1B). Under high magnification, the mutant showed a thinned out radial pathway (arrows in Fig. 1D) followed by a short stretch that did not run tangentially but ended on the pia (Fig. 1D, arrowheads). Antibody detection of GFAP (another major radial glial marker) together with Ki-67 (a marker of dividing cells) (Gerdes *et al.*, 1983) on wild-type revealed the scaffolding of the fissure (Fig. 2A, asterisk) as well as numerous progenitor cells migrating on GFAP-positive processes (Fig. 2A), as described (Eckenhoff & Rakic, 1984, 1988; Rickmann *et al.*, 1987; Altman & Bayer, 1990a,b). In the mutant, the abortive radial glial fibres (arrow in Fig. 2B) supported the migration of only a few progenitors (arrowheads in Fig. 2B). These results indicate that dentate radial glial fibres are extremely reduced in number and have severely altered morphology in the *Emx2*^{-/-} brain. Subpial migration of astrocyte precursors has a role in the formation of the normally developing fissure (Sievers *et al.*, 1992). Accordingly, in the subpial region of the mutant we were able to observe GFAP- and Ki67-positive cells, although in very small numbers (Fig. 2C).

Emx2 is specifically responsible for the growth of OMZ + DMZ (not IMZ)

Next, we analysed the state of the marginal zones around the developing fissure (Fig. 2D) in the mutant. *Lhx6* is a LIM-homeobox gene (Grigoriou *et al.*, 1998) expressed by a subpopulation of basal ganglia-born cells that migrate tangentially into the cortical marginal zone (Lavdas *et al.*, 1999). In wild-type, *Lhx6*-expressing cells arrived at the hippocampal primordium by E15.5 (not shown). At E18.5, *Lhx6* mRNA was detected in the IMZ, and absent from the hippocampal fissure region (OMZ + DMZ) (Fig. 3A). In the *Emx2* mutant at that age, *Lhx6* mRNA was distributed in the IMZ (Fig. 3B and C). The neocortical marginal zone showed *Lhx6*-expressing cells and could be followed to the point (arrow in Fig. 3C) where it divides into *Lhx6*-

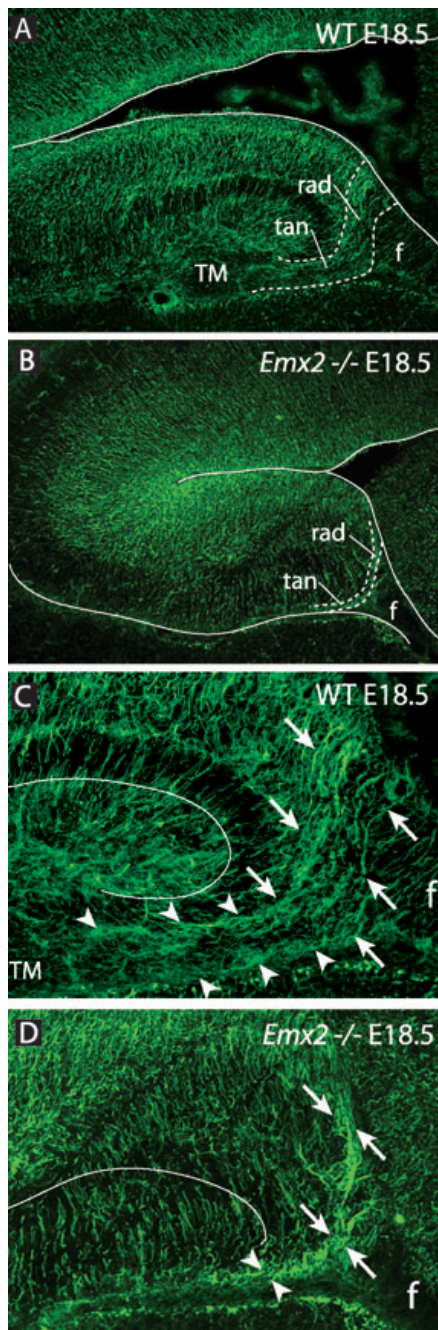


FIG. 1. Abnormal nestin expression in the *Emx2*^{-/-} hippocampus. Anti-nestin antibody labelling on sagittal sections of E18.5 wild-type (A and C) and *Emx2*^{-/-} (B and D) hippocampus. (C and D) High-magnification views of A and B, respectively. (A) Nestin fibres in wild-type hippocampus delineate the radial (rad) and tangential (tan) portions of the pathway (delineated with dotted lines) leading from the dentate neuroepithelium to the tertiary matrix (TM). (B) Nestin fibres in the *Emx2*^{-/-} dentate are sparse and form only very shortened radial (rad) and tangential (tan) pathways (delineated with dotted lines). (C) High-magnification view of (A) showing the radial migration pathway of the dentate (arrows) followed by the tangential pathway (arrowheads); the fimbria (f) shows abundant parallel nestin-positive fibres. (D) High-magnification view of (B) showing the abnormally short and narrow nestin-positive migration pathway in the mutant (arrows, radial portion; arrowheads, tangential portion); the fimbria (f) is almost completely devoid of nestin-positive parallel fibres. A continuous line in (C) and (D) shows the ventral boundary of the CA pyramidal layer.

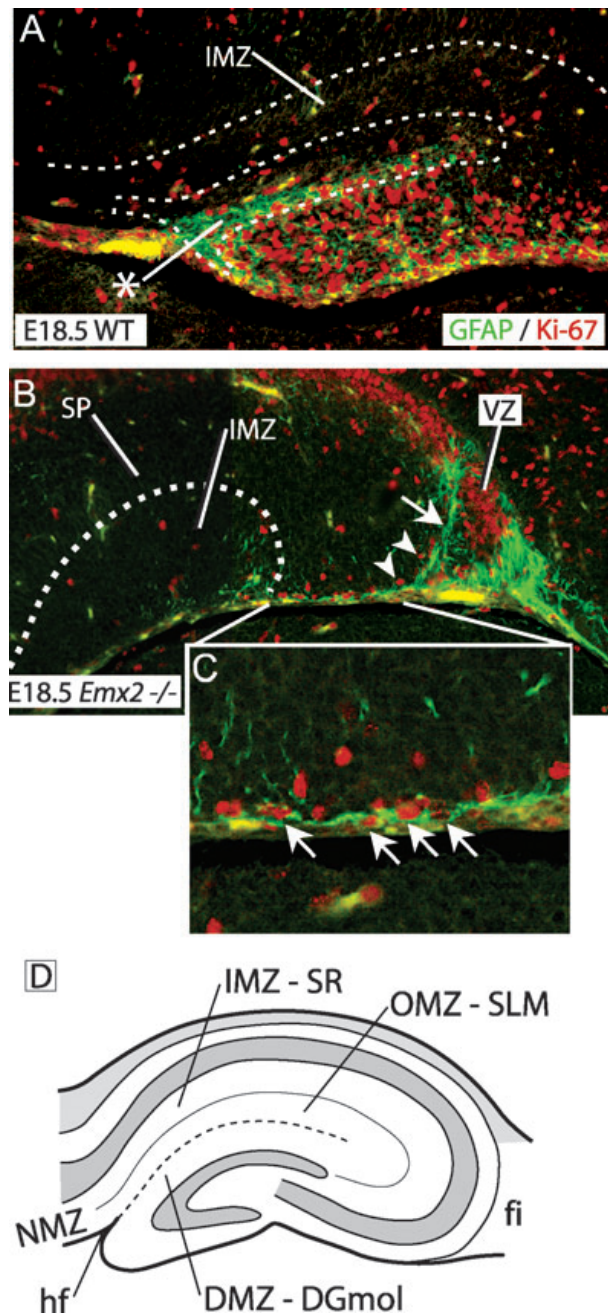


FIG. 2. Abnormal glial fibrillary acidic protein (GFAP) expression in the *Emx2*^{-/-} hippocampus. (A–C) Antibody localization of GFAP (green) and Ki-67 (red) on E18.5 wild-type (A) and *Emx2*^{-/-} (B and C) hippocampus. Asterisk in (A) points at fissure scaffolding. Notice the scarce progenitors (arrowheads) that migrate on the radial glial processes (arrow) of the mutant (B). (C) A magnified portion of B shows some subpial migrating GFAP-positive cells (arrows) in the mutant. (D) Diagram showing the marginal zones around the developing fissure region. Abbreviations: DGmol, molecular layer of dentate gyrus; DMZ, marginal zone of dentate gyrus; fi, fimbria; hf, hippocampal fissure; IMZ, inner marginal zone; NMZ, neocortical marginal zone; OMZ, outer marginal zone; SLM, stratum lacunosum-moleculare; SP, stratum pyramidale; SR, stratum radiatum; VZ, ventricular zone.

expressing IMZ and non-*Lhx6*-expressing OMZ + DMZ. *Lhx6* expression in the mutant, acting as a 'negative staining', defined the mutant OMZ + DMZ as a narrow band of cells between the IMZ

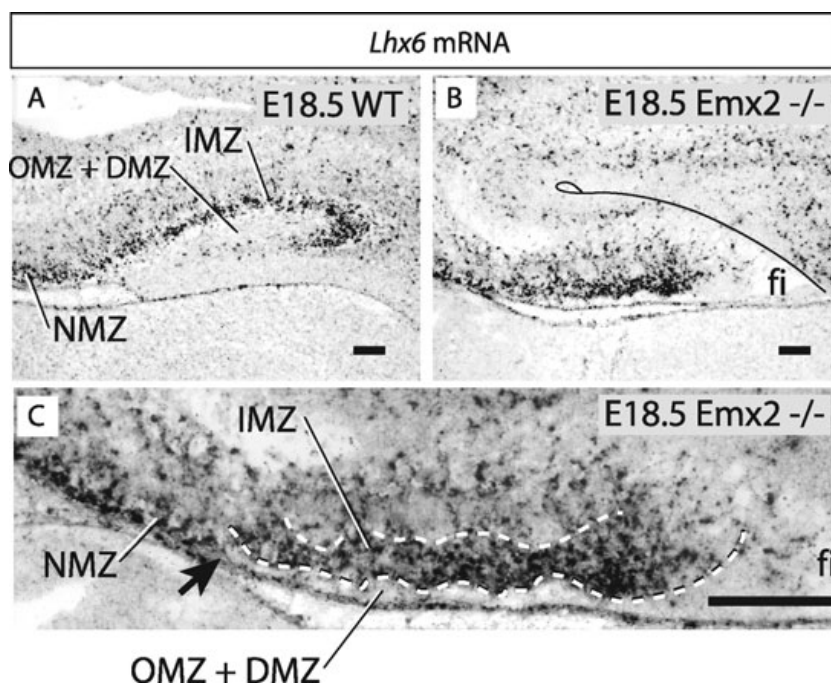


FIG. 3. Atrophic hippocampal fissure region in the *Emx2*^{-/-} hippocampus. (A) By E18.5, *Lhx6*-expressing cells have entered the wild-type hippocampus and distribute along the inner marginal zone (IMZ) but not the outer marginal zone (OMZ). (B) In the E18.5 *Emx2*^{-/-} hippocampus there is *Lhx6* expression in the IMZ. (C) A high-magnification view of (B), which shows that in the E18.5 *Emx2*^{-/-} hippocampus, *Lhx6* expression in the IMZ (between dotted lines) acts as a 'negative staining' of the OMZ + dentate marginal zone (DMZ), which are devoid of *Lhx6* and appear very reduced. Arrow shows the 'entrance' to the hippocampal marginal zone, where NMZ divides into IMZ and OMZ. Abbreviations: fi, fimbria; NMZ, neocortical marginal zone. Scale bars: 100 μ m.

(dorsally) and the pia (ventrally). The separation between both was remarkably well respected in the mutant (Fig. 3C).

These findings indicate that the marginal zones around the *Emx2*^{-/-} hippocampal fissure region are correctly specified and located, and that at least the IMZ is populated by the appropriate cells. However, the mutant OMZ + DMZ are unable to grow to their normal size (they are atrophic).

Reln-expressing cells in the *Emx2*^{-/-} developing hippocampal fissure region

Next we wanted to analyse the cells of the OMZ + DMZ. A very prominent cell group in these layers is the one formed by the *Reln*-expressing cells (Alcantara *et al.*, 1998). We detected characteristically large amounts of *Reln*-expressing cells in wild-type marginal zone (Fig. 4A), while the *Emx2*^{-/-} dentate (Fig. 4B) showed a very decreased number of them, located at the pial border in the presumptive localization of the hippocampal fissure (where the hippocampal primordium slightly folds in). Some *Reln*-expressing cells migrated dorsally into the IMZ, as observed also in wild-type (Fig. 4A and B).

We then analysed the expression of the LIM-homeobox gene *Lhx5*, a marker of the *Reln*-expressing cells of the marginal zone (Yamazaki *et al.*, 2004) expressed in the developing hippocampus (Bertuzzi *et al.*, 1996; Sheng *et al.*, 1997; Hobert & Westphal, 2000). The brains of mice carrying null mutations of *Lhx5* show a hippocampal phenotype similar to that of *Emx2*^{-/-}, with loss of fissure region, dentate gyrus and *Reln*-expressing cells in the marginal zone (Zhao *et al.*, 1999). We detected *Lhx5* mRNA in the wild-type neocortical marginal zone (not shown) and in the hippocampus (Fig. 4C), where abundant *Lhx5* cells were present in the OMZ + DMZ. This pattern was very similar to that

of *Reln*, except that only very few *Lhx5* cells entered the wild-type IMZ (compare Fig. 4A to C). In the mutant, *Lhx5* expression disappeared from the neocortical marginal zone (not shown), but was conserved in the reduced OMZ + DMZ (Fig. 4D). The pattern of *Lhx5* in the mutant (Fig. 4D) was similar to that of *Reln* (Fig. 4B), with the only exception that (as in wild-type) very few *Lhx5*-expressing cells entered the IMZ (Fig. 4C). The results in Figs 3 and 4 show that, at the point where the neocortex meets the hippocampal primordium, the marginal zone divides into two regions (IMZ and OMZ + DMZ), differentially expressing *Lhx6* (the IMZ; Fig. 3A) or *Lhx5* (the OMZ + DMZ; Fig. 4C). The OMZ + DMZ are atrophic in the *Emx2* mutant, and their *Reln*-expressing cells are severely decreased in number.

Reln-expressing cells of the fissure region express *Emx2*

Emx2 is a known marker of *Reln*-expressing cells of the marginal zone (Hevner *et al.*, 2003). The fact that a certain number of *Lhx5*- and *Reln*-expressing cells remain in the *Emx2*-deficient fissure region could indicate the existence of some non-*Emx2*-expressing *Reln*-expressing cells in this area. In order to investigate this possibility, we used *in situ* hybridization for *Emx2* mRNA with a probe against the 3' UTR of *Emx2* mRNA and were able to detect *Emx2* transcriptional activation (*Emx2*-TA) in homozygous brains. At E18.5, *Emx2* was strongly expressed in all portions of the dentate gyrus, and also in the OMZ, but not in the IMZ (Fig. 4E). In the mutant, *Emx2*-TA could be detected in a small group of cells (Fig. 4F) similar in size and position to that expressing *Reln* and *Lhx5*. A few labelled cells were inside the IMZ (arrowheads in Fig. 4F).

The labelling of *Reln*, *Lhx5* and *Emx2* expression in the mutant (Fig. 4) provides a 'positive staining' of the OMZ + DMZ matching the 'negative staining' of these layers imparted by IMZ-marker *Lhx6*

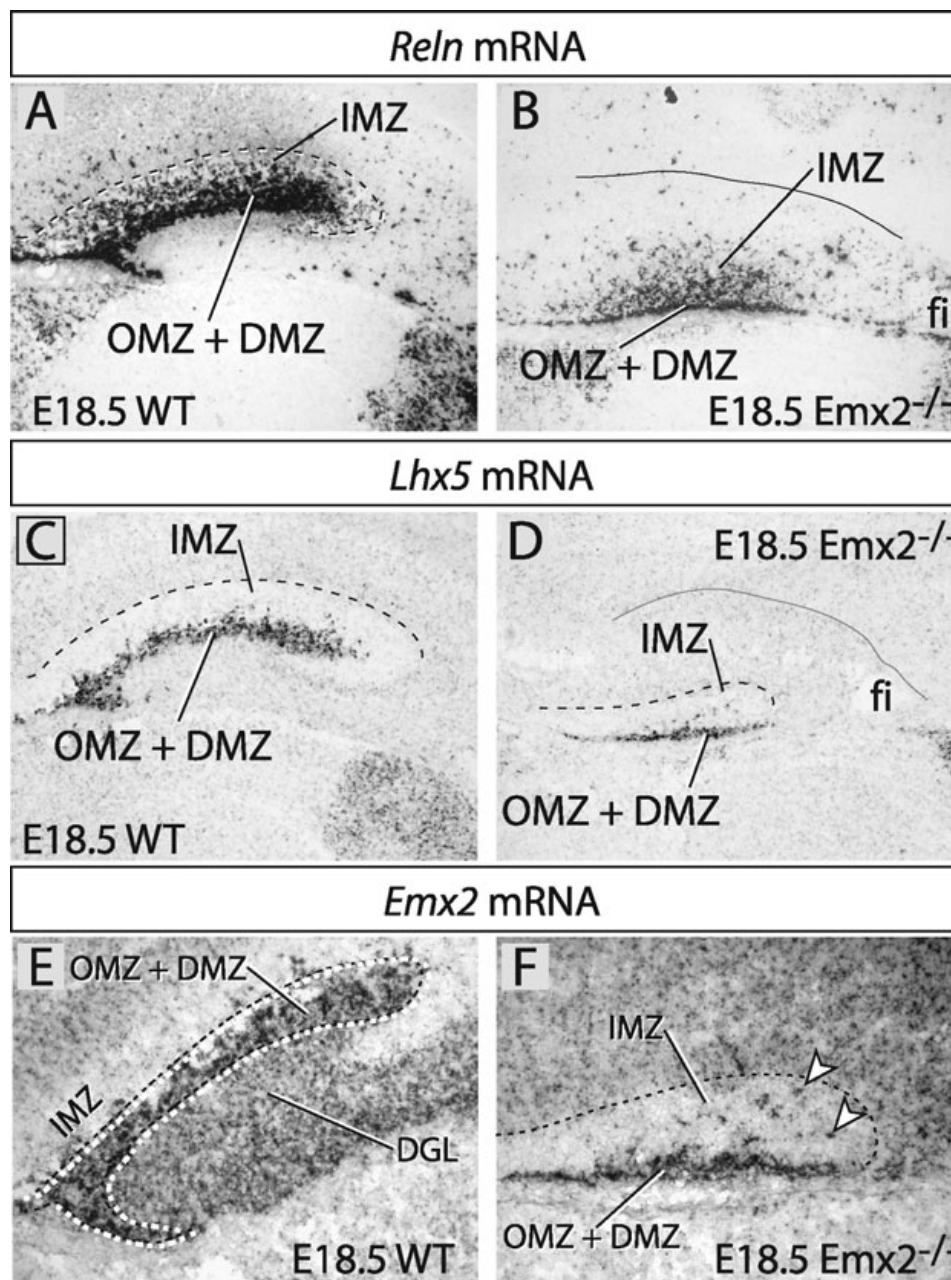


FIG. 4. *Reln*-expressing cells are very reduced in *Emx2*^{-/-} hippocampus. (A and B) *reelin* mRNA in wild-type (A) and *Emx2*^{-/-} (B) E18.5 hippocampus. (C and D) *Lhx5* mRNA in wild-type (C) and *Emx2*^{-/-} (D) E18.5 hippocampus. (E, F) *Emx2* mRNA in wild-type (E) and *Emx2*^{-/-} (F) E18.5 hippocampus. Abbreviations: DGL, dentate granular layer; DMZ, dentate marginal zone; fi, fimbria; IMZ, inner marginal zone; OMZ, outer marginal zone.

(Fig. 3). Furthermore, our data indicate that the few *Reln*-expressing cells of the mutant hippocampal fissure region do express *Emx2* (i.e. show *Emx2*-TA) and that, however, they do not need the *Emx2* protein to be produced, correctly localized and express at least some of their specific markers.

Further characterization of the *Reln*-expressing cells in the *Emx2*^{-/-} fissure

At this point we wanted to characterize further this population of *Reln*-expressing cells of the fissure region, which express *Emx2* but, as

opposed to the rest, do not need this gene as an essential requirement. Subdivision of marginal zone cells in the neocortex has been tried by different methods, each with advantages and disadvantages (see Discussion). We decided to use *in situ* hybridization to characterize the expression by these cells of five additional marker genes known to be expressed in the marginal zone. Calretinin (*Calb2*) is a gene expressed by all reelin-expressing cells of the marginal zone from early on in development (Takiguchi-Hayashi *et al.*, 2004); expression of this gene can be used for instance to identify Cajal-Retzius cells in reeler mutants, which do not express reelin (Coulin *et al.*, 2001). We found abundant *Calb2* mRNA in the wild-type fissure (Fig. 5A) as expected, and we could ascertain expression of *Calb2* also in the mutant fissure

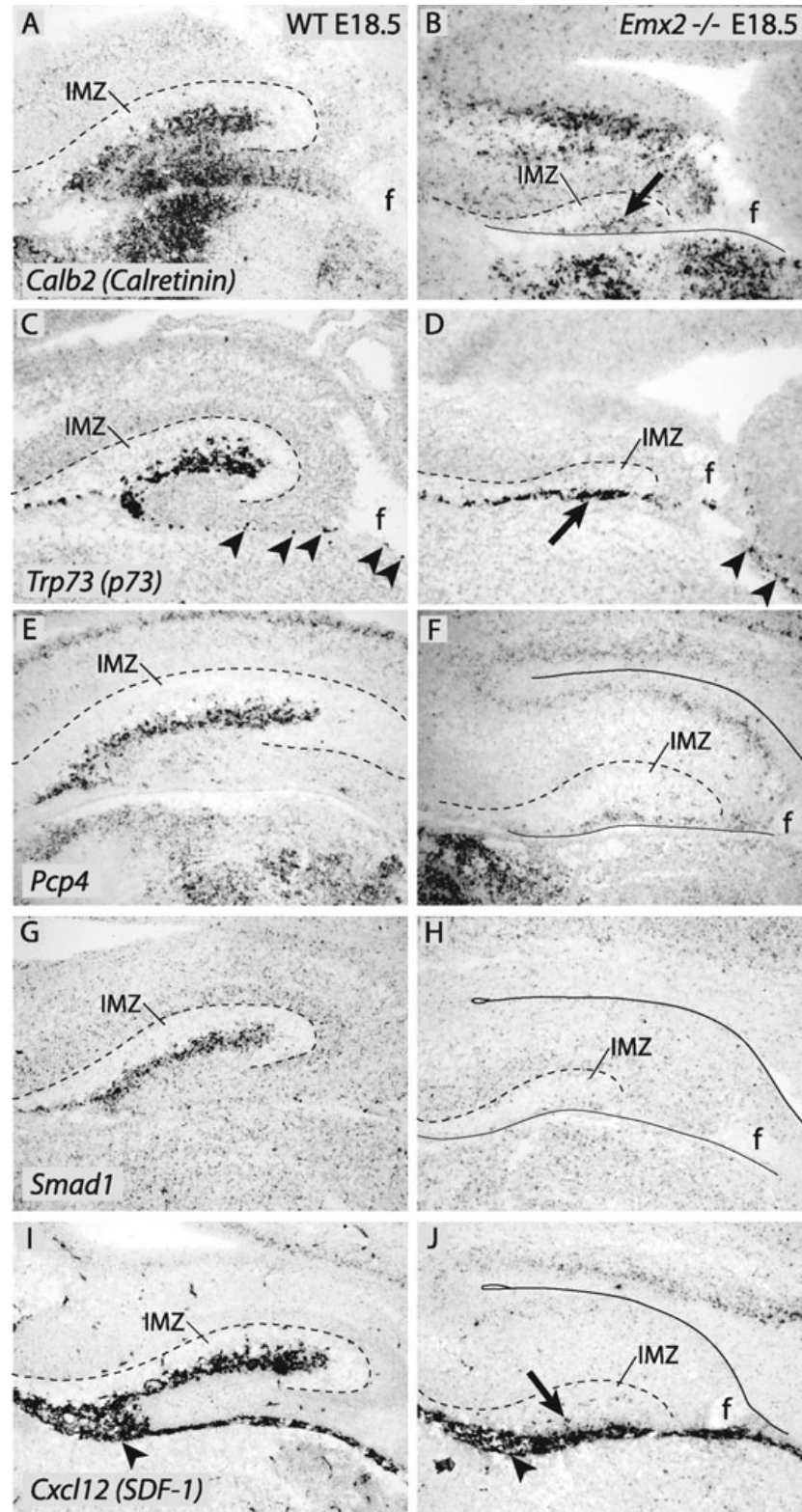


FIG. 5. Genetic marker expression in the *Emx2*^{-/-} hippocampus. (A and B) Detection of *Calretinin* (*Calb2*) mRNA in the E18.5 wild-type (A) and *Emx2*^{-/-} (B) hippocampus. Arrow in (B) points at remnants of *Calb2* expression in the mutant. (C and D) Detection of *Trp73* mRNA in the E18.5 wild-type (C) and *Emx2*^{-/-} (D) hippocampus. Arrowheads in C and D show a trail of *Trp73* expression from the cortico-choroid region to the hippocampus. Arrow in D shows *Trp73* expression in the mutant hippocampal marginal zone. (E and F) Detection of *Pcp4* mRNA in the E18.5 wild-type (E) and *Emx2*^{-/-} (F) hippocampus. (G and H) Detection of *Smad1* mRNA in the E18.5 wild-type (G) and *Emx2*^{-/-} (H) hippocampus. (I and J) Detection of *Calretinin* (*Calb2*) mRNA in the E18.5 wild-type (I) and *Emx2*^{-/-} (J) hippocampus. Arrowhead in I and J points at pial expression. Arrow in J shows a few labelled cells in the mutant. Abbreviations: f, fimbria; IMZ, inner marginal zone.

(Fig. 5B), consistently in a pattern similar but not exactly matching that of *Reln*, *Lhx5* or *Emx2* (Fig. 4B, D and F). Expression of transcription factor gene *p73* (*Trp73*) together with *Reln* is considered characteristic of Cajal-Retzius cells (Abraham *et al.*, 2004). We found strong expression of *p73/Trp73* in the wild-type hippocampal marginal zone as expected (Fig. 5C). A trail of labelled cells could be seen apparently originated in the former 'hem' region (cortico-choroidal border) (arrowheads in Fig. 5C). In the mutant, labelled cells formed a compact, strongly expressing group (arrow in Fig. 5D), with the same position and appearance as markers *Reln*, *Lhx5* and *Emx2* (Fig. 4B, D and F). A trail of cells from the former 'hem' could be followed also in the mutant (arrowheads in Fig. 5D). *Pcp4* encodes a modulator of calcium-signalling cascades (Slemmon *et al.*, 1996) and has been recently identified as a marker of *Reln*-expressing cells of the marginal zone (Yamazaki *et al.*, 2004). We detected it in the wild-type developing fissure region (Fig. 5E), but it was virtually absent or only very weakly expressed from the mutant hippocampal marginal zone (Fig. 5F). *Smad1* is a transcription factor gene essential for the transduction of the BMP signalling pathway (Angley *et al.*, 2003) as well as a key player in angiogenesis (Goumans *et al.*, 2003). It has also been identified as a marker of *Reln*-expressing cells of the marginal zone (Yamazaki *et al.*, 2004). Accordingly, we found *Smad1* expression in the wild-type foetal fissure (Fig. 5G), but completely absent in the mutant (Fig. 5H). Finally, *Cxcl12/SDF-1* is a cytokine gene essential in hippocampal development (Bagri *et al.*, 2002) and in angiogenesis (Mirshahi *et al.*, 2000; Salcedo & Oppenheim, 2003), and a marker of *Reln*-expressing cells of the marginal zone (Yamazaki *et al.*, 2004). We detected its expression in the fissure region of the wild-type foetus (Fig. 5I), as well as in pial structures of vascular appearance (arrowhead in Fig. 5I). It was still present in the mutant pia (arrowhead in Fig. 5J), but absent from the hippocampus except for a few isolated cells (arrow in Fig. 5J).

Our results at this point suggested that the *Reln*-expressing cells remaining in the mutant hippocampus belong to a group normally expressing *Reln*, *Lhx5*, *Emx2* and *p73/Trp73*, but not *Smad1*, *Pcp4* or *Cxcl12/SDF-1*. Additionally, the presence of *p73/Trp73* expression in the mutant, as well as in a trail of cells starting in the cortico-choroidal region, suggests that the 'survivor' cells are originated in the hem.

Development of Reln-expressing cells in the Emx2^{-/-} hippocampal marginal zone

We then analysed the development of *Reln*-expressing cells of the marginal zone in the hippocampal region with anti-reelin antibodies in wild-type and mutant (Fig. 6). The distribution of *Reln*-expressing cells was similar in wild-type and mutant at E12.5. The hippocampal primordium showed only a few *Reln*-expressing cells, situated on the pial side (arrows in Fig. 6A and B). At E14.5, *Reln*-expressing cells were more abundant in the hippocampal primordium of the wild-type than in that of the mutant (Fig. 6C and D). In the mutant, the medial neocortical primordium (asterisk in Fig. 6D) showed at this age an abnormal and transient accumulation of neocortical *Reln*-expressing cells, which has been described (Mallamaci *et al.*, 2000). We did not observe this transient accumulation in the hippocampus, which is the object of our study (separated from the neocortex by a dotted line in Fig. 6D). Later on, as in wild-type the hippocampal fissure started to develop, numerous *Reln*-expressing cells began to accumulate in it (Fig. 6E). In the mutant, however, only a few labelled cells were found. They were aligned in a row in the place where the pallium folds in slightly, indicating the region of the abortive hippocampal fissure (Fig. 6F). This region showed in the mutant already at this age the same appearance as later at E18.5 (compare Fig. 6F with Fig. 4B). In order to quantify the reduction in

Reln-expressing cells in the mutant, we counted the *Reln*-expressing cells in the hippocampal marginal zone in all sections of two wild-type and two mutant brains at E18.5. The average number of reelin-expressing cells in the mutant hippocampal marginal zone at this age was less than 20% of the number in the wild-type (Fig. 6G). Thus, in the *Emx2^{-/-}* hippocampal primordium, *Reln*-expressing cells are sparse from early on, gradually becoming rarer except for one group that forms in the vestige of the hippocampal fissure.

Reln-expressing cells of the hippocampal fissure are born at normal ages but in reduced numbers in the Emx2^{-/-} mutant

Our data at this point showed a loss of *Reln*-expressing cells in the *Emx2* mutant marginal zone (except for a specific subpopulation). We asked what could be the mechanism of that loss. Cells can be reduced in number either because of reduced proliferation, or because of increased cell death, or because they migrate away and are not to be found where usually expected. In the neocortex of the *Emx2^{-/-}* mutant there is a loss of *Reln*-expressing cells (Mallamaci *et al.*, 2000; Shinozaki *et al.*, 2002), although the mechanism is still not clear. In addition, and contrary to the situation in the hippocampus, the mutant neocortex does not show any specific remnant population of *Reln*-expressing cells.

First of all, to investigate hippocampal *Reln*-expressing cell proliferation in wild-type and mutant, we injected pregnant mice with BrdU at different gestation ages. Previous work (Takiguchi-Hayashi *et al.*, 2004) has shown that *Reln*-expressing cells of the marginal zone of the cortex are born from E10.5 to E13.5, so we injected BrdU at these ages. We then used antibodies to detect reelin (cytoplasm) and BrdU (nucleus) in *Reln*-expressing cells of this region at E18.5 (Fig. 7A and B). At E18.5, both wild-type and *Emx2^{-/-}* hippocampal fissure region (Fig. 7C) contain *Reln*-expressing cells born at E11.5, E12.5 and E13.5. Surprisingly, counting cells at E18.5 we did not find *Reln*-expressing cells labelled at E10.5. No *Reln*-expressing cells of this region were born at E14.5 (not shown). However, consistent with our previous results (Fig. 6), the total number of *Reln*-expressing cells in the mutant fissure region was much smaller than in wild-type. One *Emx2*-expressing neuroepithelial region characterized as a major source of *Reln*-expressing cells and immediately adjacent to the hippocampus is the cortical hem (Shinozaki *et al.*, 2002; Takiguchi-Hayashi *et al.*, 2004). Therefore, our result suggests that reduced production of *Reln*-expressing cells by the *Emx2^{-/-}* cortical hem is the main cause of the absence of these cells in the mutant hippocampal primordium. This points to a possible answer to the question of the mechanism of disappearance of *Reln*-expressing cells in the *Emx2^{-/-}* hippocampus.

An early-born/early-transient population of Reln-expressing cells in wild-type and Emx2^{-/-} hippocampus

Surprisingly, and in contrast to reliable reports establishing that cortical *Reln*-expressing cells of the marginal zone originate from E10.5 on (Alcantara *et al.*, 1998; Mallamaci *et al.*, 2000; Takiguchi-Hayashi *et al.*, 2004), we did not observe in the E18.5 fissure any *Reln*-expressing cells born at E10.5 either in wild-type or in mutant. Besides, the mutant neocortex at E11.5 shows abundant *Reln*-expressing neurons (Mallamaci *et al.*, 2000), presumably born on E10.5. Therefore, to examine this question in more detail, we injected pregnant mice with BrdU at E10.5, and collected the embryos at E12.5 and E14.5. Double-labelled cells (BrdU and reelin) were consistently detected in the fissure region of wild-type and mutant at E12.5 (Fig. 8A and B) but not at E14.5 (Fig. 8C and D). Counting BrdU-

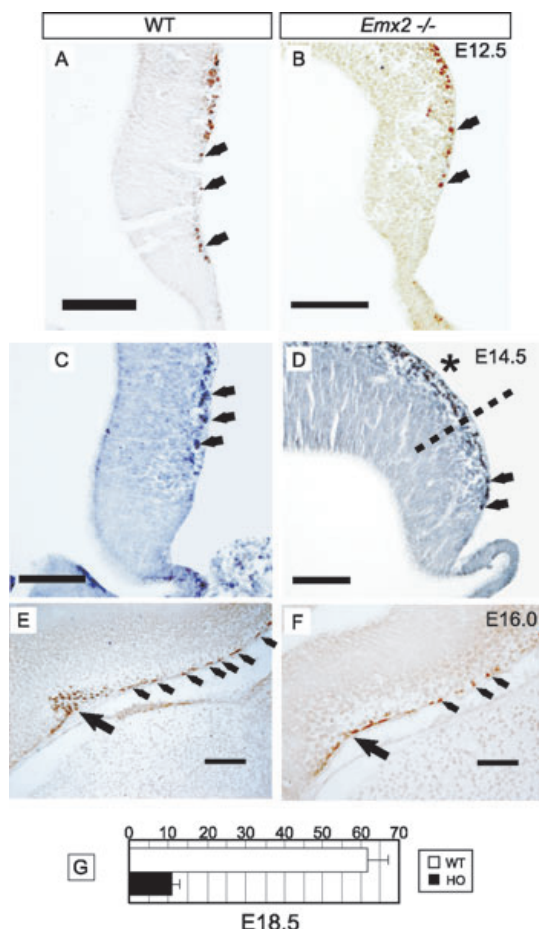


FIG. 6. Development of *Reln*-expressing cells in *Emx2*^{-/-} hippocampus. Antibody localization of reelin in the wild-type (A, C and E) and *Emx2*^{-/-} (B, D and F) medial cortex at E12.5 (A and B), E14.5 (C and D) and E16.0 (E and F). (A and B) At E12.5 both wild-type (A) and mutant (B) show scattered *Reln*-expressing cells (arrows) in presumptive hippocampus. (C and D) At E14.5, the wild-type hippocampus (C) shows a row of *Reln*-expressing cells (arrows), while the mutant hippocampus (D) shows some scattered *Reln*-expressing cells (arrows); an accumulation of *Reln*-expressing cells can be seen in the neocortex (asterisk), separated from hippocampal primordium (no accumulation) by a dotted line. (E and F) At E16.0, the wild-type hippocampus (E) shows a row of *Reln*-expressing cells (small arrows) and a larger group accumulating in the developing fissure region (large arrow). In the mutant hippocampus (F) *Reln*-expressing cells are less and scattered (small arrows), they do not accumulate in the fissure region (large arrow) and remain close to the pial border. (G) Reelin cells of the fissure per section of E18.5 brain in wild-type (white column) or *Emx2*^{-/-} (black column).

labelled neurons at E12.5 and E14.5 in the whole pallial marginal zone (presumptive cortex and hippocampus) revealed a decrease of about 60% both in wild-type and in mutant (Fig. 8E), which can be attributed to 'dilution' in a rapidly growing brain. The decrease was, however, particularly dramatic for *Reln*-expressing cells, which almost completely disappear from the telencephalic marginal zone by E14.5 (Fig. 8F). Finally, we were not able to find any E10.5-born *Reln*-expressing cell in the hippocampal anlage at E14.5, either in wild-type or in mutant (Fig. 8G). We concluded that, in the wild-type as well as in the *Emx2*^{-/-} brain there is an early-born and early-transient population of *Reln*-expressing cells. This population is born at about E10.5 and not detectable any more at E14.5, either because the cells migrate elsewhere or downregulate reelin expression (see Discussion).

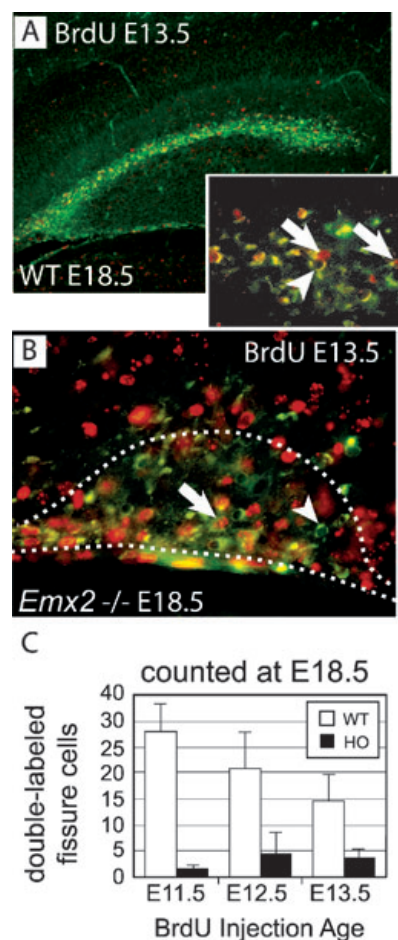


FIG. 7. Late-born *Reln*-expressing cells in the *Emx2*^{-/-} hippocampus. (A and B) Examples of antibody detection of BrdU and reelin in hippocampal fissure region at E18.5 in wild-type (A) and *Emx2*^{-/-} (B). (A) The entire fissure region, inset shows a high-magnification detail. Numerous cells are labelled green for reelin (arrowheads), of which some show red nuclei for BrdU (arrows). (C) Number of BrdU-reelin double-labelled cells in the hippocampal fissure per section (both sides) found at E18.5 after BrdU injections either at E11.5, E12.5, E13.5 or E14.5. White bars, wild type; black bars, *Emx2*^{-/-}. Error bars: standard deviation.

No increase in cell death in the *Emx2*^{-/-} marginal zone

In search of a mechanism for the reduced amount of *Reln*-expressing cells in the hippocampal marginal zone of this mutant, we reasoned that increased cell death could concur with reduced production to decrease the number of *Reln*-expressing cells. To investigate this, we performed TUNEL staining on wild-type and mutant brain sections at different ages (Fig. 9). Our analysis at E14.5, E16.5 (Fig. 9A–D) (and also at E12.5 and E18.5, not shown) revealed only a small number of cell death profiles in wild-type and mutant hippocampi, and failed to reveal any difference between the two genotypes. This is consistent with decreased production as the main cause of the *Reln*-expressing cell deficiency in the *Emx2*^{-/-} hippocampal fissure region.

Both Pax6 and Emx2 are needed in the development of the *Reln*-expressing cells of the hippocampal fissure region

The previous results suggested that the formation of the hippocampal fissure region and its colonization by *Reln*-expressing cells are specific

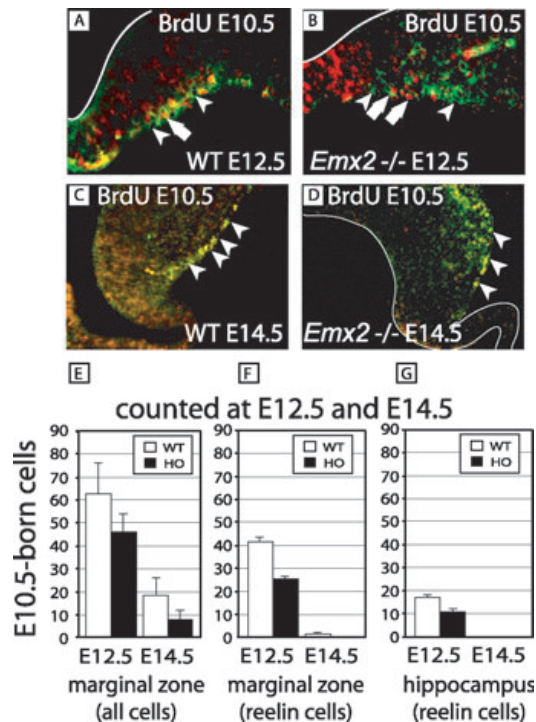


FIG. 8. Early-born *Reln*-expressing cells in the *Emx2*^{-/-} hippocampus. (A and B) Antibody detection of BrdU (injected E10.5) and reelin in hippocampus at E12.5 in wild-type (A) and *Emx2*^{-/-} (B). Numerous cells are labelled green for reelin (arrowheads), of which some show red nuclei for BrdU (arrows). (C and D) Antibody detection of BrdU (injected on E10.5) and reelin in hippocampus at E14.5 in wild-type (C) and *Emx2*^{-/-} (D). Of the cells labelled green for reelin (arrowheads), none shows red nuclei for BrdU (injected on E10.5). (E–G) Number of E10.5-born cells (detected by BrdU antibody) per histological section (both sides) at E12.5 and E14.5 in wild-type and *Emx2*^{-/-}. (E) Countings including the total marginal zone or in the case of E12.5 the outer border of the pallium. (F) Only double-labelled cells have been counted. (G) Only double-labelled cells of the hippocampal primordium have been counted. Error bars: standard deviation.

regionalization processes regulated by *Emx2*. *Pax6* is a key developmental transcription factor that functionally antagonizes *Emx2* in pallial regionalization (Bishop *et al.*, 2000, 2002). To investigate a possible role of *Pax6* in the formation of the hippocampal fissure we looked at the distribution of *Reln*-expressing cells in the fissure region of foetuses carrying the *Pax6* null allele *Small eye (Sey)* (Hill *et al.*, 1991). The *Pax6*^{Sey/Sey} neocortical marginal zone is thicker than in wild-type, containing abnormally large numbers of *Reln*-expressing cells (Stoykova *et al.*, 2003). We confirmed an increase in *Reln*-expressing cells in the *Pax6*^{Sey/Sey} neocortical marginal zone (Fig. 10A and B). However, we detected a decrease in *Reln*-expressing cells in *Pax6*^{Sey/Sey} hippocampal fissure region as compared with wild-type (compare Fig. 10C and D). The enlarged *Pax6*^{Sey/Sey} neocortical marginal zone (arrowheads in Fig. 10D) consistently showed a narrowing in the immediate vicinity of the hippocampal fissure region (arrow in Fig. 10D), i.e. a region of transition where the neocortical marginal zone kept its normal width in the *Pax6*^{Sey/Sey} mutant. Intriguingly, the reduction in *Reln*-expressing cells in *Pax6*^{Sey/Sey} was limited to the OMZ, while the DMZ seemed unaffected (Fig. 10E and F). We confirmed the reduction in *Reln* mRNA in the *Pax6*^{Sey/Sey} OMZ by measuring the intensity of *Reln* expression in neocortical marginal zone and OMZ in wild-type and mutant (Fig. 10G and H). These results show that *Pax6* has differential and opposed effects on

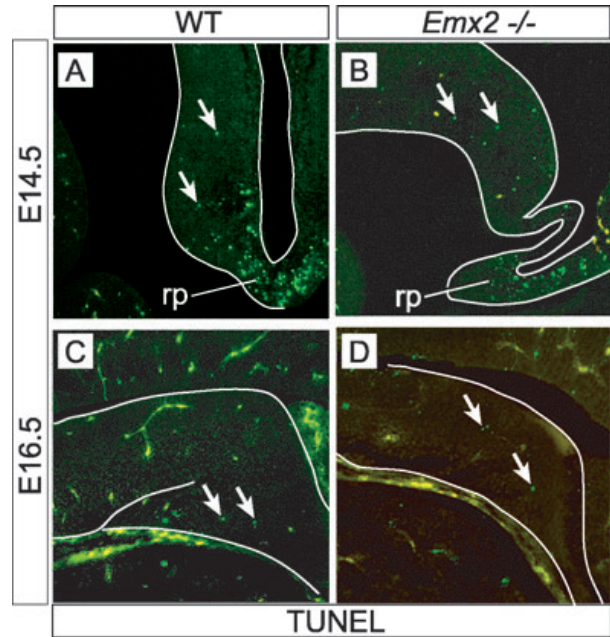


FIG. 9. Cell death in *Emx2*^{-/-} hippocampus is unchanged. TUNEL-stained sections of wild-type (A and C) and *Emx2*^{-/-} (B and D) hippocampal area at E14.5 (A and B) and E16.5 (C and D). Cell death rates are low in both wild-type and mutant at every age investigated. The telencephalic roof (rp in A and B) shows a characteristically large number of dying cells. Arrows show some typical cell death images.

neocortical vs. fissural *Reln*-expressing cells, and that both *Emx2* and *Pax6* are needed in order to obtain an OMZ of normal size and with its full complement of *Reln*-expressing cells.

Discussion

We have investigated for the first time developmental anomalies of the *Emx2*-deficient hippocampal marginal layers. In particular, we have focused on the involvement of *Emx2* in hippocampal folding (fissure formation) and in the development of the OMZ (precursor of the stratum lacunosum-moleculare). Our findings include: (i) *Emx2* is essential for the development of the radial glial scaffolding of the hippocampal fissure; (ii) the marginal zone immediately apposed to the *Emx2*^{-/-} hippocampal fissure region (OMZ) is atrophic and reduced to a vestigial size – it can be said that the mutant lacks a stratum lacunosum-moleculare; (iii) the *Reln*-expressing cells that should occupy the OMZ (as well as the DMZ) are severely decreased in the *Emx2*^{-/-} because of decreased production; (iv) we have identified a subpopulation of hippocampal *Reln*-expressing cells, probably born in the hem, expressing a specific combination of markers, and for which *Emx2* is not essentially required; (v) finally, the function of *Emx2* and *Pax6* in the formation of the presumptive stratum lacunosum-moleculare is similar, although they functionally antagonize each other in the neocortical marginal zone.

Finally, all the structures affected by the *Emx2*^{-/-} phenotypes described here (fissure region *Reln*-expressing cells, dentate neuroepithelium, neocortical hem) express *Emx2* (the present work and Oldekamp *et al.*, 2004), suggesting that these mutant phenotypes could be to a large degree cell autonomous.

Glial scaffolding and *Reln*-expressing cells in the fissure region

Radial glial cells of the dentate ventricular layer give rise to two systems of processes (Rickmann *et al.*, 1987; Sievers *et al.*, 1992; Yuasa, 2001).

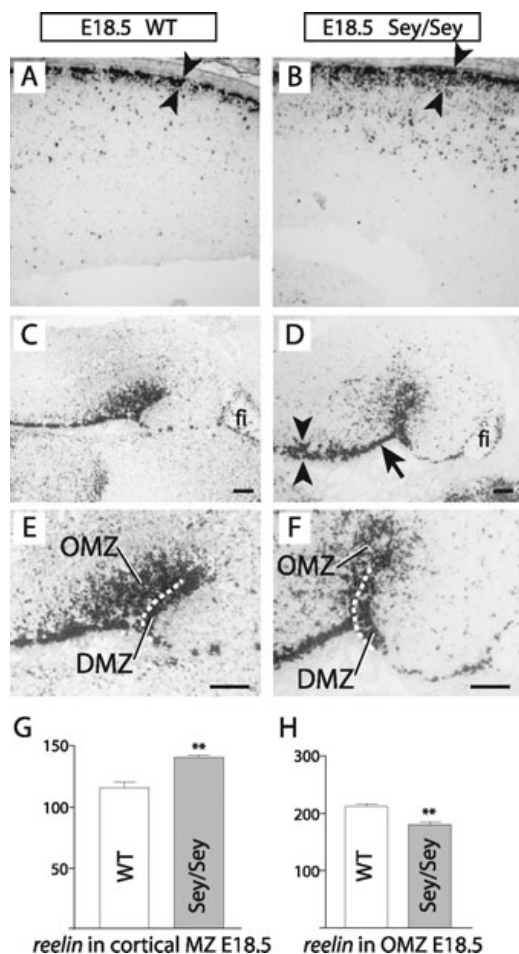


FIG. 10. Both *Emx2* and *Pax6* are involved in outer marginal zone (OMZ) formation. (A and B) *In situ* hybridization for *Reln* mRNA on E18.5 wild-type (A) and *Pax6*^{Sey/Sey} mutant (B) neocortex. Pairs of arrowheads show the marginal zone thicker in (B) (*Pax6*^{Sey/Sey}) than in (A) (wild-type). (C) *Reln* expression on a sagittal section of E18.5 wild-type brain. (D) *Reln* expression on a sagittal section of E18.5 *Pax6*^{Sey/Sey} brain. Arrowheads show the thickened neocortical marginal zone in the mutant. Arrow points at narrow band of mutant marginal zone immediately adjacent to hippocampal fissure. (E) High-magnification detail of C with a dotted line separating the labelled dentate marginal zone (DMZ, right side) from the labelled OMZ (left side). (F) High-magnification detail of D showing that the reduction in *Reln* expression is mostly on the OMZ side. (G and H) Densitometric analysis of *Reln* expression intensity confirms significant increase in *Pax6*^{Sey/Sey} neocortical marginal zone (G) and significant decrease in *Pax6*^{Sey/Sey} hippocampal fissure (H). Error bars: standard deviation. Abbreviations: fi, fimbria; WT, wild type. Scale bars: 100 μ m. ***P* < 0.01.

One of them follows a straight course immediately adjacent to the fimbria towards the pial side (radial migratory pathway, Fig. 1A and C) and then turns in the direction of the future dentate granular layer (tangential migratory pathway, Fig. 1A and C). The second system of processes courses towards the developing fissure, whose scaffolding it forms. As a third glial component, GFAP-expressing astrocytes able to divide migrate tangentially under the pia, enter the developing fissure and spread along its scaffolding forming two–three cell rows (Sievers *et al.*, 1992). Our results here show that in the *Emx2*^{-/-} dentate the various glial components are differentially altered. The long radial glial processes forming the scaffolding of the fissure are completely missing (Fig. 2A and B); the processes forming the migratory pathway are present but dramatically reduced in number and length (Figs 1B and D,

and 2B). Finally, some of the subpial migratory-dividing astrocytes are present in the mutant, although they fail to form or colonize the fissure region, remaining close to the pia (Fig. 2C).

Our analysis emphasizes the existence of trophic interactions between the different elements of the fissure region. Although *reeler* mutants are able to develop a hippocampal fissure (Hamburgh, 1963), reelin is essential for the proper development of the radial glia of cortex and cerebellum (Soriano *et al.*, 1997; Hartfuss *et al.*, 2003). Because *Emx2* is expressed both by *Reln*-expressing cells and dentate gyrus neuroepithelium, probably in the *Emx2*^{-/-} brain both elements are altered, and later these defects compound.

Reln-expressing cells and hippocampal folding

The OMZ + DMZ of the *Emx2*^{-/-} is extremely reduced in size (Fig. 3). Neither reports by other authors nor our own observations (not shown) have found comparable atrophy in the *Emx2*^{-/-} neocortical marginal zone. This suggests specific trophic effects of *Reln*-expressing cells on the growth of the marginal zones around the fissure region. Because the proper growth of these marginal zones would lead to hippocampal folding, maybe this observation can be put in the context of other mutant phenotypes, including at least the *Lhx5* (Zhao *et al.*, 1999) and *p73* mutants (Meyer *et al.*, 2004), characterized by a decrease in *Reln*-expressing cells together with failure of hippocampal folding. This adds to growing evidence of a role of the *Reln*-expressing cells in cortical folding involving probably other molecules than reelin (Alcantara *et al.*, 2006).

A specific subpopulation of *Reln*-expressing cells in the hippocampus does not require *Emx2*

The marginal zone contains a morphologically heterogeneous population of *Reln*-expressing cells, which has been subclassified by using the Golgi method (Marin-Padilla, 1998) and by means of antibodies against calbindin and calretinin (reviewed in Soriano & Del Rio, 2005). More recently, detection of gene expression by *in situ* hybridization has revealed that different groups of *Reln*-expressing cells of the marginal zone express specific markers, perhaps revealing their different points of origin in the telencephalon (Lavdas *et al.*, 1999; Hevner *et al.*, 2003; Yamazaki *et al.*, 2004). We have used nine marker genes known to be expressed at least in some reelin-expressing cells of the marginal zone in order to characterize the unique group of *Reln*-expressing cells, located in the hippocampus, which are preserved in the *Emx2* mutant. These cells express indeed *Reln* and *Emx2*, as well as *Lhx5* and *p73/Trp73* (Figs 3–5). A few of them seem to weakly express *Calb2* (*calretinin*) and *Cxcl12/SDF-1* (Fig. 5B and J). Finally, none of them expresses *Pcp4* or *Smad1* (Fig. 5F and H). *Cxcr4* encodes the receptor for cytokine *Cxcl12* and is also expressed in the hippocampal fissure region (Lu *et al.*, 2002; Yamazaki *et al.*, 2004). However, our data (not shown) indicate that it is also expressed abundantly in the IMZ, making it difficult to assess in the mutant hippocampus. Expression of *Reln* and *p73/Trp73* in the marginal zone has been considered a defining trait of Cajal-Retzius cells (Meyer *et al.*, 2002, 2004; Abraham *et al.*, 2004); therefore, at least some of the ‘survivor’ cells in the mutant hippocampus can be considered Cajal-Retzius cells.

Mechanism of disappearance of *Reln*-expressing cells of the hippocampal fissure in the *Emx2* mutant

Several mechanisms can contribute to the absence of a certain cell population from the place where it would usually be expected: reduced

proliferation, increased cell death, abnormal migration or a combination thereof. According to our results, it would seem that the decrease in *Reln*-expressing cells in the *Emx2* mutant hippocampal marginal zone is due to a decrease in production. Most, if not all, *Reln*-expressing cells of the marginal zone of the medial cortex (including hippocampus) originate in the immediately adjacent cortical hem (Shinozaki *et al.*, 2002; Takiguchi-Hayashi *et al.*, 2004; Yoshida *et al.*, 2006), an *Emx2*-expressing neuroepithelial area severely decreased in size in the *Emx2*^{-/-} brain (Shinozaki *et al.*, 2002, 2004). Accordingly, the distribution of reelin in the developing hippocampus (Fig. 6) plus the birthdate labellings (Fig. 7) point to important reduction in *Reln*-expressing cell production in *Emx2*^{-/-} brains. The second important mechanism that could contribute to a reduction in the number of *Reln*-expressing cells could be increased cell death. Our results with TUNEL labelling (Fig. 9) on wild-type brains agree with reports that most developmental cell death in wild-type rodent pallium is postnatal (Ferrer *et al.*, 1990; Gould *et al.*, 1991), and that prenatal cell death in the wild-type marginal zone is negligible (Thomaidou *et al.*, 1997). In addition, we found no change in the *Emx2*^{-/-} brain, excluding cell death as the mechanism of disappearance. Finally, the *Reln*-expressing cells of the *Emx2* mutant could migrate away from the telencephalon to some other place. However, the *Emx2*^{-/-} cortex has demonstrable tangential migration defects (Shinozaki *et al.*, 2002), which precludes migration as an explanation.

An early transient population of Reln-expressing cells in the wild-type pallium

Cortical *Reln*-expressing cells are transient and disappear early postnatally (Derer & Derer, 1990). Unexpectedly, we have found in wild-type as well as *Emx2*^{-/-} brains a population of *Reln*-expressing cells born at E10.5 that seems to disappear within the next 3 days (Fig. 8). Analysis of *Reln*-expressing cells in the *Emx2*^{-/-} neocortex (Mallamaci *et al.*, 2000) detected a discrepancy between actual histological detection of reelin cells in the mutant at E11.5, and BrdU + reelin cell counting at E19.5 showing that cells born at E12.5 were absent. Mallamaci *et al.* (2000) solved this discrepancy by postulating the existence of two different populations of *Reln*-expressing cells: an early transient, not dependent on *Emx2*; and a late population, still detectable around birth, dependent on *Emx2*. In the present study, we have actually injected BrdU much earlier, at E10.5 and at E11.5, and we have in the hippocampus (and in the neocortex) data that permit to confirm this conjecture. Their disappearance cannot be in this case attributed to reduced proliferation, and our data with the TUNEL method preclude cell death as the mechanism. Intriguingly, these early transient *Reln*-expressing cells are able to migrate and invade the pallial marginal zone also in the *Emx2*^{-/-} brain, suggesting that, unlike the ones born later, they do not depend on *Emx2* for tangential migration. Accordingly, their disappearance could mean that they migrate away from the pallium; alternatively, they could downregulate *Reln* as part of their normal differentiation.

Different development of neocortical vs. hippocampal Reln-expressing cells

In *Emx2*^{-/-} brains, the neocortical marginal zone keeps its normal thickness and neocortical *Reln*-expressing cells transiently accumulate and then completely disappear (Mallamaci *et al.*, 2000). Our results, however, indicate that the region around the developing mutant fissure region shows atrophic marginal zones but no abnormal accumulation or complete disappearance of *Reln*-expressing cells. This differential

phenotype is consistent with reported differential survival of neocortical and hippocampal *Reln*-expressing cells (Del Rio *et al.*, 1996; Drakew *et al.*, 1998; Abraham & Meyer, 2003). Here we show that *Pax6*^{Sev/Sev} has differential effects on neocortical and hippocampal *Reln*-expressing cells of the marginal zone as well (very increased in neocortex vs. slightly reduced in the fissure). Intriguingly, while *Pax6* and *Emx2* are antagonists in neocortical regionalization (Bishop *et al.*, 2000, 2002; Shinozaki *et al.*, 2002) and have opposite effects on neocortical *Reln*-expressing cells of the marginal zone (Stoykova *et al.*, 2003), in the developing hippocampal fissure both mutations translate into a reduced number of *Reln*-expressing cells (although the role of *Pax6* is less dramatic and seems restricted to the OMZ, not DMZ). Hippocampal and neocortical marginal zone *Reln*-expressing cells have differential, specialized roles in the formation of layer-specific hippocampal connections (Del Rio *et al.*, 1997) and in neocortical organization (Alcantara *et al.*, 2006), respectively. Our results indicate that, in keeping with this functional diversity, the *Reln*-expressing cells found in the neocortex and hippocampus show differential developmental processes.

Acknowledgements

Dr Thomas Theil (Anatomical Institute, Tuebingen, Germany) commented on the manuscript. Dr Xunlei Zhou (Max Planck Institute, Hannover, Germany) helped with genotyping. This work was supported by the Max Planck Society.

Abbreviations

CA, Cornu Ammonis, Ammon's horn; DMZ, dentate marginal zone; GFAP, glial fibrillary acidic protein; IMZ, inner marginal zone; OMZ, outer marginal zone; TA, transcriptional activation.

References

- Abraham, H. & Meyer, G. (2003) Reelin-expressing neurons in the postnatal and adult human hippocampal formation. *Hippocampus*, **13**, 715–727.
- Abraham, H., Perez-Garcia, C.G. & Meyer, G. (2004) p73 and reelin in Cajal-Retzius cells of the developing human hippocampal formation. *Cereb. Cortex*, **14**, 484–495.
- Adams, J.C. (1992) Biotin amplification of biotin and horseradish peroxidase signals in histochemical stains. *J. Histochem. Cytochem.*, **40**, 1457–1463.
- Alcantara, S., Pozas, E., Ibanez, C.F. & Soriano, E. (2006) BDNF-modulated spatial organization of Cajal-Retzius and GABAergic neurons in the marginal zone plays a role in the development of cortical organization. *Cereb. Cortex*, **16**, 487–499.
- Alcantara, S., Ruiz, M., D'Arcangelo, G., Ezan, F., de Lecea, L., Curran, T., Sotelo, C. & Soriano, E. (1998) Regional and cellular patterns of reelin mRNA expression in the forebrain of the developing and adult mouse. *J. Neurosci.*, **18**, 7779–7799.
- Altman, J. & Bayer, S.A. (1990a) Mosaic organization of the hippocampal neuroepithelium and the multiple germinal sources of dentate granule cells. *J. Comp. Neurol.*, **301**, 325–342.
- Altman, J. & Bayer, S.A. (1990b) Migration and distribution of two populations of hippocampal granule cell precursors during the perinatal and postnatal periods. *J. Comp. Neurol.*, **301**, 365–381.
- Amaral, D.G. & Witter, M.P. (1995) Hippocampal formation. In Paxinos, G. (Ed.), *The Rat Nervous System*, 2nd Edn. Academic Press, San Diego, pp. 443–493.
- Angley, C., Kumar, M., Dinsio, K.J., Hall, A.K. & Siegel, R.E. (2003) Signaling by bone morphogenetic proteins and Smad1 modulates the postnatal differentiation of cerebellar cells. *J. Neurosci.*, **23**, 260–268.
- Bagri, A., Gurney, T., He, X., Zou, Y.R., Littman, D.R., Tessier-Lavigne, M. & Pleasure, S.J. (2002) The chemokine SDF1 regulates migration of dentate granule cells. *Development*, **129**, 4249–4260.
- Bertuzzi, S., Sheng, H.Z., Copeland, N.G., Gilbert, D.J., Jenkins, N.A., Taira, M., Dawid, I.B. & Westphal, H. (1996) Molecular cloning, structure, and chromosomal localization of the mouse LIM/homeobox gene *Lhx5*. *Genomics*, **36**, 234–239.

- Bishop, K.M., Goudreau, G. & O'Leary, D.D. (2000) Regulation of area identity in the mammalian neocortex by Emx2 and Pax6. *Science*, **288**, 344–349.
- Bishop, K.M., Rubenstein, J.L. & O'Leary, D.D. (2002) Distinct actions of Emx1, Emx2, and Pax6 in regulating the specification of areas in the developing neocortex. *J. Neurosci.*, **22**, 7627–7638.
- Coulin, C., Drakew, A., Frotscher, M. & Deller, T. (2001) Stereological estimates of total neuron numbers in the hippocampus of adult reeler mutant mice: evidence for an increased survival of Cajal-Retzius cells. *J. Comp. Neurol.*, **439**, 19–31.
- Del Rio, J.A., Heimrich, B., Borrell, V., Forster, E., Drakew, A., Alcantara, S., Nakajima, K., Miyata, T., Ogawa, M., Mikoshiba, K., Derer, P., Frotscher, M. & Soriano, E. (1997) A role for Cajal-Retzius cells and reelin in the development of hippocampal connections. *Nature*, **385**, 70–74.
- Del Rio, J.A., Heimrich, B., Super, H., Borrell, V., Frotscher, M. & Soriano, E. (1996) Differential survival of Cajal-Retzius cells in organotypic cultures of hippocampus and neocortex. *J. Neurosci.*, **16**, 6896–6907.
- Derer, P. & Derer, M. (1990) Cajal-Retzius cell ontogenesis and death in mouse brain visualized with horseradish peroxidase and electron microscopy. *Neuroscience*, **36**, 839–856.
- Drakew, A., Frotscher, M., Deller, T., Ogawa, M. & Heimrich, B. (1998) Developmental distribution of a reeler gene-related antigen in the rat hippocampal formation visualized by CR-50 immunocytochemistry. *Neuroscience*, **82**, 1079–1086.
- Eckenhoff, M.F. & Rakic, P. (1984) Radial organization of the hippocampal dentate gyrus: a Golgi, ultrastructural, and immunocytochemical analysis in the developing rhesus monkey. *J. Comp. Neurol.*, **223**, 1–21.
- Eckenhoff, M.F. & Rakic, P. (1988) Nature and fate of proliferative cells in the hippocampal dentate gyrus during the life span of the rhesus monkey. *J. Neurosci.*, **8**, 2729–2747.
- Ferrer, I., Bernet, E., Soriano, E., del Rio, T. & Fonseca, M. (1990) Naturally occurring cell death in the cerebral cortex of the rat and removal of dead cells by transitory phagocytes. *Neuroscience*, **39**, 451–458.
- Gerdes, J., Schwab, U., Lemke, H. & Stein, H. (1983) Production of a mouse monoclonal antibody reactive with a human nuclear antigen associated with cell proliferation. *Int. J. Cancer*, **31**, 13–20.
- Gould, E., Woolley, C.S. & McEwen, B.S. (1991) Naturally occurring cell death in the developing dentate gyrus of the rat. *J. Comp. Neurol.*, **304**, 408–418.
- Goumans, M.J., Lebrin, F. & Valdimarsdottir, G. (2003) Controlling the angiogenic switch: a balance between two distinct TGF- β receptor signaling pathways. *Trends Cardiovasc. Med.*, **13**, 301–307.
- Grigoriou, M., Tucker, A.S., Sharpe, P.T. & Pachnis, V. (1998) Expression and regulation of Lhx6 and Lhx7, a novel subfamily of LIM homeodomain encoding genes, suggests a role in mammalian head development. *Development*, **125**, 2063–2074.
- Hamburger, M. (1963) Analysis of the postnatal developmental effects of 'Reeler', a neurological mutation in mice. A study in developmental genetics. *Dev. Biol.*, **19**, 165–185.
- Hartfuss, E., Forster, E., Bock, H.H., Hack, M.A., LePrince, P., Luque, J.M., Herz, J., Frotscher, M. & Gotz, M. (2003) Reelin signaling directly affects radial glia morphology and biochemical maturation. *Development*, **130**, 4597–4609.
- Herzig, U., Cadenas, C., Sieckmann, F., Sierralta, W., Thaller, C., Visel, A. & Eichele, G. (2001) Development of high-throughput tools to unravel the complexity of gene expression patterns in the mammalian brain. *Novartis Found. Symp.*, **239**, 129–146; Discussion 146–159.
- Hevner, R.F., Neogi, T., Englund, C., Daza, R.A. & Fink, A. (2003) Cajal-Retzius cells in the mouse: transcription factors, neurotransmitters, and birthdays suggest a pallial origin. *Brain Res. Dev. Brain Res.*, **141**, 39–53.
- Hill, R.E., Favor, J., Hogan, B.L., Ton, C.C., Saunders, G.F., Hanson, I.M., Prosser, J., Jordan, T., Hastie, N.D. & van Heyningen, V. (1991) Mouse small eye results from mutations in a paired-like homeobox-containing gene. *Nature*, **354**, 522–525.
- Hobert, O. & Westphal, H. (2000) Functions of LIM-homeobox genes. *Trends Genet.*, **16**, 75–83.
- Hockfield, S. & McKay, R.D. (1985) Identification of major cell classes in the developing mammalian nervous system. *J. Neurosci.*, **5**, 3310–3328.
- Lavdas, A.A., Grigoriou, M., Pachnis, V. & Parnavelas, J.G. (1999) The medial ganglionic eminence gives rise to a population of early neurons in the developing cerebral cortex. *J. Neurosci.*, **19**, 7881–7888.
- Lu, M., Grove, E.A. & Miller, R.J. (2002) Abnormal development of the hippocampal dentate gyrus in mice lacking the CXCR4 chemokine receptor. *Proc. Natl Acad. Sci. USA*, **99**, 7090–7095.
- Mallamaci, A., Mercurio, S., Muzio, L., Cecchi, C., Pardini, C.L., Gruss, P. & Boncinelli, E. (2000) The lack of Emx2 causes impairment of Reelin signaling and defects of neuronal migration in the developing cerebral cortex. *J. Neurosci.*, **20**, 1109–1118.
- Marin-Padilla, M. (1998) Cajal-Retzius cells and the development of the neocortex. *Trends Neurosci.*, **21**, 64–71.
- Meyer, G., Cabrera Socorro, A., Perez Garcia, C.G., Martinez Millan, L., Walker, N. & Caput, D. (2004) Developmental roles of p73 in Cajal-Retzius cells and cortical patterning. *J. Neurosci.*, **24**, 9878–9887.
- Meyer, G., Perez-Garcia, C.G., Abraham, H. & Caput, D. (2002) Expression of p73 and Reelin in the developing human cortex. *J. Neurosci.*, **22**, 4973–4986.
- Mirshahi, F., Pourtau, J., Li, H., Muraine, M., Trochon, V., Legrand, E., Vannier, J., Soria, J., Vasse, M. & Soria, C. (2000) SDF-1 activity on microvascular endothelial cells: consequences on angiogenesis in vitro and in vivo models. *Thromb. Res.*, **99**, 587–594.
- Muzio, L., DiBenedetto, B., Stoykova, A., Boncinelli, E., Gruss, P. & Mallamaci, A. (2002a) Emx2 and Pax6 control regionalization of the pre-neurogenic cortical primordium. *Cereb. Cortex*, **12**, 129–139.
- Muzio, L., DiBenedetto, B., Stoykova, A., Boncinelli, E., Gruss, P. & Mallamaci, A. (2002b) Conversion of cerebral cortex into basal ganglia in Emx2(-/-) Pax6(Sey/Sey) double-mutant mice. *Nat. Neurosci.*, **5**, 737–745.
- Muzio, L. & Mallamaci, A. (2003) Emx1, emx2 and pax6 in specification, regionalization and arealization of the cerebral cortex. *Cereb. Cortex*, **13**, 641–647.
- Oldekamp, J., Kraemer, N., Alvarez-Bolado, G. & Skutella, T. (2004) bHLH gene expression in the Emx2-deficient dentate gyrus reveals defective granule cells and absence of migrating precursors. *Cereb. Cortex*, **14**, 1045–1058.
- Pellegrini, M., Mansouri, A., Simeone, A., Boncinelli, E. & Gruss, P. (1996) Dentate gyrus formation requires Emx2. *Development*, **122**, 3893–3898.
- Rickmann, M., Amaral, D.G. & Cowan, W.M. (1987) Organization of radial glial cells during the development of the rat dentate gyrus. *J. Comp. Neurol.*, **264**, 449–479.
- Salcedo, R. & Oppenheim, J.J. (2003) Role of chemokines in angiogenesis: CXCL12/SDF-1 and CXCR4 interaction, a key regulator of endothelial cell responses. *Microcirculation*, **10**, 359–370.
- Savaskan, N.E., Alvarez-Bolado, G., Glumm, R., Nitsch, R., Skutella, T. & Heimrich, B. (2002) Impaired postnatal development of hippocampal neurons and axon projections in the Emx2(-/-) mutants. *J. Neurochem.*, **83**, 1196–1207.
- Sheng, H.Z., Bertuzzi, S., Chiang, C., Shawlot, W., Taira, M., Dawid, I. & Westphal, H. (1997) Expression of murine Lhx5 suggests a role in specifying the forebrain. *Dev. Dyn.*, **208**, 266–277.
- Shinozaki, K., Miyagi, T., Yoshida, M., Miyata, T., Ogawa, M., Aizawa, S. & Suda, Y. (2002) Absence of Cajal-Retzius cells and subplate neurons associated with defects of tangential cell migration from ganglionic eminence in Emx1/2 double mutant cerebral cortex. *Development*, **129**, 3479–3492.
- Shinozaki, K., Yoshida, M., Nakamura, M., Aizawa, S. & Suda, Y. (2004) Emx1 and Emx2 cooperate in initial phase of archipallium development. *Mech. Dev.*, **121**, 475–489.
- Sievers, J., Hartmann, D., Pehlemann, F.W. & Berry, M. (1992) Development of astroglial cells in the proliferative matrices, the granule cell layer, and the hippocampal fissure of the hamster dentate gyrus. *J. Comp. Neurol.*, **320**, 1–32.
- Slemmon, J.R., Morgan, J.I., Fullerton, S.M., Danho, W., Hilbush, B.S. & Wengenack, T.M. (1996) Camstatins are peptide antagonists of calmodulin based upon a conserved structural motif in PEP-19, neurogranin, and neuromodulin. *J. Biol. Chem.*, **271**, 15911–15917.
- Soriano, E., Alvarado-Mallart, R.M., Dumesnil, N., Del Rio, J.A. & Sotelo, C. (1997) Cajal-Retzius cells regulate the radial glia phenotype in the adult and developing cerebellum and alter granule cell migration. *Neuron*, **18**, 563–577.
- Soriano, E. & Del Rio, J.A. (2005) The cells of cajal-retzius: still a mystery one century after. *Neuron*, **46**, 389–394.
- Soriano, E., Del Rio, J.A., Martinez, A. & Super, H. (1994) Organization of the embryonic and early postnatal murine hippocampus. I. Immunocytochemical characterization of neuronal populations in the subplate and marginal zone. *J. Comp. Neurol.*, **342**, 571–595.
- Stoykova, A., Hatano, O., Gruss, P. & Gotz, M. (2003) Increase in reelin-positive cells in the marginal zone of Pax6 mutant mouse cortex. *Cereb. Cortex*, **13**, 560–571.
- Super, H., Del Rio, J.A., Martinez, A., Perez-Sust, P. & Soriano, E. (2000) Disruption of neuronal migration and radial glia in the developing cerebral cortex following ablation of Cajal-Retzius cells. *Cereb. Cortex*, **10**, 602–613.

- Takahashi, T., Nowakowski, R.S. & Caviness, V.S. Jr (1993) Cell cycle parameters and patterns of nuclear movement in the neocortical proliferative zone of the fetal mouse. *J. Neurosci.*, **13**, 820–833.
- Takiguchi-Hayashi, K., Sekiguchi, M., Ashigaki, S., Takamatsu, M., Hasegawa, H., Suzuki-Migishima, R., Yokoyama, M., Nakanishi, S. & Tanabe, Y. (2004) Generation of reelin-positive marginal zone cells from the caudomedial wall of telencephalic vesicles. *J. Neurosci.*, **24**, 2286–2295.
- Thomaidou, D., Mione, M.C., Cavanagh, J.F. & Parnavelas, J.G. (1997) Apoptosis and its relation to the cell cycle in the developing cerebral cortex. *J. Neurosci.*, **17**, 1075–1085.
- Walther, C. & Gruss, P. (1991) Pax-6, a murine paired box gene, is expressed in the developing CNS. *Development*, **113**, 1435–1449.
- Wilkinson, D.G. & Nieto, M.A. (1993) Detection of messenger RNA by in situ hybridization to tissue sections and whole mounts. *Meth. Enzymol.*, **225**, 361–373.
- Yamazaki, H., Sekiguchi, M., Takamatsu, M., Tanabe, Y. & Nakanishi, S. (2004) Distinct ontogenic and regional expressions of newly identified Cajal-Retzius cell-specific genes during neocorticalogenesis. *Proc. Natl Acad. Sci. USA*, **101**, 14509–14514.
- Yang, H., Wanner, I.B., Roper, S.D. & Chaudhari, N. (1999) An optimized method for in situ hybridization with signal amplification that allows the detection of rare mRNAs. *J. Histochem. Cytochem.*, **47**, 431–446.
- Yoshida, M., Assimacopoulos, S., Jones, K.R. & Grove, E.A. (2006) Massive loss of Cajal-Retzius cells does not disrupt neocortical layer order. *Development*, **133**, 537–545.
- Yoshida, M., Suda, Y., Matsuo, I., Miyamoto, N., Takeda, N., Kuratani, S. & Aizawa, S. (1997) Emx1 and Emx2 functions in development of dorsal telencephalon. *Development*, **124**, 101–111.
- Yuasa, S. (2001) Development of astrocytes in the mouse hippocampus as tracked by tenascin-C gene expression. *Arch. Histol. Cytol.*, **64**, 149–158.
- Zhao, Y., Sheng, H.Z., Amini, R., Grinberg, A., Lee, E., Huang, S., Taira, M. & Westphal, H. (1999) Control of hippocampal morphogenesis and neuronal differentiation by the LIM homeobox gene Lhx5. *Science*, **284**, 1155–1158.

Author's contribution - Emx2 in developing fissure

Maintain the mouse lines used in paper and harvest the appropriate embryos at certain stage. Processing tissues into blocks and cut the block into ready to use sections.

All the immunohistochemistry work

All the Brdu injection /detection and Tunnel assay

Most of the Cell counting (except Figure 10) and part of ISH work (Figure2 A-D)

Chapter 2

Publication #2: Cajal-Retzius neurons that produce Vascular Endothelial Growth Factor have a role in cortical Angiogenesis

Thoma Skutella, Sbanine Conrad, **Tianyu Zhao**, Murat Cankaya, Ana Matinez-Herhandez and Gonzalo Alvarez-Bolado. Submitted

Cajal-Retzius neurons that produce Vascular Endothelial Growth Factor have a Role in Cortical Angiogenesis

Thomas Skutella*^{1§}, Sabine Conrad^{1§}, Tianyu Zhao^{2§}, Murat Çankaya³, Ana Martínez-Hernández² and Gonzalo Alvarez-Bolado*²

¹ Dept. Tissue Engineering, Institute of Anatomy, University of Tübingen, D-72074 Germany; ² Dept.

Genes and Behavior, Max Planck Institute, Göttingen, D-37077 Germany; ³ Dept. Chemistry, Faculty of

Arts and Science, Atatürk University, 25240 Erzurum, Turkey; §equal contribution; *corresponding authors

Corresponding authors: Thomas Skutella, Institute of Anatomy, Österbergstrasse 3, Tübingen, 72074

Germany, Phone: +49 7071 29 73429 / Fax 29 5124 tskutella@anatom.uni-tuebingen.de; Gonzalo

Alvarez-Bolado, Max Planck Institut bpC, Am Fassberg 11, Göttingen, 37077 Germany, Phone: +49 551

201 2713 / Fax 201 2705 gonzalo.alvarez-bolado@mpibpc.mpg.de

Abbreviations: CPL, cortical plate; C-R, Cajal-Retzius; HUVEC, human umbilical vein endothelial cells; MZ, marginal zone; PVP, perineural vascular plexus; Vegfa, vascular endothelial growth factor A

Cajal-Retzius (C-R) cells are a transient population of neurons residing in the outermost layer of the developing cerebral cortex, and have essential roles in cortical development and evolution. The mechanism by which these special neurons influence cortical development is currently the object of active research, but the details are still elusive. Vegfa is a cytokine promoting the sprouting of blood vessels into developing organs. Here we report the ability of C-R neurons to produce and secrete Vegfa. We also found C-R cells to be able to direct migration of vascular endothelial cells *in vitro*. Since C-R cells are in close vicinity to the meninges and their rich vascular network, our results suggested an involvement of C-R cells in the sprouting of new blood vessels into the developing cortex. We analyzed neocortical vascularization of mouse embryos mutant for transcription factor gene *Emx2*, which are deficient in C-R cells since early in development. The upper neocortical layers of these mutants showed a dramatically reduced blood vessel supply. Our findings indicate that at least part of the influence of C-R cells on cortical histogenesis and evolution could be exerted through modulation of cortical angiogenesis.

The outermost layer of the developing cerebral cortex is the marginal zone (MZ). It contains a transient population of neurons, the C-R cells, which die perinatally (1). C-R cells are thought to play an essential role in the development and evolution of the cortical layers as well as in some human neurological disorders (2-4). C-R cells characteristically express *Reelin* (*Reln*), whose product is essential for cortical development (5-7). The exact details of the mechanism of action of C-R cells on the developing cortex are still being elucidated (2, 8, 9). C-R cells reside in close vicinity to the pia, a layer of connective tissue apposed to the brain. Around the pia there is a rich vascular network, the “perineural vascular plexus” (PVP). Around mid-gestation, PVP sprouts enter the cortical primordium and grow, branch, remodel and differentiate to create the intricate vascular networks of the cortex (10), a process called angiogenesis (11). Some pia and PVP cells express *Vegfa* (vascular endothelial growth factor A), which encodes a cytokine essential for vascular development (12). *Vegfa* exists in several isoforms able to induce proliferation, differentiation and survival of endothelial cells, as well as directed blood vessel sprouting and endothelial cell migration (13). *Vegfa* is expressed by the deepest layer of the cortical primordium, the neuroepithelium, at the time of entrance of vascular sprouts from the PVP (14). Here we show that C-R cells produce and secrete *Vegfa*, and that they are able to induce directed migration of vascular endothelial cells. These results predict deficient vascularization in a developing cortex with reduced Cajal-Retzius cells. Accordingly, we analyzed vascularization in the cortex of the *Emx2* mutant, which loses

its C-R cells abnormally early (15, 16). In accordance with our hypothesis, this cortex has dramatically reduced vascularization in the upper cortical layers. Our results indicate a novel function for C-R neurons in cortical angiogenesis, and show that these cells are at the crossroads between vascular and neuronal development in the cortex.

RESULTS

***Vegfa*-expressing cells in the cortical MZ.** We found *Vegfa* expression in a discrete cell population in the MZ (arrowheads in Fig. 1A, B, C). The *Vegfa*-expressing cells expressed *Reln* as well (Fig. 1D, E, F). Comparison of the position of these cells to that of known pial (*Vegfr2*, *Decorin*, *Cxcl12*) and MZ (*Cxcr4*) marker gene expression indicated that the *Vegfa*- and *Reln*-expressing cells were true MZ cells rather than deeply seated pia/PVP cells, (Fig. 1G, H, I, J, K) and therefore could be classified as C-R cells.

Vegfa is expressed in several isoforms which have differential properties depending on their solubility. *Vegfa* isoforms 188 and 164 are able to bind to the extracellular matrix forming spatially restricted cues that induce formation of branches in newly formed vessels; isoforms 120 and 115 are soluble and favor increase in diameter over branching (17, 18). Therefore, we counted *Vegfa*-expressing cells in the MZ of wildtype and *Emx2*^{-/-} mice at E12.5, E15.5 and E18.5 using isoform-specific probes as well as a probe for the 3'UTR common to all of them. *Vegfa* expression in the wildtype MZ was negligible at E12.5 (not shown). At E15.5 and E18.5 (Fig. 1L, white bars) both number of *Vegfa*-expressing cells and variety of expressed isoforms increased gradually.

Absence of *Vegfa*-expressing cells in the *Emx2*-deficient MZ. Since the MZ is narrow, and it is surrounded by the *Vegfa*-expressing CPL (cortical plate) and pia-PVP, we

designed an additional negative control to make certain that the *Vegfa*-expressing cells in question reside indeed in the MZ. *Emx2* is a transcription factor gene expressed in C-R cells and in the cortical neuroepithelium (19, 20). In *Emx2*-deficient mice, C-R cells disappear one week earlier than in wildtype, and cannot be detected beyond embryonic day (E)13.5 (15, 16). Thus, by counting *Vegfa*-cells in the *Emx2*^{-/-} MZ it can be determined whether the *Vegfa* cells are indeed C-R neurons. *Vegfa* expression in the mutant MZ was absent at E12.5 (not shown). *Vegfa*-positive cell counting in the MZ of *Emx2*^{-/-} mice at E15.5 and E18.5 showed insignificant results, as expected (Fig. 1L, black bars).

C-R cells secrete Vegfa. It remained to be demonstrated that C-R cells secrete Vegfa in an angiogenic form. First, we devised a procedure to isolate and cultivate C-R cells *in vitro*. *Cxcr4* is a membrane receptor protein specifically expressed by C-R neurons but not by the PVP or pia (21, 22). After removing pia and PVP we microdissected the MZ of wildtype E15.5 mouse brains. Then we separated *Cxcr4*-expressing cells by magnetic activated cell sorting (MACS; Fig. 2A; see Methods) and plated them on culture dishes. 95% of the cells isolated in this way showed a small round shape (Fig. 2B) and complete viability after 72 hours in culture. About 75% of the MACS-sorted cells were immunoreactive for C-R cell marker reelin (Fig. 2C). A full 80% of these reelin-immunoreactive cells were also labeled by antibodies against Vegfa (Fig. 2D, E).

To carry out its function, Vegfa must first be secreted. Therefore, we investigated the presence of Vegfa in the culture medium of C-R neurons. We found steady concentrations of Vegfa in the medium after 1, 2 and 3 days of culture (Fig. 2F). Since C-R cells dying in culture would release Vegfa (although we did not detect significant levels of cell death in our cultures), we tested the cells for actual Vegfa secretion by stimulating them with deferoxamine (DFO) (23). As expected, we measured large increases of Vegfa in the culture medium of C-R neurons upon stimulation after a latency period of one day (Fig. 2F).

C-R cells have angiogenic properties. *Vegfa* is essential for angiogenesis, and endothelial cells typically respond to Vegfa stimulation by proliferation and migration (24). Endothelial cells from the human umbilical vein (HUVEC) cultivated either in Vegfa-containing medium or in the presence of C-R neurons extended significantly longer filopodia than those in control cultures (Fig. 2G), indicating active migration (25). In order to influence the branching of PVP sprouts into the brain, C-R neurons should also be able to attract migrating endothelial cells in a certain direction (directed migration or chemotaxis), a property which can be conferred by *Vegfa* (26).

Vegfa-expressing C-R cells are specially abundant in a particular region of the cortical MZ called hippocampal fissure region (not shown). We co-cultured HUVEC in the presence of E14.5 explants from this region or from a control region (Fig. 3A, B). As

control we used the mantle layer of the caudate-putamen, where *Vegfa* expression is virtually absent at that age (by *in situ* hybridization; not shown). The MZ was able to attract endothelial cells significantly better than control tissue (Fig. 3C, D, E).

Dramatic decrease in vascularization in the *Emx2*-deficient cortex after E12.5. On the basis of our results up to this point, we predicted that in the absence of C-R neurons, the upper cortical layers would be less vascularized. Removal of C-R neurons is possible by surgical or pharmacological methods (9, 27), but not without damaging the pia and PVP (and consequently altering angiogenesis). Therefore, we turned to an analysis of the cortex of *Emx2*^{-/-} embryos, which lose their C-R cells abnormally early (15, 16).

However, lack of *Emx2* could in principle cause *Vegfa* expression decrease in the neuroepithelium, which, together with the C-R cells, forms part of the *Emx2* expression domain in the cortex. Therefore, we first ascertained that *Vegfa* remains expressed correctly in the *Emx2*^{-/-} cortex (apart of course from the MZ) at the same ages (Fig. 4A-D). Afterwards, in order to quantitate the degree of vascularization of the cortex, we labeled the brain blood vessels on histological sections by *in situ* hybridization for vascular endothelial-specific marker gene *Col4a1* (28, 29) (Fig. 5A to D). Then we measured the surface area occupied by blood vessels vs total cortical area. Consistent with the absence of *Vegfa* in the MZ at E12.5, the mutant and wildtype showed no difference in vascularization at this age (Fig. 5E). At E15.5 in the wild type, the upper

layers are significantly more vascularized than the lower layers (Fig. 5F). The C-R cell-deficient *Emx2*^{-/-} mutant, however, showed dramatic impairment of upper layer vascularization at E15.5, reflected by a lack of significant difference between upper and lower layers (Fig. 5F; “n.s.” in red). Additionally, the mutant upper layers were significantly less vascularized than in wildtype (Fig. 5F; $P < 0.001$). The lower layers showed comparable degrees of vascularization in wildtype and mutant at E15.5 (Fig. 5F; “n.s.” in blue). This phenotype was maintained through E18.5 (Fig. 5G) –the wild type upper layers were significantly more vascularized than the lower, while in the mutant there was no significant difference between them (Fig. 5G; “n.s.” in red). The impairment of vascularization in the mutant lower layers at E18.5 (Fig. 5G; * in blue) can be understood as a delayed consequence of the vascularization defect in upper levels. Finally, we counted the number of radially oriented vessels coursing through the MZ and found a dramatic reduction in the *Emx2*^{-/-} at E15.5 and E18.5 (Fig. 5H).

DISCUSSION

***Vegfa* in C-R cells.** The exact way in which C-R cells influence cortical development and evolution is still elusive (2, 7). The intricate natural history (30) and dynamic gene expression (22, 31) of C-R cells suggest complex functions. These could be mediated by several proteins. Our study was prompted by the novel finding of *Vegfa* expression in C-R cells. Previous detailed characterizations of C-R cell-specific expression have not detected *Vegfa* (22, 31). The probable reason is that the widespread *Vegfa* expression in the developing brain prevents it from being detected on a specific group of cells by methods relying on transcriptome comparison. *Vegfa*, a multifunctional protein involved not only in angiogenesis but in neurogenesis and axonal outgrowth as well (32, 33), could confer functional diversity to C-R cells.

C-R cells and cortical vascularization. Cortical vascularization is an extended process consisting of several phases of sprouting, branching, degeneration and remodeling (10). As these processes go on, C-R cells are generated then migrate tangentially around the cortex (34). An early population of C-R cells is present in both WT and *Emx2*^{-/-} brains (15, 16). Our data show that they do not express *Vegfa*. At the same early stages, the first PVP sprouts grow straight through the upper cortical layers and branch preferentially in the lower layers (10). Later, at midgestation, C-R cells are absent in the *Emx2*-deficient brain (15, 16). Consistent with this, we have found *Vegfa*-expressing C-R cells in the

wildtype MZ, but not in the mutant, during this period. As they migrate, the *Vegfa*-expressing C-R cells would lay down spatially restricted branching cues consisting of their predominantly expressed *Vegfa* isoforms, 188 and 164 (18) (Fig. 1L). Around the same gestational time, newly entered sprouts course radially through the MZ to branch preferentially in the upper layers (10). As we show here, this inverts the relation between upper and lower layer vascularization, which favored lower layers at earlier stages. It is precisely this turnaround that fails in the *Emx2*-deficient cortex, which also shows very reduced number of radially oriented blood vessels in the MZ.

Our model attributes to *Vegfa*-expressing C-R cells a supporting role in cortical vascularization. At the same time, other important functions of these cells might be mediated by the same multifunctional cytokine.

MATERIALS AND METHODS

Animals

All animal experiments were conducted in compliance with the German Law on Animal Welfare.

C-R cells for *in vitro* culture were isolated from C57BL/6 mice.

Emx2 heterozygous female mice (C129Sv/J-C57Bl6) were mated with *Emx2*⁺ males of same background and inspected for vaginal plug at 9.00 A.M. next day. Pregnant mice were anesthetized with isoflurane and killed by cervical dislocation on the desired gestation day. Embryos were dissected out and processed for histology or other procedures.

Immunocytochemistry

Antibodies: anti-reelin monoclonal 1:100 (Chemicon), anti-mouse Cxcr4 rat monoclonal 1:100 (BD Pharmingen), anti-VEGF rabbit polyclonal 1:200 (Abcam), anti-mouse VEGF goat polyclonal 1:100 (R&D Systems).

***In situ* hybridization**

Tissue collection, sectioning, RNA probe synthesis and hybridization were as described (35). Quality control and quantitation of riboprobes were assessed with a Bioanalyzer (Agilent Technologies, Waldbronn, Germany). For the double detection of *Vegfa* mRNA and reelin protein, *in situ* hybridization of *Vegfa* with alkaline phosphatase labeling was

followed by anti-reelin immunohistochemistry detected with diaminobenzidine.

Primers for the *Col4a1* probe:

forward: ctactcttactggctgtccacgc

reverse: gccatgacttccacaaaagcagc

Probe size: 1037 bp

Primers for *Vegfa* probes:

Vegfa 3'UTR Probe size: 916

forward: agactcttcgaggagcactttgg; location: 1187

reverse: aagatgaggaagggttaagccactc; location: 2102

Ref sequence: NM_001025250.1; a new version is now available on NCBI.

Vegfa188 Probe size: 407

forward: gaagtcccatgaagtgatcaag; location: exon 2-3 junction: 14bp(exon 2)+9bp(exon 3)

reverse: aacaaggctcacagtgaacgct; location: exon 6-7 junction: 5bp(exon 6)+17bp(exon 7)

Vegfa164 Probe size: 333

forward: gaagtcccatgaagtgatcaag; location: exon 2-3 junction: 14bp(exon 2)+9bp(exon 3)

reverse: caaggctcacagtgattttctggc; location: exon 5-7 junction: 9bp(exon 5)+15bp(exon 8)

Vegfa120 Probe size: 330

forward: gaagtcccatgaagtgatcaag; location: exon 2-3 junction: 14bp(exon 2)+9bp(exon 3)

reverse: cggctgtcacattttctggc (Note: c appears in ref seq as T); location: exon 5-8
junction: 9bp(exon 5)+12bp(exon 8)

Magnetic cell sorting of Cxcr4-positive cells of the MZ

For each experiment, the brains of 30 to 40 mouse embryos (E14.5) were dissected out and the meninges removed. Forebrains were cut with into 300 µm thick transverse slices. Cortical MZ was microdissected and enzymatically digested following standard procedures. The cells were labeled with a biotinylated anti-CXCR-4 antibody for 15 min at 4°C, incubated with magnetic beads covered with anti-biotin antibody (anti-Biotin MicroBeads from Miltenyi Biotech, Bergisch Gladbach, Germany), and then separated on selecting magnetic columns (LS columns, Miltenyi Biotech) following the manufacturer's instructions. The selected cells were plated, counted and tested for viability as usual.

Cell culture

1. Reagents

Recombinant human VEGF was from ProTech (Rocky Hill, New Jersey, USA), media and sera from LifeTechnologies, Inc. (Gaithersburg, Maryland, USA). Other reagents were from PAA Laboratories GmbH (Pasching, Austria), unless otherwise specified.

2. HUVEC

Endothelial cells used for *in vitro* assays were HUVECs. Primary HUVECs were prepared from neonatal human umbilical cords by trypsin digestion. HUVEC were cultured on collagen type I-coated plastic wells, in Endothelial Cell Medium (from PAA), glutamine (2 mmol/L), and penicillin/streptomycin. Experiments were performed using subcultures between the fourth and eighth passage.

3. C-R neurons

C-R neurons were plated on laminin-coated 24 well plates (4×10^5 cells per well) in Neurobasal medium, 5% FCS, 1% B27 supplement, 1% L-glutamine and 1% penicillin/streptomycin and incubated in a humidified atmosphere of 5% CO₂ at 37°C for a maximum of 72 hrs. To induce VEGF secretion we stimulated the cells with 5 μM deferoxamine mesylate (DFO) 12 hrs after plating (23). For VEGF detection in the culture medium see below.

4. HUVEC plus C-R co-cultures

4×10^5 cells per well of freshly prepared C-R cells were plated on laminin-coated 24 well dishes. After 12 hrs of incubation, the same number of HUVEC were added. As controls, C-R and HUVEC cells were cultivated separately (8×10^5 cells/well). Control HUVEC were cultivated with or without VEGF (10ng/ml) stimulation. All cells were cultivated (or co-cultivated) for a maximum of 72 hrs. At the end of the culture period, the cells were fixed with 4% paraformaldehyde and stained with anti-vW antibody (endothelial cell marker).

5. Migration analysis

The length of endothelial filopodia was measured with AxioVision LE 4.4 software (Carl Zeiss AG, Oberkochen, Germany). For the MZ/endothelial co-culture cell migration assays, explants were microdissected from the cortical MZ (hippocampal fissure region) and medial ganglionic eminence of E14.5 embryonic mouse brains and placed in culture.

1 μ l endothelial cells (5×10^6 cells/ml) was embedded in a drop of collagen I. After polymerization, the collagen drops were placed at an approximate distance of 500 μ m to the explants and covered with 20 μ l collagen I. Medium (Neurobasal medium plus 5% FCS, 1% B27, 1% L-glutamine, 1% penicillin/streptomycin) was added and the plates were incubated for up to 72 hrs. The migration distance from the endothelial aggregate was measured with AxioVision LE 4.4.

VEGF detection by enzymatic immunoassay (ELISA)

The Quantikine Mouse VEGF ELISA kit (R&D Systems, Minneapolis, USA) was used to measure mouse VEGF164 and VEGF120 in cell culture supernatants, following manufacturer's instructions.

Cell counting

Cells of the cortical MZ were labeled for different Vegfa isoforms by *in situ* hybridization (see above). For each Vegfa isoform, four sections of each of 3 mouse embryos (ages E12.5 [results not shown], E15.5 and E18.5) were counted on 25 micrometer thick histological sections. The sections were sagittal (to ensure same degree of development through the section, since the cortex develops with a marked lateral-early to medial-late gradient). The sections selected for counting were at a medio-lateral level including the center of the olfactory bulb, for consistency. Cells were identified under the microscope with normal optics (40x oil immersion numerical aperture 1.00 and 63x oil immersion numerical aperture 1.40) and their localization in the MZ or above the MZ was

individually determined by Differential Interference Optics (DIC), which shows clearly the boundaries of the different tissues. Only cells unequivocally located in the MZ as opposed to the pia were counted.

Morphometry

Morphometrical analysis of cortical vascularization was carried out on histological slides with 25 micrometer thick sections from embryonic mouse brains (E12.5, E15.5 or E18.5) labeled by non-isotopic *in situ* hybridization with probes against endothelial-specific marker gene *Col4a1*. Then we used Cell-F software (Olympus SIS, Münster, Germany) to measure the labeled surface area and expressed the result as a percentage of the total area in upper (MZ plus CPL) vs. lower cortical layers. The sections were taken along the sagittal plane to ensure that the cortical slice they contained was in a homogeneous developmental stage. Transverse sections would have included a developmental gradient from more mature (lateral) to less mature (medial). The slides were digitally photographed at a resolution of 1.6 micrometer/pixel using a microscope with a motorized scanning stage and a digital camera (Leica Microsystems GmbH, Wetzlar, Germany), and saved as tiff files. Eight sections from each of three embryos for every age and genotype were chosen for analysis. For consistency, all sections selected for morphometrical evaluation were taken from a medio-lateral level that included the olfactory bulb. Besides, sections in this level are the most perpendicular to the cortical layers (i.e., they do not cut tangentially or sidewise through the layers). A parallel series

of Nissl-stained sections was used to determine the limits of “upper” and “lower” layers.

Statistics

Statistical analyses were carried out with GraphPad Prism 4 (GraphPad Software Inc., San Diego, USA). Details can be found in the figure legends.

ACKNOWLEDGMENTS

The “Robotic *in situ* Hybridization Team” of the Dept. Genes and Behavior (Max Planck Institute, Göttingen) performed some *in situ* labelings. This work was funded through the Deutsche Forschungsgemeinschaft and the Max Planck Society.

1. Derer, P. & Derer, M. (1990) *Neuroscience* **36**, 839-56.
2. Soriano, E. & Del Rio, J. A. (2005) *Neuron* **46**, 389-94.
3. Pollard, K. S., Salama, S. R., Lambert, N., Lambot, M. A., Coppens, S., Pedersen, J. S., Katzman, S., King, B., Onodera, C., Siepel, A., Kern, A. D., Dehay, C., Igel, H., Ares, M., Jr., Vanderhaeghen, P. & Haussler, D. (2006) *Nature* **443**, 167-72.
4. Gressens, P. (2000) *Pediatr Res* **48**, 725-30.
5. D'Arcangelo, G., Miao, G. G., Chen, S. C., Soares, H. D., Morgan, J. I. & Curran, T. (1995) *Nature* **374**, 719-23.
6. Ogawa, M., Miyata, T., Nakajima, K., Yagyu, K., Seike, M., Ikenaka, K., Yamamoto, H. & Mikoshiba, K. (1995) *Neuron* **14**, 899-912.
7. Tissir, F. & Goffinet, A. M. (2003) *Nat Rev Neurosci* **4**, 496-505.
8. Yoshida, M., Assimacopoulos, S., Jones, K. R. & Grove, E. A. (2006) *Development* **133**, 537-45.
9. Super, H., Del Rio, J. A., Martinez, A., Perez-Sust, P. & Soriano, E. (2000) *Cereb Cortex* **10**, 602-13.
10. Strong, L. H. (1964) *J Comp Neurol* **123**, 121-38.
11. Pardanaud, L., Yassine, F. & Dieterlen-Lievre, F. (1989) *Development* **105**, 473-85.
12. Carmeliet, P., Ferreira, V., Breier, G., Pollefeyt, S., Kieckens, L., Gertsenstein, M., Fahrig, M., Vandenhoeck, A., Harpal, K., Eberhardt, C., Declercq, C., Pawling, J., Moons, L., Collen, D., Risau, W. & Nagy, A. (1996) *Nature* **380**, 435-9.
13. Coultas, L., Chawengsaksophak, K. & Rossant, J. (2005) *Nature* **438**, 937-45.
14. Breier, G., Albrecht, U., Sterrer, S. & Risau, W. (1992) *Development* **114**, 521-32.
15. Mallamaci, A., Mercurio, S., Muzio, L., Cecchi, C., Pardini, C. L., Gruss, P. & Boncinelli, E. (2000) *J Neurosci* **20**, 1109-18.
16. Zhao, T., Kraemer, N., Oldekamp, J., Cankaya, M., Szabo, N., Conrad, S., Skutella, T. & Alvarez-Bolado, G. (2006) *Eur J Neurosci* **23**, 2895-907.
17. Ruhrberg, C., Gerhardt, H., Golding, M., Watson, R., Ioannidou, S., Fujisawa, H., Betsholtz, C. & Shima, D. T. (2002) *Genes Dev* **16**, 2684-98.
18. Ruhrberg, C. (2003) *Bioessays* **25**, 1052-60.
19. Simeone, A., Gulisano, M., Acampora, D., Stornaiuolo, A., Rambaldi, M. & Boncinelli, E. (1992) *Embo J* **11**, 2541-50.
20. Mallamaci, A., Iannone, R., Briata, P., Pintonello, L., Mercurio, S., Boncinelli, E. & Corte, G. (1998) *Mech Dev* **77**, 165-72.
21. Tissir, F., Wang, C. E. & Goffinet, A. M. (2004) *Brain Res Dev Brain Res* **149**, 63-71.
22. Yamazaki, H., Sekiguchi, M., Takamatsu, M., Tanabe, Y. & Nakanishi, S. (2004) *Proc Natl Acad Sci U S A* **101**, 14509-14.
23. Beerepoot, L. V., Shima, D. T., Kuroki, M., Yeo, K. T. & Voest, E. E. (1996) *Cancer Res* **56**, 3747-51.
24. Ferrara, N. (2001) *Am J Physiol Cell Physiol* **280**, C1358-66.

25. Wood, W. & Martin, P. (2002) *Int J Biochem Cell Biol* **34**, 726-30.
26. Gerhardt, H., Golding, M., Fruttiger, M., Ruhrberg, C., Lundkvist, A., Abramsson, A., Jeltsch, M., Mitchell, C., Alitalo, K., Shima, D. & Betsholtz, C. (2003) *J Cell Biol* **161**, 1163-77.
27. Super, H., Martinez, A. & Soriano, E. (1997) *Brain Res Dev Brain Res* **98**, 15-20.
28. Urabe, N., Naito, I., Saito, K., Yonezawa, T., Sado, Y., Yoshioka, H., Kusachi, S., Tsuji, T., Ohtsuka, A., Taguchi, T., Murakami, T. & Ninomiya, Y. (2002) *Arch Histol Cytol* **65**, 133-43.
29. Gould, D. B., Phalan, F. C., Breedveld, G. J., van Mil, S. E., Smith, R. S., Schimenti, J. C., Aguglia, U., van der Knaap, M. S., Heutink, P. & John, S. W. (2005) *Science* **308**, 1167-71.
30. Meyer, G., Soria, J. M., Martinez-Galan, J. R., Martin-Clemente, B. & Fairen, A. (1998) *J Comp Neurol* **397**, 493-518.
31. Garcia-Frigola, C., Burgaya, F., Calbet, M., Lopez-Domenech, G., de Lecea, L. & Soriano, E. (2004) *Brain Res Mol Brain Res* **122**, 133-50.
32. Sondell, M., Lundborg, G. & Kanje, M. (1999) *J Neurosci* **19**, 5731-40.
33. Jin, K., Zhu, Y., Sun, Y., Mao, X. O., Xie, L. & Greenberg, D. A. (2002) *Proc Natl Acad Sci U S A* **99**, 11946-50.
34. Takiguchi-Hayashi, K., Sekiguchi, M., Ashigaki, S., Takamatsu, M., Hasegawa, H., Suzuki-Migishima, R., Yokoyama, M., Nakanishi, S. & Tanabe, Y. (2004) *J Neurosci* **24**, 2286-95.
35. Yaylaoglu, M. B., Titmus, A., Visel, A., Alvarez-Bolado, G., Thaller, C. & Eichele, G. (2005) *Dev Dyn* **234**, 371-86.

FIGURE LEGENDS

Figure 1. *Vegfa* expression in Cajal-Retzius neurons

(A, B, C) *In situ* hybridization of *Vegfa* in the neocortical MZ (arrowheads) and pia/PVP (arrows). Wildtype mouse, E15.5 (A) and E18.5 (B, C). Probes: *Vegfa*-3'UTR (A, B) and *Vegfa*164 (C). Horizontal lines represent the boundaries between pia/MZ and MZ/cortical plate (CPL).

(D, E, F) *Vegfa*- and *Reln*-expressing neurons in the neocortical MZ by *in situ* hybridization against *Vegfa*-3'UTR (purple/blue) and anti-reelin antibody (brown) (wildtype, E18.5). Insets show neurons indicated by arrowheads at high-magnification.

(G, H, I, J, K) *Vegfa*- and *Reln*-expressing neurons in neocortical MZ can be distinguished from *Vegfa*-expressing cells of the pia/PVP. E18.5 mouse neocortex.

(G) Arrowheads point at *Vegfa*- (3'UTR) and *Reln*-(antibody) expressing neurons in cortical MZ. White arrowheads: pia/MZ boundary. Arrows show *Vegf*-expressing cells (blue) in the pia/PVP.

(H-J) *In situ* hybridization of *Vegfr2* (*Vegf* receptor 2), *Dcn* (*Decorin*) and *Cxcl12*, markers of pia but not MZ.

(K) *In situ* hybridization of MZ-marker *Cxcr4*.

(L) Number of MZ cells expressing *Vegfa* isoforms on sections at E15.5 (left) and E18.5 (right) in wildtype (white bars) and *Emx2*^{-/-} (black bars). Mean±SEM, n.s., not significant; * $P<0.05$, ** $P<0.01$, *** $P<0.001$.

CPL, cortical plate; MZ, marginal zone. Scale bars: 50 micrometers.

Figure 2. Isolation and functional assays of cortical marginal zone neurons co-expressing *Cxcr4*, *Reln* and *Vegfa*

(A) Procedure for the sorting and isolation of C-R cells from the marginal zone (MZ) of E15.5 mouse cerebral cortex.

(B, C, D, E) A group of 3 C-R cells in culture under phase contrast and the same cells labeled with nuclear staining DAPI and with fluorescent antibodies against reelin (C), and Vegfa (D). (E) shows Vegfa and reelin labelings merged.

(F) VEGFA quantitation in C-R culture medium by enzymatic immunoassay. C-R cells spontaneously secrete VEGFA to the medium; DFO stimulation leads to very increased secretion after a 24 h delay. (Mean \pm SD; n=15; ***P<0.001).

(G) C-R neurons induce migratory activity in endothelial cells. Quantification of HUVEC filopodial length after 1, 2 or 3 days in culture medium, plus VEGF or co-cultured with C-R neurons. (Mean \pm SD; n=5; ***P<0.001).

Figure 3. The MZ induces directed migratory activity in endothelial cells

(A) Non-directional migratory activity of HUVEC in the presence of a control explant (left side of picture).

(B) HUVEC are attracted by the MZ explant (left side of picture). (C) and (D) show

high-magnification views of the fields enclosed in (A) and (B) respectively.

(E) Quantification of directional migratory activities. Mean \pm SD from 5 experiments (left bar, 24 ± 5.911 ; right bar, 75.41 ± 8.350 ; unpaired t-test, two-tail P value <0.0002).

Figure 4. *Vegfa* expression is not altered in the *Emx2*^{-/-} CPL or neuroepithelium.

Cortical expression of *Vegfa* in the developing wildtype (A, C) and *Emx2*^{-/-} (B, D) neocortex, at E15.5 (A, B) and E18.5 (C, D). Expression was detected by *in situ* hybridization with the 3'UTR probe (see Methods). The distribution of *Vegfa*-positive cells in the mutant pia, CPL and ventricular zone (VZ) is the same as in the wildtype.

Figure 5. Vascularization deficit in upper cortical layers of a mutant without Cajal-Retzius cells

(A-D) Expression of *Col4a1* (A, B, C, D) in E15.5 and E18.5 mouse cortex of wildtype and *Emx2*^{-/-}.

(E, F, G) Quantitation of vascularization in upper and lower layers of developing wildtype (white bars) and *Emx2*^{-/-} cortex (black bars) at E12.5 (E), E15.5 (F) and E18.5 (G). At E12.5, upper layers are less vascularized in both wildtype and mutant; at E15.5 and E18.5 the upper layers are significantly better vascularized than the lower in the wildtype, but not in the *Emx2*^{-/-} (n.s. in red). The lower layers have a comparable degree of vascularization in wildtype and mutant at E15.5 (n.s. in blue), but show certain defects

in vascularization at E18.5 (* in blue). Mean±SEM; n=21 to 23; n.s., not significant;

* $P < 0.05$; *** $P < 0.001$

(H) Quantitation of number of radial features expressing *Col4a1* in the MZ of wildtype and *Emx2*^{-/-} at E12.5, E15.5 and E18.5. Mean±SEM; n=16 to 32

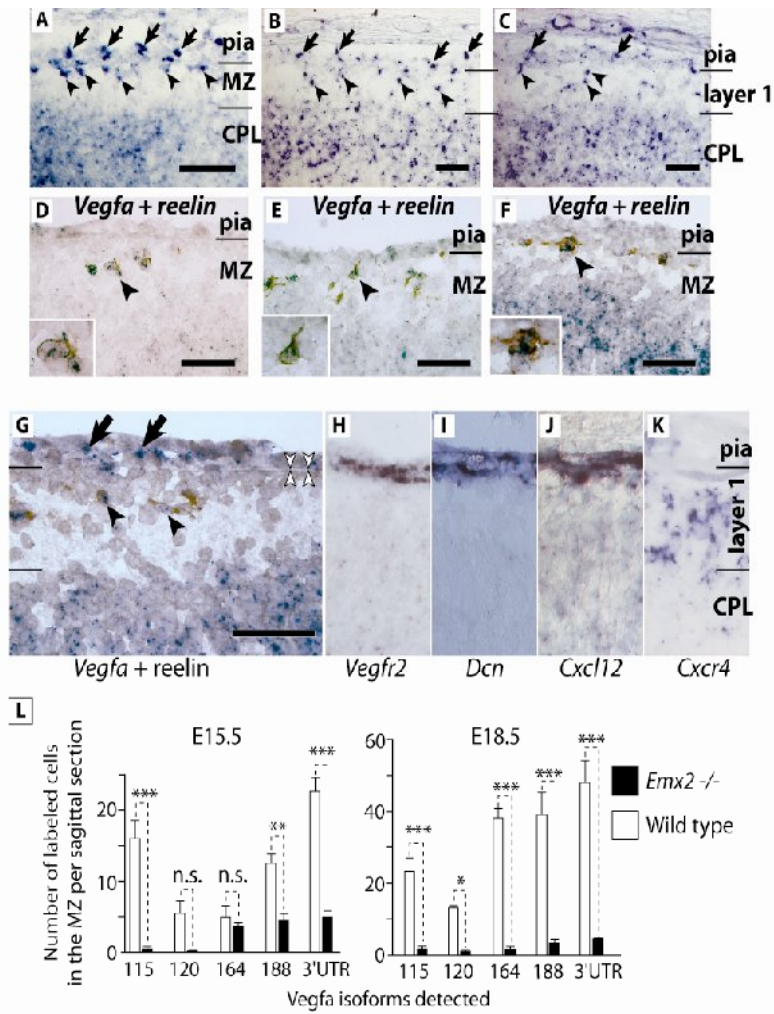


Fig. 1

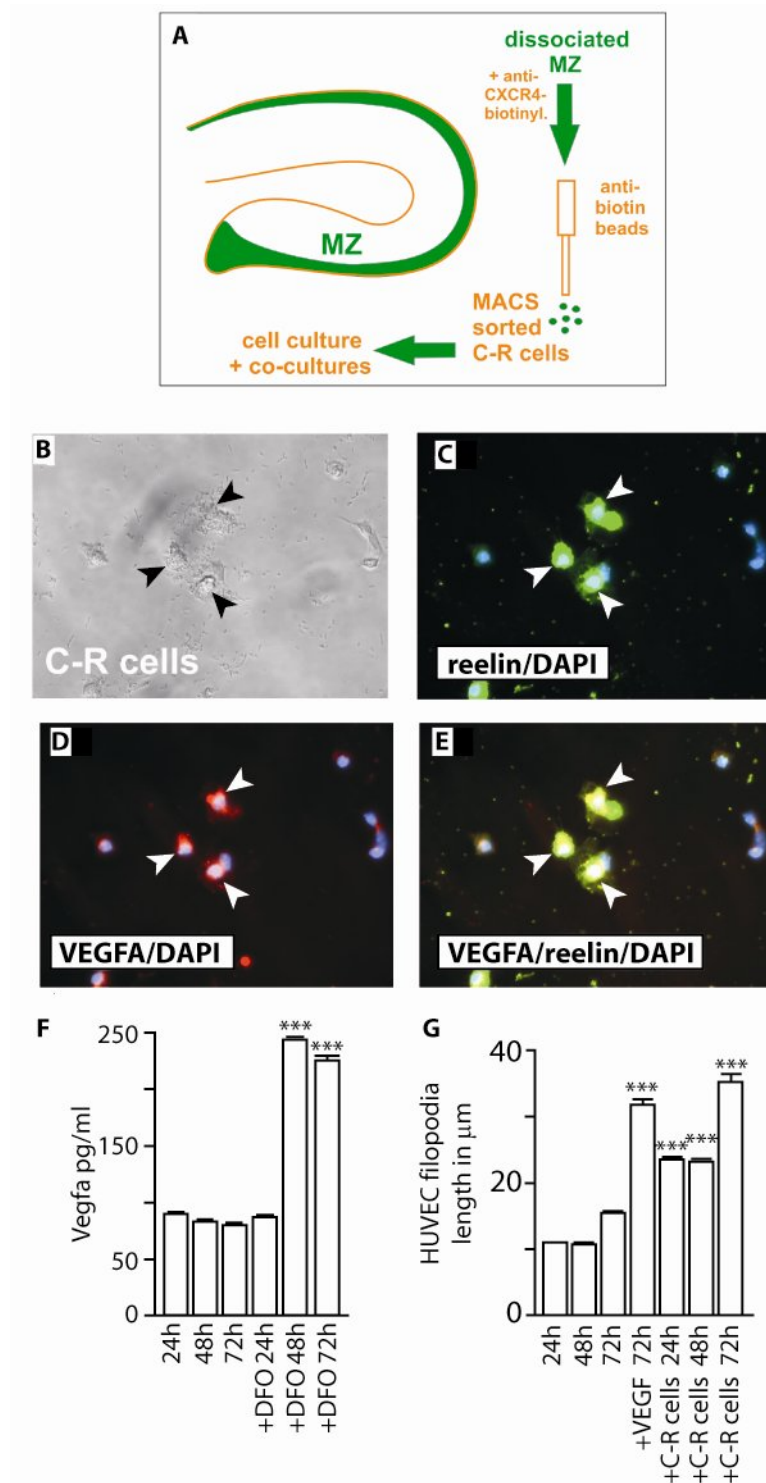


Figure 2

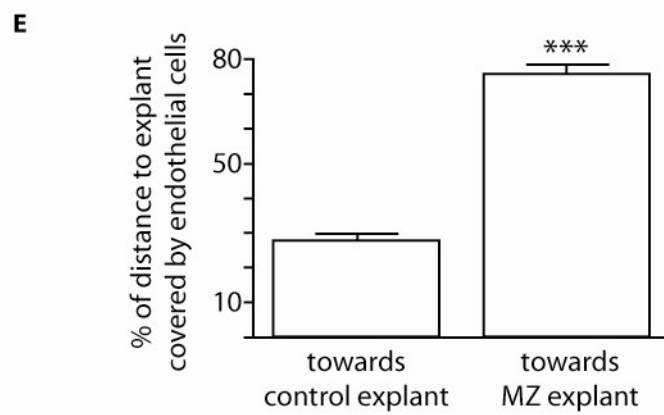
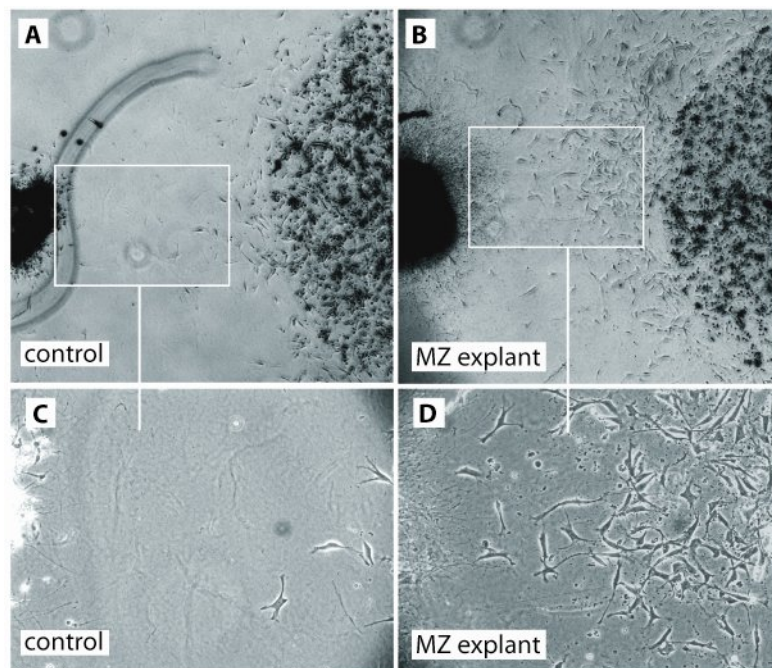
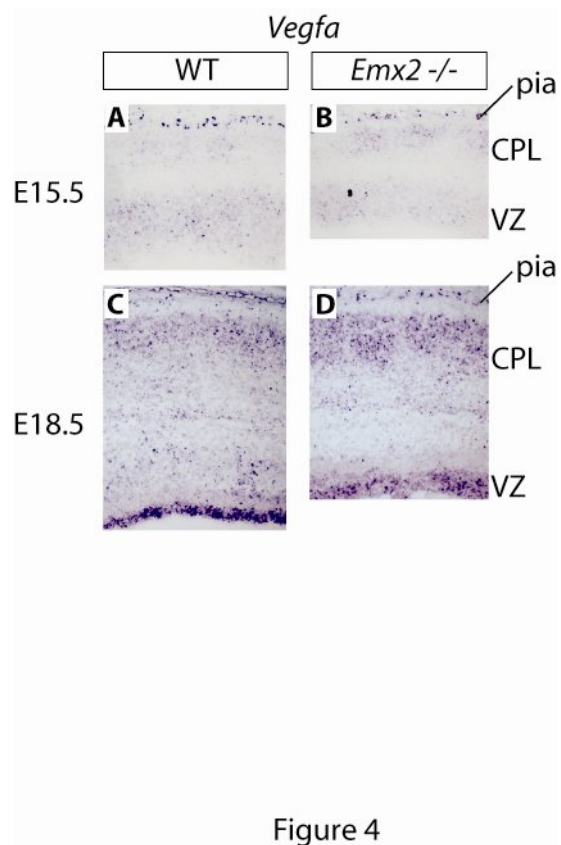


Figure 3



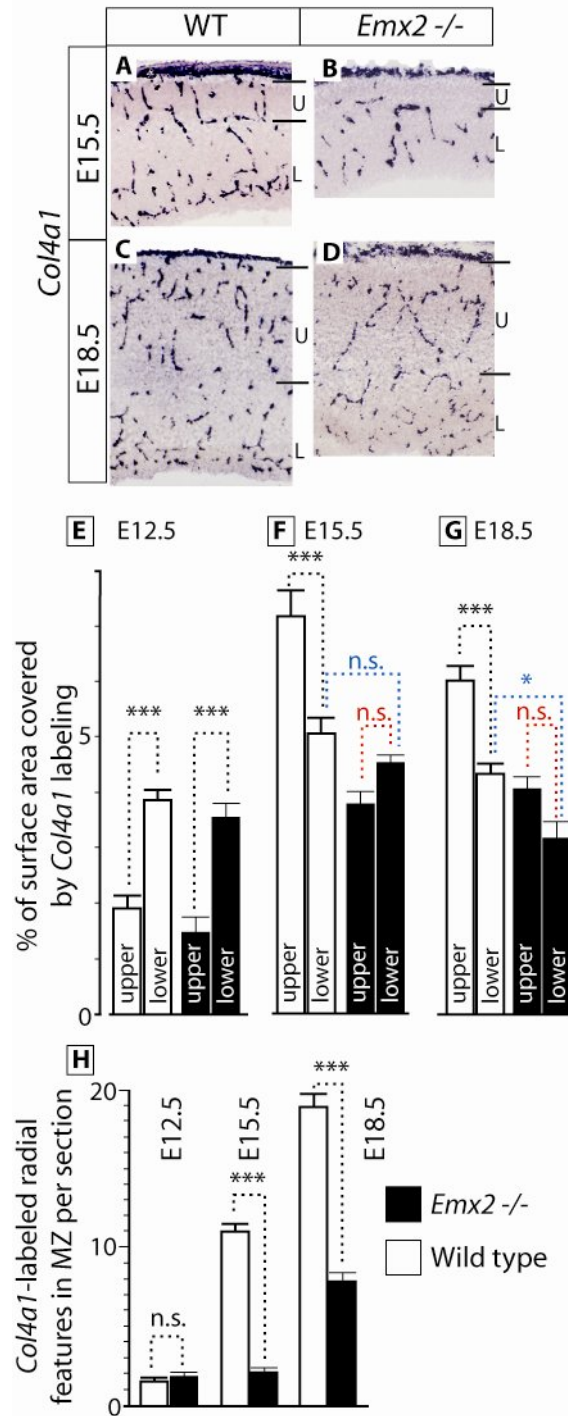


Figure 5

Author's contribution: Cajal-Retzius neurons that produce Vascular Endothelial Growth Factor have a role in cortical angiogenesis

Maintained the *Emx2* mouse line in parallel with the group of Tübingen

Performed large scale screening on angiogenesis markers in cortical tissues by ISH and choose the marker *Vegfa* and *Col4a1*

Performed large scale ISH of *Col4a1* on different stages of *Emx2* null mutants as well as comparable wild type mice

Did the statistics of the ISH results

Chapter 3

Publication#3: *Foxb1*-driven Cre expression in somites and the neuroepithelium of diencephalon, brainstem, and spinal cord.

Tianyu Zhao, Xunlei Zhou, Nora Szabo, Micheal Leitges and Gonzalo Alvarez-Bolado. *Genesis* 45:781-787 (2007)

This article is not included in this thesis because of copyright reasons.

Author's contribution - Foxb1-driven Cre expression in somites and the neuroepithelium of diencephalon, brainstem, and spinal cord

Cross the original Foxb1cre line with FLP mouse line to eliminated neo-cassette.
Maintain all the mouse lines used in paper and harvest the appropriate embryos at certain stage.

Performed all the whole mount detection of Beta- galactosidase activity

Performed all the whole mount detection of HPAP

Chapter 4

Publication#4: Genetic mapping of *Foxb1*-cell lineage shows migration from caudal diencephalons to telencephalon and lateral hypothalamus

Tianyu Zhao, Nora Szabo, Jun Ma, Lingfei Luo, Xunlei Zhou and Gonzalo Alvarez-Bolado. *European Journal of Neuroscience* (2008) *in press*

Genetic mapping of *Foxb1*-cell lineage shows migration from caudal diencephalon to telencephalon and lateral hypothalamus

Tianyu Zhao^{1,2}, Nora Szabó^{1,2}, Jun Ma³, Lingfei Luo³, Xunlei Zhou¹ and Gonzalo Alvarez-Bolado^{1*}

¹ Dept. 11100, Brain Development Group, Max Planck Institute of Biophysical Chemistry, 37077 Göttingen, Germany

² equal contribution

³ Dept. of Molecular Developmental Biology, School of Life Sciences, Southwest University, Beibei, 400715 Chongqing, China

* author for correspondence: Gonzalo Alvarez-Bolado, Max Planck Institute bpC, Am Fassberg 11, 37077 Göttingen, Germany

Phone +49(0)551-201-2713; Fax +49(0)551-201-2705

gonzalo.alvarez-bolado@mpibpc.mpg.de

Running title: *Foxb1*-lineage in the diencephalon

Key words: axon-dependent, forkhead genes, prethalamus, tangential, thalamus

Number of pages: 40

Number of Figures: 11

Number of words in whole manuscript: 9, 008

Number of words in Abstract: 198

Number of words in Introduction: 475

ABSTRACT

The hypothalamus is a brain region with vital functions, and alterations of its development can cause human disease. However, we still do not have a complete description of how this complex structure is put together during embryonic and early postnatal stages. Radially oriented, outside-in migration of cells is prevalent in the developing hypothalamus. In spite of this, cell contingents from outside the hypothalamus as well as tangential hypothalamic migrations have also an important role. Here we study migrations in the hypothalamic primordium by genetically labeling the *Foxb1* diencephalic lineage. *Foxb1* is a transcription factor gene expressed in the neuroepithelium of the developing neural tube with a rostral expression boundary between caudal and rostral diencephalon, and therefore appropriate to mark migrations from caudal levels into the hypothalamus. We have found a large, longitudinally oriented migration stream apparently originated in the thalamic region and following an axonal bundle to end in the anterior portion of the lateral hypothalamic area. Additionally, we have mapped a specific expansion of the neuroepithelium into the rostral diencephalon. The expanded neuroepithelium generates abundant neurons for the medial hypothalamus at the tuberal level. Finally, we have uncovered novel diencephalon-to-telencephalon migrations into septum, piriform cortex and amygdala.

INTRODUCTION

The hypothalamus is a brain region subserving vital functions, and alterations of its development can cause disease. Obtaining a complete description of how this complex structure is put together during embryonic and early postnatal stages will be helpful to understand human pathological conditions (Michaud, 2001; Caqueret *et al.*, 2005). The hypothalamus originates in the rostral diencephalon, which, because of its situation between telencephalon and caudal diencephalon (including the thalamic region) (Fig. 1), undergoes particularly complex patterning (Puelles & Rubenstein, 2003). The longitudinal axis of the neural tube divides the primordium into dorsal and ventral portions (Shimamura *et al.*, 1995). The hypothalamus is subdivided into four areas (preoptic, anterior, tuberal and mammillary) (Swanson, 1987; Simerly, 2004), of which the first two are dorsal and the last two are ventral (according to embryonic topology, Fig. 1), although they appear arranged rostro-caudally in the adult brain.

Birthdating shows that most of the hypothalamus develops by waves of neurogenesis from the rostral diencephalic neuroepithelium, followed by radially oriented, outside-in migration (Altman & Bayer, 1986), and gene expression studies confirm this general pattern (Alvarez-Bolado *et al.*, 1995; Caqueret *et al.*, 2006). However, cells from outside the hypothalamus (Muske & Moore, 1988; Schwanzel-Fukuda & Pfaff, 1989; Wray *et al.*, 1989; Henderson *et al.*, 1999) as well as tangential intra-hypothalamic migrations (Alvarez-Bolado *et al.*, 2000a) have also an important role. In addition,

differential control of migration underlies important functional features like the sexual dimorphism of some hypothalamic structures (Tobet, 2002). Neuroepithelial expansion is another mechanism resulting in increased cellular heterogeneity in brain regions. As the embryo grows, the neuroepithelium expands by symmetric ("horizontal") mitosis (Rakic, 1988; Chenn & McConnell, 1995). Differential expansion of neuroepithelial subpopulations could contribute to regionalization (Alvarez-Bolado *et al.*, 1995). Alternatively, neuroepithelial cells can simply migrate inside the neuroepithelium (Fishell *et al.*, 1993; Arnold-Aldea & Cepko, 1996; Golden & Cepko, 1996). The displaced neuroepithelial cells will generate cells for the region where they settle. Ultimately, every forebrain region including the hypothalamus is a composite of cells from different origins (Marin & Rubenstein, 2003). Knowledge of the cell migrations involved is necessary to understand its development.

Genetic neuroanatomy (Joyner & Zervas, 2006; Dymecki & Kim, 2007) is being successfully used to unravel the development of complex brain regions like the cerebellum (Zervas *et al.*, 2005; Sillitoe & Joyner, 2007). Similar approaches will be very useful to work out the different cell migrations and lineages in the hypothalamus. Here we have labeled the *Foxb1* diencephalic lineage by crossing a *Foxb1-Cre* mouse line (Zhao *et al.*, 2007) with reporter mouse lines. *Foxb1* is a transcription factor gene widely expressed in the neural tube, with a rostral expression boundary between caudal and rostral diencephalon (Kaestner *et al.*, 1996; Wehr *et al.*, 1997; Alvarez-Bolado *et al.*, 1999; Alvarez-Bolado *et al.*, 2000a) which makes this gene useful to study cell

migration into the hypothalamic primordium.

METHODS

Mouse lines

All experiments with animals were carried out in accordance with the European Communities Council Directive of 24 November 1986 (86/609/EEC) and under authorization Az 32.22/Vo (Ordnungsamt der Stadt Göttingen).

In the *Foxb1^{Cre}* mouse line (Zhao et al., 2007) (kept in the C57BL/6 background), the *Foxb1* coding sequence was replaced by the Cre recombinase cDNA by homologous recombination. It expresses Cre under the control of the regulatory sequences of *Foxb1*. To characterize the Cre activity encoded by *Foxb1^{Cre}*, we crossed our mice with the ROSA26R (Soriano, 1999) or Z/AP (Lobe et al., 1999) reporter mouse lines (C57BL/6). All mice used for lineage-labeling were heterozygous for *Foxb1^{Cre}* and therefore they were heterozygous for *Foxb1*. *Foxb1* heterozygotes show normal phenotype (Labosky et al., 1997; Wehr et al., 1997; Alvarez-Bolado et al., 2000b; Kloetzli et al., 2001). No homozygotes were used in this study.

To obtain embryos, timed-pregnant females of the appropriate crossings were killed by cervical dislocation.

Lineage labeling

In the *ROSA26R* animals, the reporter gene β -galactosidase is inserted in the constitutively active ROSA locus downstream a floxed stop codon. Upon Cre-mediated recombination, the stop codon is deleted and β -galactosidase is constitutively produced.

Therefore, this reporter is a lineage marker: in mice carrying both the *Foxb1*^{Cre} and the ROSA26R alleles, cells expressing *Foxb1* and any cell derived from them will permanently express β -galactosidase. Similar principles apply to the use of Z/AP mice, which carry human placental alkaline phosphatase (hPLAP) as reporter. Since hPLAP attaches to axonal membranes, it is a very good marker of axons of lineage-labeled neurons (Fields-Berry *et al.*, 1992; Gustincich *et al.*, 1997; Leighton *et al.*, 2001). The expression of lineage markers is "cumulative" (Louvi *et al.*, 2007), since the lineage domain enlarges as progressively more cells start expressing the marker (here *Foxb1*). In addition, when lineage labeling appears beyond the expression domain of the marker, it is indicative of migration.

We analyzed the *Foxb1* lineage in *ROSA26* crossings at the following ages: embryonic day (E)8.75, E9.5, E11.5, E12.5, E14.5, E15.5, E18.5 and postnatal day 0 (P0). In Z/AP crossings: E12.5, E13.5 and P(0). For every embryonic age up to E12.5 we examined 2 to 5 litters, and from E15.5 on we examined 2 to 4 brains for each age. Each of the Figures 6 and 7 shows material from one brain, for consistency. We identified structures in the brain according to current reference works (Alvarez-Bolado & Swanson, 1996; Paxinos & Franklin, 2001).

In situ hybridization (ISH)

Whole-mount ISH was performed as described (Wilkinson, 1992). The *Foxb1* probe was cloned by PCR (forward primer atc gct agg gag tac aag atg cc; reverse gat cag tga gtt ggt ctt gtg gc). Briefly, the embryos were fixed in formaldehyde 4% in phosphate

buffer saline (PBS) overnight (4°C), washed in PBS + 0.1% Tween-20 (PBT) and stored at -20°C in methanol. For ISH the embryos were rehydrated, bleached (6% H₂O₂), digested (10 µg/ml Proteinase K in PBT at RT), washed (2 mg/ml glycine/PBT), postfixed (4% PFA/0.2% glutaraldehyde/PBT), prehybridized for 1-2h (70°C) and hybridized overnight (70°C). They were then washed (50% formamide, 5x SSC, pH4.5, 1% SDS at 70°C), rinsed (100 mM Maleic acid, 150 mM NaCl, 2 mM Levamisole, 0.1% Tween-20 (MAB)) and incubated in 10% sheep serum in MAB/2% Blocking Reagent (Roche Diagnostics GmbH, Mannheim, Germany) for 2-3h (RT), then in anti-DIG AP antibody (Roche) overnight (4°C). The embryos were rinsed, then left in MAB overnight (4°C). The embryos were then incubated in BM-Purple (Roche) with Levamisole (RT) and, after color developed, washed in PBT (pH4.5), fixed in 4% formaldehyde/0.1% glutaraldehyde overnight (4°C), and transferred into 80% Glycerol/PBT.

β-galactosidase activity detection

β-galactosidase activity was detected as described (Koenen *et al.*, 1982). Embryos from timed pregnancies were collected, washed with cold PBS and fixed 30-50 minutes (1% paraformaldehyde, 0.2% glutaraldehyde, 0.02% NP40/PBS). The embryos were then rinsed and incubated in staining solution (1mg/ml Xgal, 2mM MgCl₂, 5mM K₃Fe(CN)₆ and 5mM K₄Fe(CN)₆/PBS) overnight in the dark (RT). For animals older than E12.5, the brains were dissected out, fixed (4% paraformaldehyde) 60 minutes (4°C), embedded in agarose and cut into sections (150 micrometers). The sections were

fixed on ice 30 minutes, washed with PBS, incubated with staining solution and fixed again (4% paraformaldehyde) 60 minutes.

Alkaline phosphatase activity detection

Material was collected, fixed (4% paraformaldehyde) on ice 60 minutes, embedded in agarose and cut into sections (150 micrometers). The sections were fixed again (4% paraformaldehyde/0.2% glutaraldehyde) on ice 60 minutes, rinsed, incubated 30 minutes (72°C) to inhibit endogenous phosphatase activity, rinsed in alkaline phosphatase-buffer (100mM Tris-Cl, pH 9.5, 100mM NaCl, 10mM MgCl₂), incubated with staining solution (250µl NBT +187.5µl BCIP per 50ml in alkaline phosphatase-buffer) overnight (4°C), and fixed (4% paraformaldehyde) 60 minutes (4°C) (Lobe *et al.*, 1999).

Immunohistochemistry

Paraffin sections (15 micrometer) of P0 *Foxb1^{Cre}/ROSA26R* mouse brains were dewaxed, preincubated in PBT/10% fetal calf serum and incubated overnight (4°C) in antibody. Alexa (Molecular Probes-Invitrogen, Karlsruhe, Germany) fluorescent secondary antibodies were used for visualization (1/500). Antibodies: anti-MCH (rabbit, 1/100) Phoenix Pharmaceuticals, Burlingame, California; anti-orexin (mouse, 1/10) R&D Systems GmbH, Wiesbaden, Germany; anti-GAD "pan" antibody (rabbit, 1/100) Abcam, Cambridge, UK; anti-Calbindin (rabbit, 1/100) Chemicon-Millipore GmbH, Schwalbach, Germany; anti-Calretinin (rabbit, 1/200) Swant, Bellinzona,

Switzerland; anti- β -galactosidase (chicken, 1/100) Abcam; anti-GFAP (rabbit, 1/200) DakoCytomation; anti-neurofilaments (2H3, 1/5, this mouse monoclonal antibody, developed by T. M. Jessell and J. Dodd, was obtained from the Developmental Studies Hybridoma Bank developed under the auspices of the NICHD and maintained by The University of Iowa, Department of Biology, Iowa City, IA 52242).

Microscopy

Leica DMR and MZ APO microscopes (Leica Mikrosysteme, Wetzlar, Germany), Olympus DP50 cameras (Olympus, Tokyo, Japan) and Cell-F 2.6 software (Olympus Soft Imaging Solutions GmbH, Münster, Germany) were used for analysis and photography. Image contrast was enhanced by applying Photoshop 7.0 (Adobe Systems Inc., San José, California) software tools to one whole image file at a time.

RESULTS

Lineage-labeling with the *Foxb1-Cre* mouse line

The *Foxb1-Cre* mouse line (Zhao *et al.*, 2007) carries the recombinase *Cre* under the control of the regulatory sequences of *Foxb1*. To use this line as a marker of the *Foxb1* lineage, we crossed it with reporter mouse lines, engineered to carry inactive reporter genes (e.g. easily detected enzymes like β -galactosidase or alkaline phosphatase) in every cell. In the mouse progeny that we obtained upon crossing the *Foxb1-Cre* mouse line with a reporter mouse line, every cell expressing *Foxb1* carried a reporter gene made permanently active by the *Cre* recombinase. Since the active reporter gene is inherited by any cells derived from *Foxb1*-expressing neuroepithelium, the full *Foxb1* lineage was labeled (see Methods). The mice showed otherwise normal appearance and behavior.

To identify cell migration by lineage-labeling, we compared the location of cells expressing *Foxb1* with the location of *Foxb1*-lineage cells: of necessity, any lineage-labeled cells found beyond the *Foxb1* expression boundary have either migrated from the *Foxb1*-expressing domain or are derived from mitotic neuroepithelium that has expanded from the *Foxb1*-expressing domain. For this reason, we first recorded the expression domains of *Foxb1* in the early diencephalon (Figs. 2-3), using the nomenclature summarized in Fig. 1 (Puelles & Rubenstein, 2003).

Transient expression but extended lineage of *Foxb1* in the diencephalon

Aspects of the *Foxb1* expression pattern have been reported, particularly at postnatal-late prenatal stages (Kaestner *et al.*, 1996; Alvarez-Bolado *et al.*, 1999). For our lineage analysis we needed a complete and systematic exploration of the dynamic changes in the rostral expression boundary, not yet available in the literature.

Foxb1 is expressed in the neural plate from diencephalon to spinal cord (Fig. 2 A) (Ang *et al.*, 1993; Zhao *et al.*, 2007). Early *Foxb1-Cre/ROSA26R* embryos stained *in toto* for β -galactosidase activity showed a general distribution of labeling similar to that of *Foxb1* mRNA (Fig. 2 B). Relatively weak and transient expression in the early diencephalon makes it difficult to assess the distribution of *Foxb1* mRNA in the open neural tube (Fig. 2 C). Lineage labeling, however, yielded a clear picture, although it appeared with a short time lag after *Foxb1* expression (after the *Foxb1* locus becomes active, the Cre recombinase has to be produced at high enough levels to render the reporter gene active, and the reporter enzyme has to be synthesized). Careful examination revealed *Foxb1* lineage-labeled cells in the ventral midline of the presumptive diencephalon and midbrain (Fig. 2 D), as was confirmed by sectioning (inset in Fig. 2 D).

At E9.5, *Foxb1* expression is disappearing from the ventral side of the diencephalon and the ventral midline is not labeled anymore (Fig. 2 E). Lineage-labeling showed a faithful record of previous *Foxb1* expression in the ventral midline (cumulative labeling, Louvi *et al.*, 2007), which was labeled up to eye levels (asterisk in Fig. 2 F). The ventral portion of the diencephalon, including the infundibular region, was labeled

as well. At this age, *Foxb1* expression is high in the dorsal portion of the neural tube, including caudal diencephalon (thalamic region) and midbrain (Fig. 2 E). Accordingly, lineage-labeling began to appear in these regions (Fig. 2 F). At E9.5 the telencephalon is free from *Foxb1* expression (Fig. 2 E) and *Foxb1*-lineage cells (Fig. 2 F).

***Foxb1* expression in the caudal diencephalon peaks early and disappears**

At E11.5, expression of *Foxb1* reaches its peak of intensity in the caudal diencephalon, including a large thalamic (dorsal thalamic) domain and a small prethalamic (ventral thalamic) domain (Fig. 3 A). Expression in the rostral diencephalon (including the hypothalamic primordium) labeled strongly and specifically the mammillary body (Fig. 3 A). Horizontal sections however demonstrated that *Foxb1* is at this stage expressed in the mantle but not in the neuroepithelium anymore (not shown). In the caudal diencephalon, thalamus and tegmentum were heavily labeled while the prethalamus showed labeled and unlabeled cells. In the rostral diencephalon, the dorsal portion did not show any *Foxb1*-lineage cells. In the ventral portion, the mammillary area and adjacent regions were labeled, as well as some cells in the tuberal area (Fig. 3 B). The *Foxb1* lineage in the ventral midline extended rostrally into the retrochiasmatic portion of the basal plate and reached the level of the lamina terminalis (asterisk in Fig. 3 B). At this point, in some cases, the labeled neuroepithelium extended into the basal ganglia (arrow).

At E12.5 the major brain regions are recognizable by specific gene expression

(Shimamura *et al.*, 1995). At this age, *Foxb1* expression has almost completely vanished from the caudal diencephalic neuroepithelium, except for very weak domains in the thalamus and prethalamus (Fig. 3 C), separated by a clear boundary corresponding to the zona limitans interthalamica (arrowhead in Fig. 3 C). In the rostral diencephalon, the mantle layer (postmitotic neurons) of the mammillary body is very strongly labeled also at this age (Fig. 3 C). Lineage-labeling at E12.5 covered the thalamus as well as part of the prethalamus in the caudal diencephalon (Fig. 3 D). The ventral portion of the caudal diencephalon was also completely labeled (Fig. 3 D). In the rostral diencephalon, mammillary area labeling covered a domain larger than the actual *Foxb1* expression in the mammillary body. Numerous labeled cells were also present in the tuberal area (Fig. 3 D). The labeled ventral midline seemed to have ceased expanding rostrally, and its rostral end was at this stage caudal to eye levels (asterisk in Fig. 3 D). However, scattered labeled cells were found at the level of the lamina terminalis (arrows in Fig. 3 D).

In transverse sections, the thalamic neuroepithelium was intensely labeled while the prethalamic neuroepithelium showed labeled and unlabeled cells. Both domains were clearly separated by a sharp boundary (zona limitans) (arrowheads in Fig. 3 E). Fig. 3 F summarizes our findings.

Neuroepithelial migration from diencephalon into the early telencephalon

Foxb1 has been reported as a diencephalic marker, not expressed in the early

telencephalon of the mouse or zebrafish (Kaestner *et al.*, 1996; Wehr *et al.*, 1997; Varga *et al.*, 1999). We confirm this (Figs. 2 E, 3 A, C), indicating that any *Foxb1* lineage cell found in the telencephalon would have migrated from diencephalic levels. Since labeled cells could have been overlooked due to the evagination of the telencephalic vesicles after E10.5, we examined lineage-labeled, transversally sectioned E11.5 brains (Fig. 4 A-D). Surprisingly, at the level where diencephalon and telencephalon are continuous, a trail of labeled neuroepithelial cells entered the cortex (arrowheads in Fig. 4 A-D). The apparent origin of the migrating neuroepithelial cells was in the prethalamus (Fig. 4 B-D). No labeled cells were found in the telencephalon at levels rostral or caudal to the ones shown in Fig. 4 A or Fig. 4 D, respectively.

Extension of axons into hypothalamus before the beginning of migration

To explore the relation of the *Foxb1* lineage with the early thalamic axons, we used the Z/AP reporter mouse line, which carries as reporter an enzyme that attaches to axonal membranes, efficiently labeling the *Foxb1* lineage axons (see Methods). At around E12.5, the thalamo-cortical projection (internal capsule) was visible (Fig. 4 E, F). More caudally, we observed an axonal bundle directed ventrally towards the hypothalamus (Fig. 4 G). At this age, the region of the hypothalamus receiving the axons is devoid of *Foxb1*-lineage cells (Fig. 3 C, D; Fig. 4 F, H). As development proceeded, the thalamo-cortical and thalamo-hypothalamic *Foxb1*-lineage bundles elongated and became increasingly distinct (Fig. 4 I-K).

Migratory routes into ventral diencephalon and telencephalon

Mapping the relation between the *Foxb1* lineage domains and the spatiotemporal pattern of *Foxb1* expression in the forebrain (Figs. 2-3) until it becomes stable or disappears was the prerequisite to analyze cell migration into the hypothalamic primordium. From this point on, detection of *Foxb1* lineage-labeled cells rostral to the boundary would be indicative of migration. At E14.5, *Foxb1*-lineage cells apparently from the prethalamus started migrating in the rostral and ventral direction (arrowheads in Fig. 4 L, M). The migrating cells were associated with thalamo-hypothalamic axons (arrow in Fig. 4 M) and not with the internal capsule (ic in Fig. 4 L, M). This phenomenon became more clear at E15.5, when the migrating cells reached the ventralmost level of the hypothalamus (Fig. 4 N, O). At E18.5 the migrating cell group appeared completely established (Fig. 4 P, Q).

On sagittal sections at different ages (Fig. 5 A-S), we detected two additional migratory routes. Cells from the prethalamus extended rostrally into the presumptive septum on medial levels from E14.5 (arrow in Fig. 5 A) through E15.5 (arrows in Fig. 5 D, F) to E18.5 (arrows in Fig. 5 L, M). The migration into the hypothalamus (see above, Fig. 4) was also evident on sagittal sections at E14.5 (black arrowhead in Fig. 5 C), E15.5 (black arrowheads in Fig. 5 F, G, H, I) and E18.5 (black arrowheads in Fig. 5 N, O). In a third migration route, labeled cells from the caudal hypothalamus migrated into ventral levels of the telencephalon by taking advantage of the ventral diencephalon-telencephalon continuity. This migration became apparent at E15.5

(white arrowheads in Fig. 5 I, K) and was very substantial at E18.5 (white arrowheads in Fig. 5 P-S).

Rostral expansion of caudal diencephalic neuroepithelium

We went on to map the *Foxb1* lineage onto the hypothalamus and telencephalon at postnatal day 0 (P0), when regionalization and most mantle formation are over (Figs. 6, 7).

Sagittal sections through the midline showed that the boundary of the most intensely labeled neuroepithelium (white dotted line in Fig. 6 A) was readily comparable to that found at earlier stages, immediately after *Foxb1* expression has disappeared from the caudal diencephalon (Fig. 3 D). However, we observed several intriguing departures from this pattern, i.e., labeled cells located rostrally to the boundary, in keeping with the migrations observed at earlier stages (Figs. 4, 5).

A region of neuroepithelium rostral to the boundary was labeled with β -galactosidase (asterisks in Fig. 6 A), which was much more rostrally positioned than any *Foxb1* expressing cell has been, and that any *Foxb1*-lineage cell that could be seen at E12.5 (compare with Fig. 3 D). These cells demonstrate a rostral expansion of the caudal diencephalic neuroepithelium (dorsally) and of the mammillary neuroepithelium (ventrally). Transverse sections confirmed this expansion (asterisks in Fig. 7 F-J).

Migration stream from prethalamic levels into the lateral hypothalamus

In the mantle layer, we observed a striking departure from the early *Foxb1* expression and lineage boundaries. A large group of cells was positioned between the zona incerta (prethalamus or ventral thalamus) and the hypothalamus (arrow in Fig. 6 C and Fig. 7 F-H). This cell group seemed the result of the migration stream detected at E14.5 (Fig. 4 L, N and Fig. 5) and it was sharply delimited in the latero-medially (compare Fig. 6 C to Fig. 6 B, D) and rostro-caudally (arrows in Fig. 7 F to H), ending in the lateral hypothalamus at anterior levels.

The lateral hypothalamus at the tuberal level

More caudally (tuberal level), the medial and lateral hypothalamus showed abundant scattered *Foxb1*-lineage cells (Fig. 7 I, J). These cells must either migrate caudo-rostrally through the mantle layer (presumably from the mammillary area), or are generated in the expanded neuroepithelium (asterisks in Fig. 6 A and Fig. 7 I, J). A small and compact group of labeled cells was found consistently in the lateral hypothalamus at this level (arrowhead in Fig. 7 I).

The mantle in the mammillary region

We have mentioned the expansion of the labeled mammillary neuroepithelium (see above). In the rostral diencephalic mantle, the entire mammillary body was formed by cells of the *Foxb1* lineage (Fig. 6 B-D and Fig. 7 K), in agreement with the *Foxb1* expression pattern (Fig. 3 C). The posterior hypothalamus was also formed by

expanded mammillary neuroepithelium, as could be expected from the lineage labeling at E12.5 (Fig. 3 C, D).

Diencephalon-to-telencephalon migrations, medial and lateral

We have established that the early expression domain of *Foxb1* does not reach the telencephalon (Figs. 2-4). However, we found a number of *Foxb1* lineage-labeled cells in the telencephalon at P0. The presence of such labeled cells must be the result of migration from caudal levels or cell division from migrated neuroepithelium (Fig. 4). At medial levels, labeled cells formed a migration stream into the posterior septum (septo-fimbrial nucleus and triangular nucleus of the septum) which was clear on sagittal sections (Fig. 6 A, B) as well as in transverse sections (Fig. 7 A-C). At lateral levels, abundant *Foxb1*-lineage cells migrated from the thalamic region into the amygdala, globus pallidus and piriform cortex (Fig. 6 E, F; Fig. 7 A-C).

Telencephalic settling places of *Foxb1*-lineage cells

To confirm the identity of the telencephalic regions receiving *Foxb1*-lineage cells, we labeled transverse sections of *Foxb1^{Cre}-ROSA26R* neonatal brains (P0) with antibody against β -galactosidase and against glutamic acid decarboxylase (GAD). The distribution of GAD in cell bodies and axon terminals has a well-known and characteristic regional pattern (see for instance Allen Brain Atlas, <http://mouse.brain-map.org>) allowing for the identification of the major areas of the forebrain (Fig. 8). The results confirmed our previous detection of *Foxb1*-lineage cells

in the globus pallidus, amygdala and lateral hypothalamus (Figs. 5, 6).

Characterization of *Foxb1*-lineage cells in telencephalon and hypothalamus

We then carried out an initial characterization of *Foxb1*-lineage cells with antibodies against different neuronal and glial markers (Fig. 9). In the cortex, *Foxb1*-lineage cells were not abundant, and most of them expressed GAD (Fig. 9 A-C). Calretinin was a less frequent marker (Fig. 9 D, E), and we could not detect colocalization with calbindin in any case (Fig. 9 F). *Foxb1*-lineage cells in the amygdala colocalized mostly GAD (Fig. 9 G, H). Two very specific markers of cell populations in the lateral hypothalamus are hypocretin/orexin and melanin concentrating hormone (MCH) (see for instance Cvetkovic *et al.*, 2004). Some of the lateral hypothalamic *Foxb1*-lineage cells coexpressed hypocretin/orexin (Fig. 9 I) or, more often, MCH (Fig. 9 J, K). None of the *Foxb1*-lineage cells coexpressed GFAP, a glial marker. The exception was the lining of the third ventricle, where some radial glial cells (which also express GFAP) were double-labeled (Fig. 9 L), in agreement with our detection of *Foxb1*-lineage in the hypothalamic neuroepithelium (Fig. 7 F-J).

Axon-dependent migration into the lateral hypothalamus

Intriguingly, the migration from prethalamus into the lateral hypothalamus was tangential (rostro-caudal, see Fig. 1), suggesting that axons rather than radial glia could be the substrate (Fig. 10 A). In brains from *Foxb1-Cre/ZAP* crossings, we detected an important axonal bundle apparently coursing from the prethalamic region into the

lateral hypothalamus (Fig. 10 B). The β -galactosidase domain and the alkaline phosphatase domain coincided in size, shape and position (Fig. 10 A, B), suggesting the axon-dependent nature of this migration. By using anti-neurofilament antibody (monoclonal antibody 2H3, green in Fig. 10 C, D) and anti- β -galactosidase antibody (red in Fig. 10 C, D) we confirmed the existence of this axonal bundle.

Diverse migration strategies into the tuberal portion of the lateral hypothalamus

At tuberal levels, the lateral hypothalamus showed abundant labeled cells. In contrast to the compact arrangement of *Foxb1*-lineage cells at anterior levels (Fig. 10 A, B), here labeled cells were mostly scattered (Fig. 10 E). Close inspection of the settling patterns suggested that these cells could have reached their positions in the medial and lateral hypothalamus according to different strategies. In the medial hypothalamus, labeled cells were usually radially arranged and in some cases their trail could be followed to the labeled neuroepithelium (Fig. 10 E, G). In the lateral hypothalamus however, labeled cells were not disposed in radial columns and lacked an obvious connection to the neuroepithelium, suggesting a tangential migration from caudal levels (Fig. 10 E, F). Finally, another group without obvious relation to the neuroepithelium at this level was consistently found in the lateral hypothalamus, ventral to the cerebral peduncle (Fig. 10 H).

Our results are summarized in Fig. 11.

DISCUSSION

Because of the position of its rostral expression boundary, *Foxb1* lineage-labeling can detect tangential migrations from caudal levels into the rostral diencephalon and the telencephalon. One caveat is that inside the rostral diencephalon there is a source of *Foxb1*-lineage cells, the mammillary area, which contributes cells to more rostral regions (caudo-rostral intrahypothalamic migration). *Foxb1* lineage-mapping reveals overall cell migrations but is not appropriate for detailed mechanistic analysis of specific migrating cohorts whose settling point is known (see for instance Henderson *et al.*, 1999).

Tangential migration in the hypothalamus

Hypothalamic migration is mostly radial (Altman & Bayer, 1986), which does not exclude tangential migration, as most of the forebrain shows a mixed pattern of radial and non-radial migration (Balaban *et al.*, 1988). Tangential migration uses axons as a substrate (axonophilic/neuronophilic migration, Rakic, 1990; Golden *et al.*, 1997), but neurons can migrate through a permissive corridor of membrane-attached molecules (Wichterle *et al.*, 2003) or even precede the axons (Lopez-Bendito *et al.*, 2006). Several functionally important neuronal groups enter the hypothalamus following non-radial trajectories. Gonadotrophin releasing hormone-expressing neurons migrate from nasal epithelium into hypothalamus following tangential axons (Muske & Moore, 1988; Schwanzel-Fukuda & Pfaff, 1989; Wray *et al.*, 1989) in precisely regulated manner

(reviewed in Schwarting *et al.*, 2007). A unique radial-to-tangential migration stream follows radial processes from the lateral ventricle neuroepithelium (telencephalon), entering the diencephalon tangentially to settle in the medial hypothalamus, ventral to the anterior commissure (Henderson *et al.*, 1999). This estrogen-controlled migration results in sexual dimorphism in the preoptic/anterior area (Wolfe *et al.*, 2005; Knoll *et al.*, 2007).

Tangential migration of *Foxb1*-lineage cells into the lateral hypothalamus

Here we uncover a group of *Foxb1*-lineage cells extending from the prethalamus into a restricted lateral hypothalamic region as the result of tangential, axonophilic migration. Although we still do not have a full neurochemical characterization of hypothalamic *Foxb1*-lineage cells, we show that some *Foxb1*-lineage lateral hypothalamic neurons express specific lateral hypothalamic markers (hypocretin or MCH). Developmental, connectional and neurochemical heterogeneity of the MCH-expressing neurons has been reported (Brischoux *et al.*, 2001; Brischoux *et al.*, 2002; Cvetkovic *et al.*, 2004), but to our knowledge the hypocretin/orexin-expressing population has until now been considered homogeneous (Amiot *et al.*, 2005).

Other descriptions of hypothalamic development contain data compatible with this migration. Expression of calretinin shows an early caudal diencephalic domain later extending into the lateral hypothalamus (Abbott & Jacobowitz, 1999), possibly representing a migration stream similar to the one we describe here. Fate-mapping studies of the avian neural plate can provide evidence of longitudinal cell migration. In

chicken, tissue grafted in the vicinity of the thalamic eminence and prethalamus generates cells for the lateral hypothalamus (experiment QFM-38 in Cobos *et al.*, 2001) or dorsal hypothalamus and preoptic area (experiment R-173 in Garcia-Lopez *et al.*, 2004). While our mouse data agree in general with these results, it is not immediately obvious if they describe comparable phenomena.

Additionally, the lateral hypothalamus (tuberal level) contains many labeled cells not radially arranged that could originate in the mammillary area, then migrate caudo-rostrally. One example is the caudal-to-rostral migration from the mammillary body settling in a circumscribed area of the lateral hypothalamus (Fig. 7 I). Since these cells express *Foxb1* (Alvarez-Bolado *et al.*, 2000a), it is in principle possible that they do not migrate but appear to do so.

Neuroepithelial migration into cortex

Part of the lateral hypothalamic neuroepithelium actually migrates from midbrain levels (Manning *et al.*, 2006). Tangential migration of neuroepithelial cells inside the diencephalon is a known but infrequent phenomenon (Arnold-Aldea & Cepko, 1996; Golden *et al.*, 1997). We show that a reduced number of neuroepithelial cells migrates early from caudal diencephalon into telencephalon (Fig. 4 A-D), presumably originating the rare *Foxb1*-lineage cells that we have found in the cortex and which are often interneurons (coexpress GAD). As far as we know, this would be the first report of neuroepithelial migration from diencephalon into cortex giving rise to interneurons.

In the mouse, as a rule, cortical interneurons are generated in the basal ganglia (Marin & Rubenstein, 2003).

Additionally, we show what appears as clonal expansion of the neuroepithelium in a very specific hypothalamic region giving rise to cells for the tuberal level.

Different types of radial migration in the hypothalamus

Tuberal nuclei (ventromedial and arcuate) are generated locally by the neuroepithelium of the third ventricle (McClellan *et al.*, 2008). However, some radially migrating *Foxb1*-lineage cells seem to contribute to the arcuate, suggesting a contribution from "expanded" neuroepithelium. Radial migration from neuroepithelium which has previously expanded tangentially can be considered a special case of the general radial pattern found in hypothalamus. Other specific hypothalamic subpopulations show characteristic variations on radial migration, for instance the parvicellular endocrine neurons migrate tangentially but do not follow the outside-in rule (Markakis & Swanson, 1997).

Diencephalic migration into the telencephalon

No clearcut boundary separates diencephalon from telencephalon (Inoue *et al.*, 2000; Puelles *et al.*, 2000; Trujillo *et al.*, 2005), allowing for migration between them (Mitrofanis, 1994; Henderson *et al.*, 1999; Letinic & Rakic, 2001; Morante-Oria *et al.*, 2003). We have detected a novel migration stream from the dorsal diencephalon to the posterior septum and possibly the globus pallidus, as well as a migratory route from the

caudal hypothalamus into piriform cortex and amygdala. Two caveats apply here. A subpopulation of piriform cortex neurons expresses *Foxb1* at a later stage of development (around E14.5) (Alvarez-Bolado *et al.*, 1999), so they may not be related with more caudal neuroepithelium by lineage. Besides, a reduced number of *Foxb1* lineage-labeled ventral midline cells reach the lamina terminalis and enter the basal ganglia (Fig. 3 B, D), and some prethalamic neuroepithelial cells migrate into the telencephalon (Fig. 4 A-D), therefore some of the labeled cells in septum and pallidum could originate in migrated neuroepithelium (as opposed to tangentially migrating through the mantle).

***Foxb1* lineage in the ventral midline**

The dorsal and ventral portions of the early neural tube meet at optic sulcus level, marking the ventral midline's rostral end (Barth & Wilson, 1995; Shimamura *et al.*, 1995). At E8.5 and E9.5, the rostral end of the *Foxb1*-lineage domain is also at the optic level (as in zebrafish; Varga *et al.*, 1999). Later, the ventral midline *Foxb1* lineage extends briefly into dorsal levels (E11.5; Fig. 3 B) to finally end at tuberal level (E12.5; Fig. 3 D), due to differential growth of forebrain areas. In zebrafish and *Xenopus* the hypothalamus derives mostly from the ventral midline (Eagleson & Harris, 1990; Woo & Fraser, 1995; Varga *et al.*, 1999; Staudt & Houart, 2007). The present work and previous fate-mapping data (chicken, Cobos *et al.*, 2001; Fernandez-Garre *et al.*, 2002; Garcia-Lopez *et al.*, 2004; mouse, Inoue *et al.*, 2000) show that the hypothalamus of birds and mammals originates from more dorsal and lateral neuroepithelium as well.

ACKNOWLEDGEMENTS

We thank Michael Kessel (Max Planck Institute, Göttingen), Mario Wullimann (University of Munich) and Loreta Medina (Institut de Recerca Biomèdica, Lleida) for critical reading of an earlier version. Ulrike Teichmann's team took care of the mouse mutants. Supported by the Max-Planck-Gesellschaft, the National Natural Science Foundation of China (90608002 and 30700406) and the Ministry of Science and Technology of China (2007CB947100)

ABBREVIATIONS

3V, third ventricle; AHA, anterior hypothalamic area; AMY, amygdala; ARH, arcuate nucleus; DI, diencephalon; CTX, cortex; GAD, glutamic acid decarboxylase; GFAP, glial fibrillary acidic protein; GP, globus pallidus; inf, infundibulum; hPLAP, human placental alkaline phosphatase; HYP, hypothalamus; ic, internal capsule; ISH, in situ hybridization; LGd, lateral geniculate dorsal; LHA, lateral hypothalamic area; LM, lateral mammillary nucleus; LV, lateral ventricle; MAM, mammillary area; MCH, melanin concentrating hormone; MBO, mammillary body; os, optic sulcus; PBS, phosphate buffer saline; PBT, phosphate buffer Tween; PH, posterior hypothalamus; PIR, piriform cortex; PRO, preoptic area; PT, pretectum; PTh, prethalamus (ventral thalamus); TG, tegmentum; Th, thalamus (dorsal thalamus); TL, telencephalon; TUB, tuberal area; ZI, zona incerta.

REFERENCES

- Abbott, L.C. & Jacobowitz, D.M. (1999) Developmental expression of calretinin-immunoreactivity in the thalamic eminence of the fetal mouse. *Int J Dev Neurosci*, **17**, 331-345.
- Altman, J. & Bayer, S.A. (1986) *The Development of the Rat Hypothalamus*.
- Alvarez-Bolado, G., Cecconi, F., Wehr, R. & Gruss, P. (1999) The fork head transcription factor Fkh5/Mf3 is a developmental marker gene for superior colliculus layers and derivatives of the hindbrain somatic afferent zone. *Brain Res Dev Brain Res*, **112**, 205-215.
- Alvarez-Bolado, G., Rosenfeld, M.G. & Swanson, L.W. (1995) Model of forebrain regionalization based on spatiotemporal patterns of POU-III homeobox gene expression, birthdates, and morphological features. *J Comp Neurol*, **355**, 237-295.
- Alvarez-Bolado, G. & Swanson, L.W. (1996) *Developmental Brain Maps: The Structure of the Embryonic Rat Brain*. Elsevier.
- Alvarez-Bolado, G., Zhou, X., Cecconi, F. & Gruss, P. (2000a) Expression of Foxb1 reveals two strategies for the formation of nuclei in the developing ventral diencephalon. *Dev Neurosci*, **22**, 197-206.
- Alvarez-Bolado, G., Zhou, X., Voss, A.K., Thomas, T. & Gruss, P. (2000b) Winged helix transcription factor Foxb1 is essential for access of mammillothalamic axons to the thalamus. *Development*, **127**, 1029-1038.
- Amiot, C., Brischoux, F., Colard, C., La Roche, A., Fellmann, D. & Risold, P.Y. (2005) Hypocretin/orexin-containing neurons are produced in one sharp peak in the developing ventral diencephalon. *Eur J Neurosci*, **22**, 531-534.
- Ang, S.L., Wierda, A., Wong, D., Stevens, K.A., Cascio, S., Rossant, J. & Zaret, K.S. (1993) The formation and maintenance of the definitive endoderm lineage in the mouse: involvement of HNF3/forkhead proteins. *Development*, **119**, 1301-1315.
- Arnold-Aldea, S.A. & Cepko, C.L. (1996) Dispersion patterns of clonally related cells during development of the hypothalamus. *Dev Biol*, **173**, 148-161.
- Balaban, E., Teillet, M.A. & Le Douarin, N. (1988) Application of the quail-chick chimera system to the study of brain development and behavior. *Science*, **241**, 1339-1342.
- Barth, K.A. & Wilson, S.W. (1995) Expression of zebrafish nk2.2 is influenced by sonic hedgehog/vertebrate hedgehog-1 and demarcates a zone of neuronal differentiation in the embryonic forebrain. *Development*, **121**, 1755-1768.
- Brischoux, F., Cvetkovic, V., Griffond, B., Fellmann, D. & Risold, P.Y. (2002) Time of genesis determines projection and neurokinin-3 expression patterns of diencephalic neurons containing melanin-concentrating hormone. *Eur J Neurosci*, **16**, 1672-1680.

- Brischoux, F., Fellmann, D. & Risold, P.Y. (2001) Ontogenetic development of the diencephalic MCH neurons: a hypothalamic 'MCH area' hypothesis. *Eur J Neurosci*, **13**, 1733-1744.
- Caqueret, A., Boucher, F. & Michaud, J.L. (2006) Laminar organization of the early developing anterior hypothalamus. *Dev Biol*, **298**, 95-106.
- Caqueret, A., Yang, C., Duplan, S., Boucher, F. & Michaud, J.L. (2005) Looking for trouble: a search for developmental defects of the hypothalamus. *Horm Res*, **64**, 222-230.
- Chenn, A. & McConnell, S.K. (1995) Cleavage orientation and the asymmetric inheritance of Notch1 immunoreactivity in mammalian neurogenesis. *Cell*, **82**, 631-641.
- Cobos, I., Shimamura, K., Rubenstein, J.L., Martinez, S. & Puelles, L. (2001) Fate map of the avian anterior forebrain at the four-somite stage, based on the analysis of quail-chick chimeras. *Dev Biol*, **239**, 46-67.
- Cvetkovic, V., Brischoux, F., Jacquemard, C., Fellmann, D., Griffond, B. & Risold, P.Y. (2004) Characterization of subpopulations of neurons producing melanin-concentrating hormone in the rat ventral diencephalon. *J Neurochem*, **91**, 911-919.
- Dymecki, S.M. & Kim, J.C. (2007) Molecular neuroanatomy's "Three Gs": a primer. *Neuron*, **54**, 17-34.
- Eagleson, G.W. & Harris, W.A. (1990) Mapping of the presumptive brain regions in the neural plate of *Xenopus laevis*. *J Neurobiol*, **21**, 427-440.
- Fernandez-Garre, P., Rodriguez-Gallardo, L., Gallego-Diaz, V., Alvarez, I.S. & Puelles, L. (2002) Fate map of the chicken neural plate at stage 4. *Development*, **129**, 2807-2822.
- Fields-Berry, S.C., Halliday, A.L. & Cepko, C.L. (1992) A recombinant retrovirus encoding alkaline phosphatase confirms clonal boundary assignment in lineage analysis of murine retina. *Proc Natl Acad Sci U S A*, **89**, 693-697.
- Fishell, G., Mason, C.A. & Hatten, M.E. (1993) Dispersion of neural progenitors within the germinal zones of the forebrain. *Nature*, **362**, 636-638.
- Garcia-Lopez, R., Vieira, C., Echevarria, D. & Martinez, S. (2004) Fate map of the diencephalon and the zona limitans at the 10-somites stage in chick embryos. *Dev Biol*, **268**, 514-530.
- Golden, J.A. & Cepko, C.L. (1996) Clones in the chick diencephalon contain multiple cell types and siblings are widely dispersed. *Development*, **122**, 65-78.
- Golden, J.A., Zitz, J.C., McFadden, K. & Cepko, C.L. (1997) Cell migration in the developing chick diencephalon. *Development*, **124**, 3525-3533.
- Gustincich, S., Feigenspan, A., Wu, D.K., Koopman, L.J. & Raviola, E. (1997) Control of dopamine release in the retina: a transgenic approach to neural networks. *Neuron*, **18**, 723-736.
- Henderson, R.G., Brown, A.E. & Tobet, S.A. (1999) Sex differences in cell migration in the preoptic area/anterior hypothalamus of mice. *J Neurobiol*, **41**, 252-266.
- Inoue, T., Nakamura, S. & Osumi, N. (2000) Fate mapping of the mouse prosencephalic neural plate. *Dev Biol*, **219**, 373-383.

- Joyner, A.L. & Zervas, M. (2006) Genetic inducible fate mapping in mouse: establishing genetic lineages and defining genetic neuroanatomy in the nervous system. *Dev Dyn*, **235**, 2376-2385.
- Kaestner, K.H., Schutz, G. & Monaghan, A.P. (1996) Expression of the winged helix genes fkh-4 and fkh-5 defines domains in the central nervous system. *Mech Dev*, **55**, 221-230.
- Kloetzli, J.M., Fontaine-Glover, I.A., Brown, E.R., Kuo, M. & Labosky, P.A. (2001) The winged helix gene, Foxb1, controls development of mammary glands and regions of the CNS that regulate the milk-ejection reflex. *Genesis*, **29**, 60-71.
- Knoll, J.G., Wolfe, C.A. & Tobet, S.A. (2007) Estrogen modulates neuronal movements within the developing preoptic area-anterior hypothalamus. *Eur J Neurosci*, **26**, 1091-1099.
- Koenen, M., Ruther, U. & Muller-Hill, B. (1982) Immunoenzymatic detection of expressed gene fragments cloned in the lac Z gene of E. coli. *Embo J*, **1**, 509-512.
- Labosky, P.A., Winnier, G.E., Jetton, T.L., Hargett, L., Ryan, A.K., Rosenfeld, M.G., Parlow, A.F. & Hogan, B.L. (1997) The winged helix gene, Mf3, is required for normal development of the diencephalon and midbrain, postnatal growth and the milk-ejection reflex. *Development*, **124**, 1263-1274.
- Leighton, P.A., Mitchell, K.J., Goodrich, L.V., Lu, X., Pinson, K., Scherz, P., Skarnes, W.C. & Tessier-Lavigne, M. (2001) Defining brain wiring patterns and mechanisms through gene trapping in mice. *Nature*, **410**, 174-179.
- Letinic, K. & Rakic, P. (2001) Telencephalic origin of human thalamic GABAergic neurons. *Nat Neurosci*, **4**, 931-936.
- Lobe, C.G., Koop, K.E., Kreppner, W., Lomeli, H., Gertsenstein, M. & Nagy, A. (1999) Z/AP, a double reporter for cre-mediated recombination. *Dev Biol*, **208**, 281-292.
- Lopez-Bendito, G., Cautinat, A., Sanchez, J.A., Bielle, F., Flames, N., Garratt, A.N., Talmage, D.A., Role, L.W., Charnay, P., Marin, O. & Garel, S. (2006) Tangential neuronal migration controls axon guidance: a role for neuregulin-1 in thalamocortical axon navigation. *Cell*, **125**, 127-142.
- Louvi, A., Yoshida, M. & Grove, E.A. (2007) The derivatives of the Wnt3a lineage in the central nervous system. *J Comp Neurol*, **504**, 550-569.
- Manning, L., Ohyama, K., Saeger, B., Hatano, O., Wilson, S.A., Logan, M. & Placzek, M. (2006) Regional morphogenesis in the hypothalamus: a BMP-Tbx2 pathway coordinates fate and proliferation through Shh downregulation. *Dev Cell*, **11**, 873-885.
- Marin, O. & Rubenstein, J.L. (2003) Cell migration in the forebrain. *Annu Rev Neurosci*, **26**, 441-483.
- Markakis, E.A. & Swanson, L.W. (1997) Spatiotemporal patterns of secretomotor neuron generation in the parvicellular neuroendocrine system. *Brain Res Brain Res Rev*, **24**, 255-291.
- McClellan, K.M., Calver, A.R. & Tobet, S.A. (2008) GABAB receptors role in cell migration and positioning within the ventromedial nucleus of the hypothalamus.

- Neuroscience*, **151**, 1119-1131.
- Michaud, J.L. (2001) The developmental program of the hypothalamus and its disorders. *Clin Genet*, **60**, 255-263.
- Mitrofanis, J. (1994) Development of the thalamic reticular nucleus in ferrets with special reference to the perigeniculate and perireticular cell groups. *Eur J Neurosci*, **6**, 253-263.
- Morante-Oria, J., Carleton, A., Ortino, B., Kremer, E.J., Fairen, A. & Lledo, P.M. (2003) Subpallial origin of a population of projecting pioneer neurons during corticogenesis. *Proc Natl Acad Sci U S A*, **100**, 12468-12473.
- Muske, L.E. & Moore, F.L. (1988) The nervus terminalis in amphibians: anatomy, chemistry and relationship with the hypothalamic gonadotropin-releasing hormone system. *Brain Behav Evol*, **32**, 141-150.
- Paxinos, G. & Franklin, K.B.J. (2001) *The mouse brain in stereotaxic coordinates*. Academic Press, San Diego.
- Puelles, L., Kuwana, E., Puelles, E., Bulfone, A., Shimamura, K., Keleher, J., Smiga, S. & Rubenstein, J.L. (2000) Pallial and subpallial derivatives in the embryonic chick and mouse telencephalon, traced by the expression of the genes *Dlx-2*, *Emx-1*, *Nkx-2.1*, *Pax-6*, and *Tbr-1*. *J Comp Neurol*, **424**, 409-438.
- Puelles, L. & Rubenstein, J.L. (2003) Forebrain gene expression domains and the evolving prosomeric model. *Trends Neurosci*, **26**, 469-476.
- Rakic, P. (1988) Specification of cerebral cortical areas. *Science*, **241**, 170-176.
- Rakic, P. (1990) Principles of neural cell migration. *Experientia*, **46**, 882-891.
- Schwanzel-Fukuda, M. & Pfaff, D.W. (1989) Origin of luteinizing hormone-releasing hormone neurons. *Nature*, **338**, 161-164.
- Schwarting, G.A., Wierman, M.E. & Tobet, S.A. (2007) Gonadotropin-releasing hormone neuronal migration. *Semin Reprod Med*, **25**, 305-312.
- Shimamura, K., Hartigan, D.J., Martinez, S., Puelles, L. & Rubenstein, J.L. (1995) Longitudinal organization of the anterior neural plate and neural tube. *Development*, **121**, 3923-3933.
- Sillitoe, R.V. & Joyner, A.L. (2007) Morphology, molecular codes, and circuitry produce the three-dimensional complexity of the cerebellum. *Annu Rev Cell Dev Biol*, **23**, 549-577.
- Simerly, R.B. (2004) Anatomical substrates of hypothalamic integration. In Paxinos, G. (ed.) *The rat nervous system*. Elsevier, Amsterdam, pp. 335-368.
- Soriano, P. (1999) Generalized lacZ expression with the ROSA26 Cre reporter strain. *Nat Genet*, **21**, 70-71.
- Staudt, N. & Houart, C. (2007) The prethalamus is established during gastrulation and influences diencephalic regionalization. *PLoS Biol*, **5**, e69.
- Swanson, L.W. (1987) The hypothalamus. In Björklund, A., Hökfelt, T. and Swanson, L. W. (ed.) *Handbook of chemical neuroanatomy*. Elsevier, Amsterdam, pp. 1-124.
- Tobet, S.A. (2002) Genes controlling hypothalamic development and sexual differentiation. *Eur J Neurosci*, **16**, 373-376.
- Trujillo, C.M., Alonso, A., Delgado, A.C. & Damas, C. (2005) The rostral and caudal boundaries of the diencephalon. *Brain Res Brain Res Rev*, **49**, 202-210.

- Varga, Z.M., Wegner, J. & Westerfield, M. (1999) Anterior movement of ventral diencephalic precursors separates the primordial eye field in the neural plate and requires cyclops. *Development*, **126**, 5533-5546.
- Wehr, R., Mansouri, A., de Maeyer, T. & Gruss, P. (1997) Fkh5-deficient mice show dysgenesis in the caudal midbrain and hypothalamic mammillary body. *Development*, **124**, 4447-4456.
- Wichterle, H., Alvarez-Dolado, M., Erskine, L. & Alvarez-Buylla, A. (2003) Permissive corridor and diffusible gradients direct medial ganglionic eminence cell migration to the neocortex. *Proc Natl Acad Sci U S A*, **100**, 727-732.
- Wilkinson, D.G. (1992) *In situ hybridization: A practical approach*. IRL Press, Oxford.
- Wolfe, C.A., Van Doren, M., Walker, H.J., Seney, M.L., McClellan, K.M. & Tobet, S.A. (2005) Sex differences in the location of immunochemically defined cell populations in the mouse preoptic area/anterior hypothalamus. *Brain Res Dev Brain Res*, **157**, 34-41.
- Woo, K. & Fraser, S.E. (1995) Order and coherence in the fate map of the zebrafish nervous system. *Development*, **121**, 2595-2609.
- Wray, S., Grant, P. & Gainer, H. (1989) Evidence that cells expressing luteinizing hormone-releasing hormone mRNA in the mouse are derived from progenitor cells in the olfactory placode. *Proc Natl Acad Sci U S A*, **86**, 8132-8136.
- Zervas, M., Blaess, S. & Joyner, A.L. (2005) Classical embryological studies and modern genetic analysis of midbrain and cerebellum development. *Curr Top Dev Biol*, **69**, 101-138.
- Zhao, T., Zhou, X., Szabo, N., Leitges, M. & Alvarez-Bolado, G. (2007) Foxb1-driven Cre expression in somites and the neuroepithelium of diencephalon, brainstem, and spinal cord. *Genesis*, **45**, 781-787.

FIGURE LEGENDS

Figure 1. Subdivisions of the diencephalon in the E12.5 mouse embryo

Figure 2. Transient expression but extended lineage of *Foxb1* in the diencephalon

A) *Foxb1* whole mount ISH on E8.5 mouse embryo showing expression in diencephalon, not telencephalon (separated by a straight line).

B) β -galactosidase detection on *Foxb1*^{Cre}-*ROSA26R* embryo at the beginning of neurulation.

C) shows the same embryo as in (A) from the top.

D) View from top of the embryo in (B) showing the basal plate of the presumptive diencephalon. Inset shows section through the dotted line in (B). *Foxb1*-expressing cells are found in the diencephalic ventral midline and adjacent to it. Asterisks mark the rostral tip of expression in the ventral midline of (D) and inset.

E, F) At E9.5, *Foxb1* mRNA has disappeared from ventral rostral diencephalon (E), while lineage labeling shows the ventral midline labeled up to eye levels (asterisk in F).

Figure 3. *Foxb1* expression in the caudal diencephalon peaks early and disappears

A, C) *Foxb1* whole-mount ISH on hemisected embryonic mouse heads. B, D)

β -galactosidase activity detection on hemisected embryonic *Foxb1*^{Cre}-*ROSA26R* mouse heads.

A) At E11.5, *Foxb1* expression peaks in thalamus, prethalamus and midbrain. Rostral to

the mammillary body there is no expression.

B) *Foxb1* lineage labeling at E11.5 occupies the ventral midline of the entire neural tube with a rostral limit at the level of the lamina terminalis (asterisk). Arrow points at *Foxb1*-lineage cells in the basal ganglia region. Thalamus, prethalamus, mammillary area and part of the tuberal area are also labeled.

C) At E12.5, *Foxb1* expression in the caudal diencephalon is disappearing. White arrowhead, zona limitans.

D) At E12.5, the *Foxb1* lineage forms most of the dorsal and ventral caudal diencephalon, including part of the prethalamus (ventral thalamus). The mammillary and part of the tuberal areas are labeled. White arrowhead, zona limitans. Asterisk marks rostralmost extent of *Foxb1* lineage; scattered cells are found more dorsally (arrows).

E) Transverse section through the caudal diencephalon of an E11.5 embryo.

Arrowheads, zona limitans.

F) Diagram summarizing the distribution of *Foxb1*-lineage cells in the diencephalon at E12.5.

Figure 4. *Foxb1*-lineage cell migration and axonal bundle formation

Reporter detection on transverse sections through *Foxb1*^{Cre}-*ROSA26R* (A-D, F, H, L-Q) and *Foxb1*^{Cre}-*Z/AP* (E, G, I-K) brains of the ages indicated.

A-D) E11.5 brains. Arrowheads point at *Foxb1*-lineage labeled cells seemingly abandoning the diencephalon to enter the medial cortex. (A) shows the most rostral, (D)

the most caudal section. No labeled cells were found rostral to (A) or caudal to (B).

Dotted line in (D), interventricular connection.

E-H) E12.5 brains. Rostral sections (E, G) show internal capsule (ic) formation. Caudal sections (G, H) show formation of thalamo-hypothalamic axonal bundle (arrow in G) before *Foxb1*-lineage cells appear in the hypothalamus (Hy) (H).

I-K) E13.5 brains. Rostral section (I) shows internal capsule, more caudal sections show thalamo-hypothalamic axons (arrow in J, K).

L-M) E14.5 brains. The area framed in (L) is shown magnified in (M). The internal capsule (ic) can be seen together with a ventrally directed axonal bundle (arrow in M). *Foxb1*-lineage cells (arrowheads in L, M) start migrating alongside these axons.

N-O) E15.5 brains. The area framed in (N) is shown magnified in (O). Migrating cells (arrowheads) from the prethalamus stream into the hypothalamus.

P-Q) E18.5 brains. The area framed in (P) is shown magnified in (Q). The migratory stream is completely established.

Figure 5. Migration routes of *Foxb1*-lineage cells in the forebrain

Reporter detection on sagittal sections (rostral to the left) through *Foxb1*^{Cre}-*ROSA26R* brains of the ages indicated.

A-C) At E14.5, labeled cells appeared expanding in the rostral direction (arrow in A) as well as leaving the thalamic region in the ventral direction (arrowhead in C). No migrating cells were present at medial levels (A, B) or in the ventral forebrain.

D, F, H, J) E15.5 sagittal sections at low magnification and the corresponding high

magnification details (E, G, I, K) show how labeled cells from the thalamic region move towards the septum (arrows in D, F). Other labeled cells streaming from the thalamic region (black arrowheads in D-I) reach ventral levels. At lateral levels, labeled cells from the caudal hypothalamus enter the telencephalon (white arrowheads in I, K). L, N, P, R) E18.5 sagittal sections at low magnification and the corresponding high magnification details (M, O, Q, S). Arrows in L, M show the labeled septum. Black arrowheads in N, O mark the thalamo-hypothalamic migration. White arrowheads in P-S mark labeled cells at the boundary between hypothalamus and ventral telencephalon.

Figure 6. Mantle and neuroepithelium from caudal diencephalon extend into telencephalon and rostral diencephalon

A-F) Sagittal sections through postnatal day 0 (P0) *Foxb1^{Cre}-ROSA26R* mouse brain stained for β -galactosidase activity. Insets show plane of section. White dotted line in (A) shows rostral boundary of *Foxb1* lineage at E11.5 (peak expression). Red line in (A-C) marks approximate dorsal-ventral boundary. Black dotted line in A-C marks the optic chiasm (A) or optic tract (B, C).

A, B) Medial sections show migration from thalamus into posterior septum (A, B), as well as rostral expansion of the neuroepithelium (asterisks in A).

C) A stream of cells (arrow) links the caudal diencephalic mantle to the lateral hypothalamus at anterior levels.

D) Derivatives of the mammillary area belong to the *Foxb1* lineage.

E, F) Lateral sections show diencephalic migration into telencephalic regions: globus pallidus, ventral pallidum, amygdala, piriform cortex.

Figure 7. Different regions of the lateral hypothalamus show differential pattern of colonization by *Foxb1*-lineage cells

A-K) Transverse sections through a postnatal day 0 (P0) *Foxb1^{Cre}-ROSA26R* mouse brain stained for β -galactosidase activity.

A, B) Contribution of *Foxb1* lineage to the telencephalon: septum, piriform cortex and ventral pallidum.

C) The most rostral portion of the lateral hypothalamus does not receive *Foxb1*-lineage cells.

D-H) The lateral hypothalamus at anterior levels receives a stream of cells (arrow in F-H) apparently from the zona incerta.

I, J) At tuberal levels, the medial and lateral hypothalamus have abundant labeled scattered cells presumably originated in the labeled neuroepithelium. Arrowhead in (I) marks a previously known *Foxb1*-expressing population.

K) The entire mantle of the mammillary area is from *Foxb1* lineage.

Asterisk in F-J shows the *Foxb1*-lineage neuroepithelium of the third ventricle.

Figure 8. *Foxb1*-lineage cells in basal ganglia and hypothalamus

Transverse sections (A, D, G, J) and high-magnification details (B, C, E, F, H, I, K, L) at four characteristic rostro-caudal levels of a postnatal day 0 (P0) *Foxb1^{Cre}-ROSA26R*

brain labeled with antibodies for glutamic acid decarboxylase (GAD, red) and β -galactosidase (green). Scattered *Foxb1*-lineage cells are present in the hypothalamus, amygdala and globus pallidus at every level. The thalamus is devoid of GAD (except in the lateral geniculate nucleus, K) but shows abundant *Foxb1*-lineage cells (D, G, J). The prethalamus shows abundant colocalization of both markers (G, J). Dotted line in (A), fornix.

Figure 9. Characterization of *Foxb1*-lineage cells in the forebrain

A-L) Antibody detection of cell-type specific markers (red; marker as indicated on the panels) and β -galactosidase (green) in the cortex (A-F), amygdala (G, H), hypothalamus (I-K) and third ventricle (L) of P0 *Foxb1^{Cre}-ROSA26R* brains. Large arrows mark colocalization, small arrows mark *Foxb1*-lineage cells without marker colocalization, and arrowheads mark cells expressing a specific marker but no β -galactosidase.

Figure 10. Migration strategies into the hypothalamus

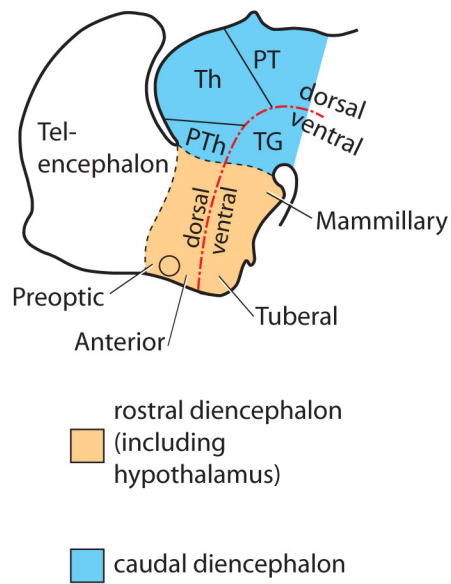
A, E-H) Transverse sections through a P0 *Foxb1^{Cre}-ROSA26R* brain stained for β -galactosidase activity. B) Transverse section through postnatal day 0 (P0) *Foxb1^{Cre}-Z/AP* mouse brain stained for alkaline phosphatase activity. C) Transverse section through a P0 *Foxb1^{Cre}-ROSA26R* brain labeled for neurofilaments (green) and β -galactosidase (red). D) High-magnification image of the area framed in (C).

A, B) A large and compact group of cells (arrowhead in A) enters the rostral portion of

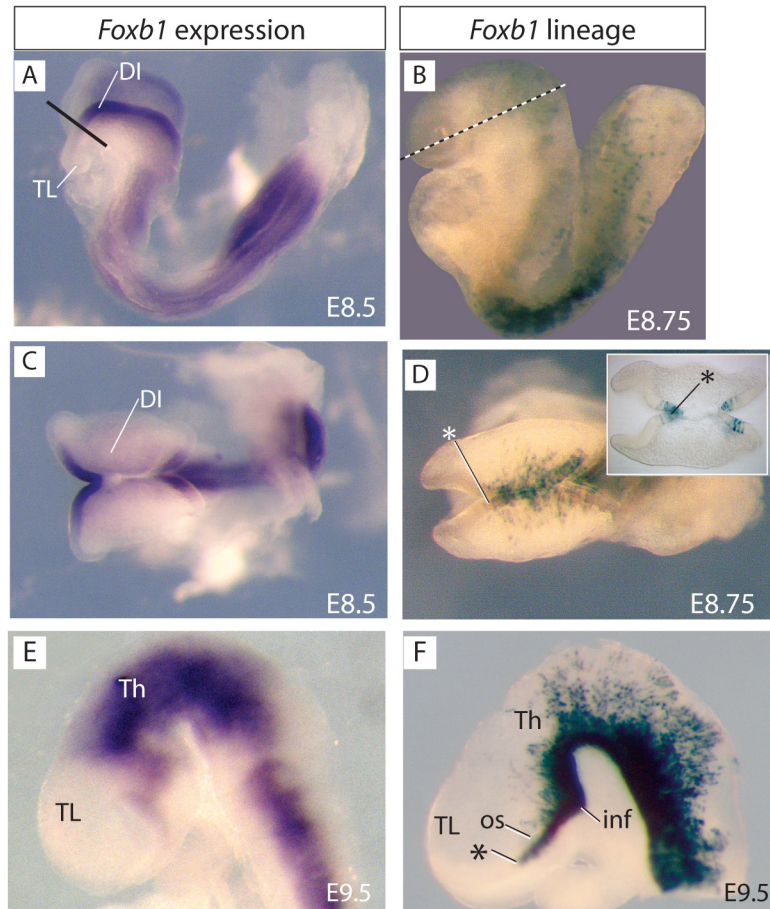
- the lateral hypothalamus from the zona incerta. Axons connecting zona incerta and lateral hypothalamus (arrowhead in B) in the same regions as the migrating cells in (A). C, D) Axons from the prethalamus enter the lateral hypothalamus (framed in C). *Foxb1*-lineage cells (red) can be seen among the axons in the high-magnification panel (D).
- E) Labeled hypothalamic neuroepithelium in the tuberal area. The areas framed in (E) are shown magnified in (F, G).
- F) Non-radially arranged cells in the lateral hypothalamus (tuberal level).
- G) Radially arranged cells in the medial hypothalamus (tuberal level). Arrows indicate direction of migration.
- H) Compact group of non-radial labeled cells (arrowhead) in the lateral hypothalamus (tuberal level).

Figure 11. Multiple diencephalon-originated rostral migrations

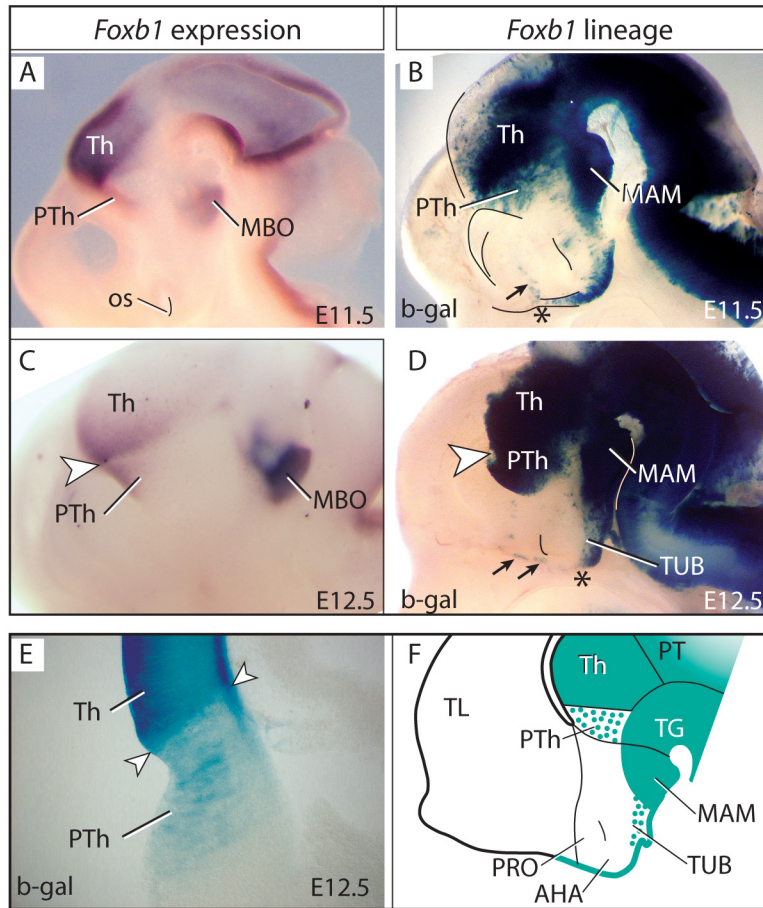
- A) Our findings summarized on a diagram of the E12.5 diencephalon.
- B) Diencephalon-to-telencephalon migrations on the lateral plane.
- C) Diencephalon-to-diencephalon migrations in the dorsal and ventral portions.
- D) Diencephalon-to-telencephalon migrations in the medial plane (red arrow), and migrations from the rostrally expanded neuroepithelium (blue arrows). Asterisk marks the expanded neuroepithelium.



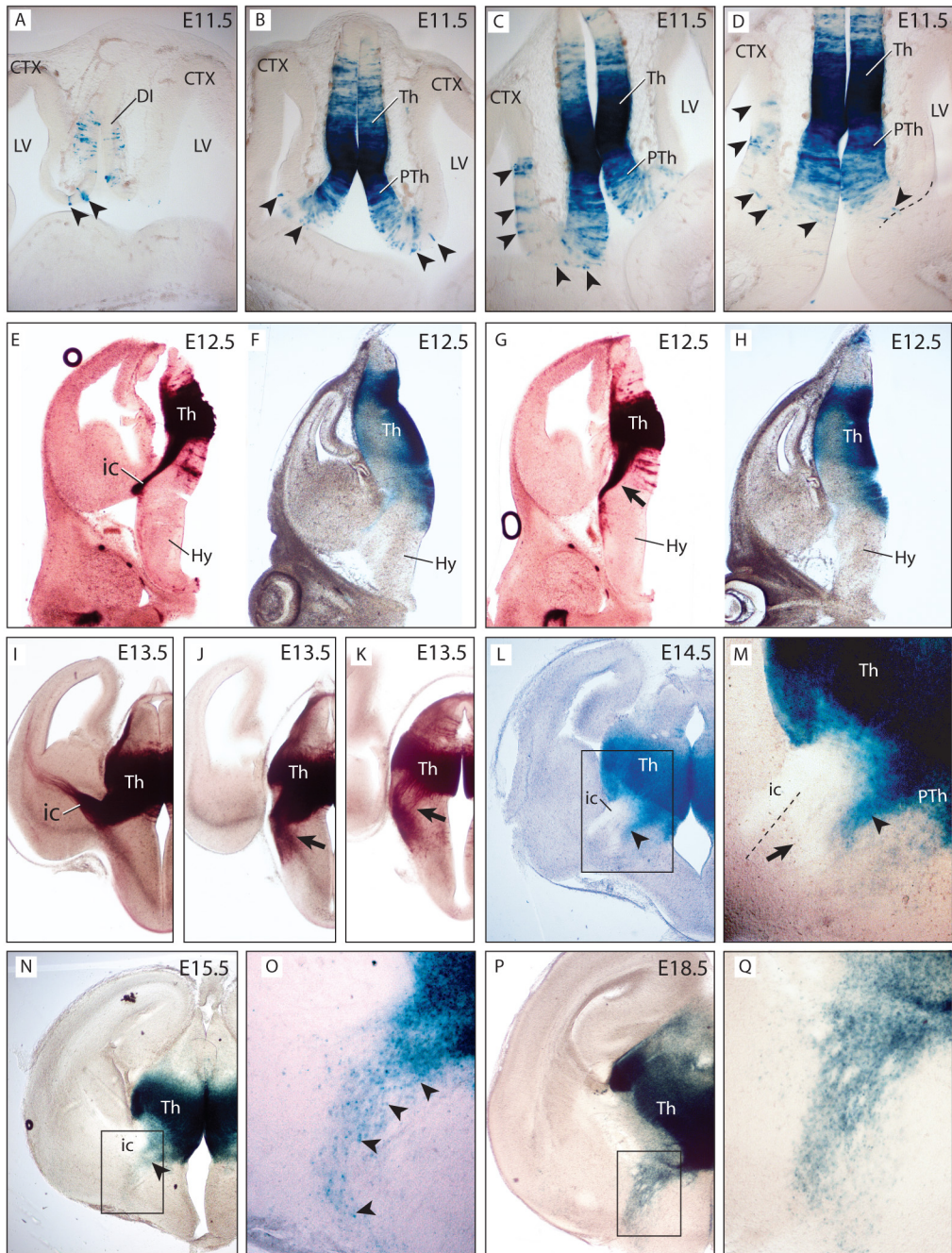
Zhao et al.
Figure 1



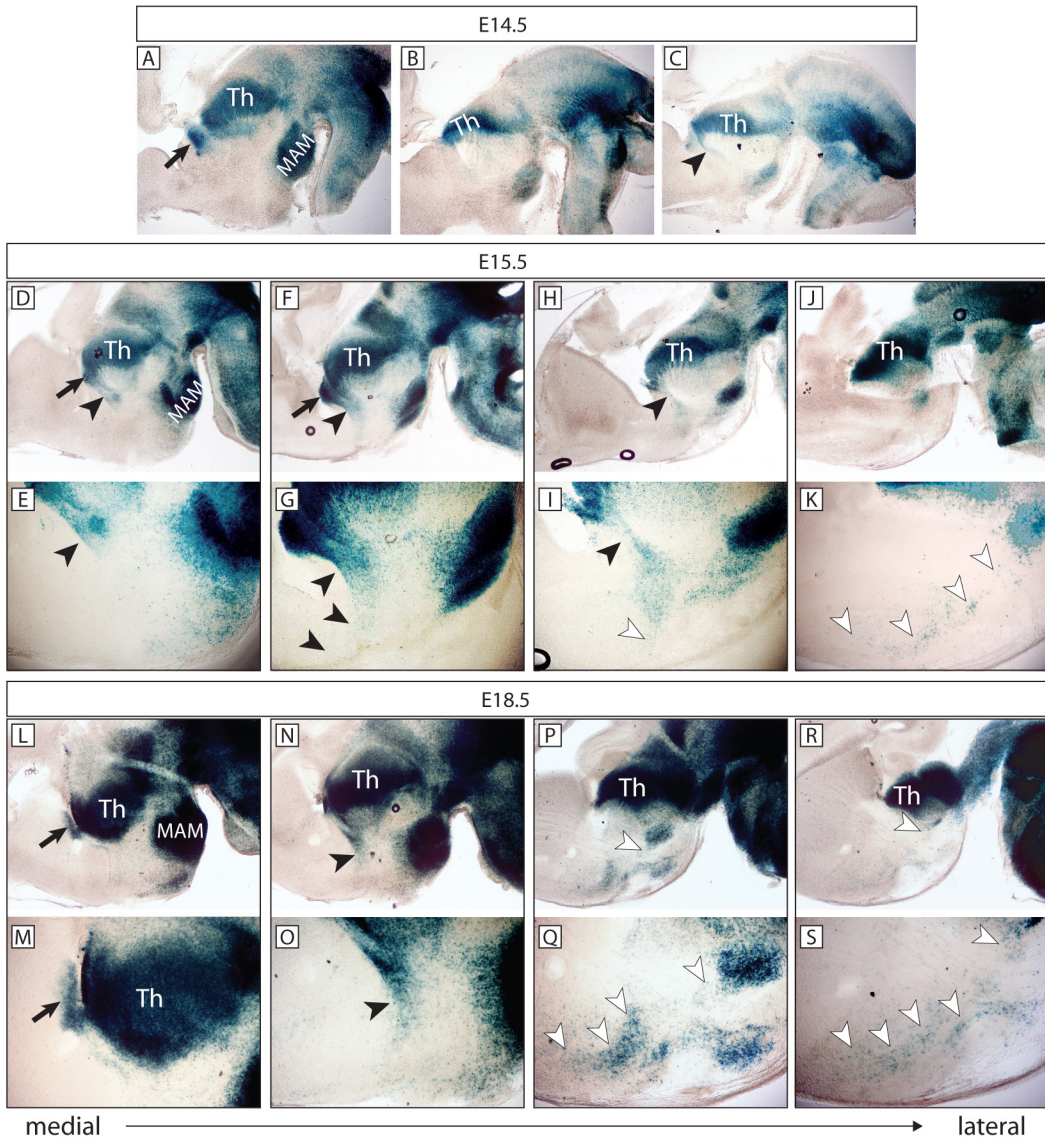
Zhao et al.
Figure 2



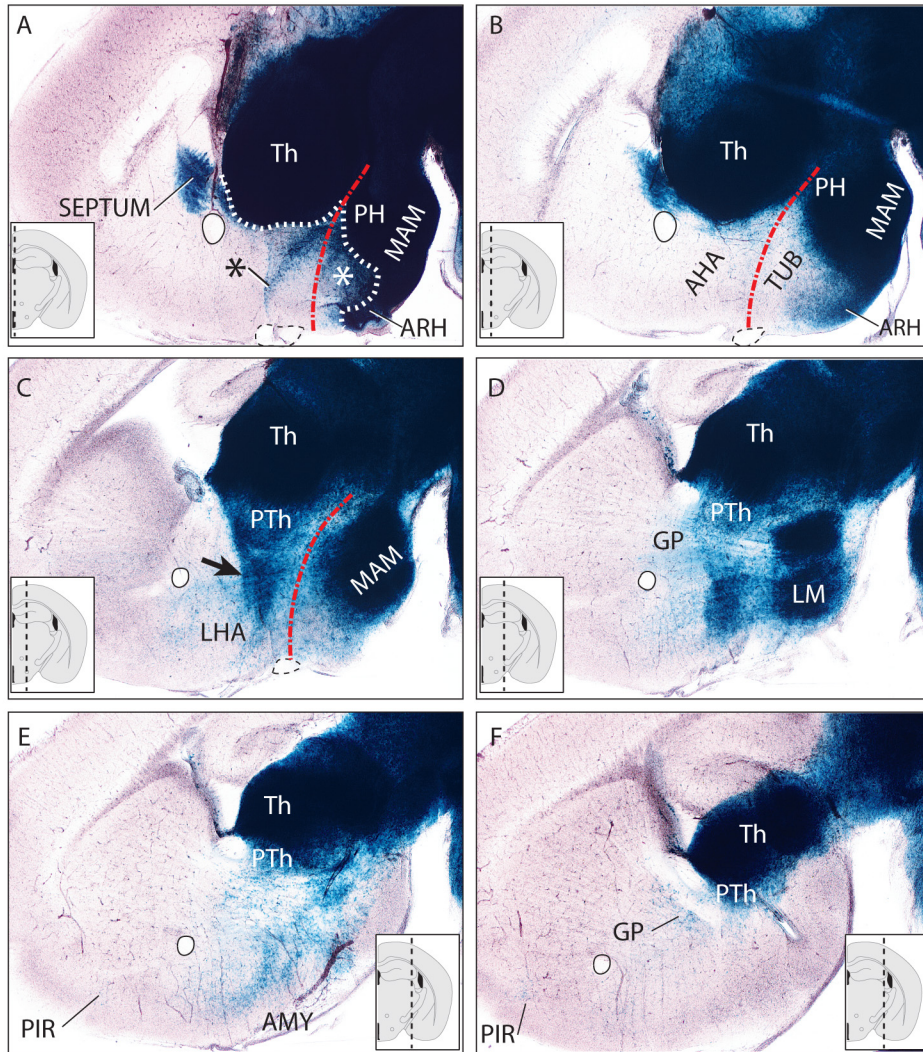
Zhao et al.
Figure 3



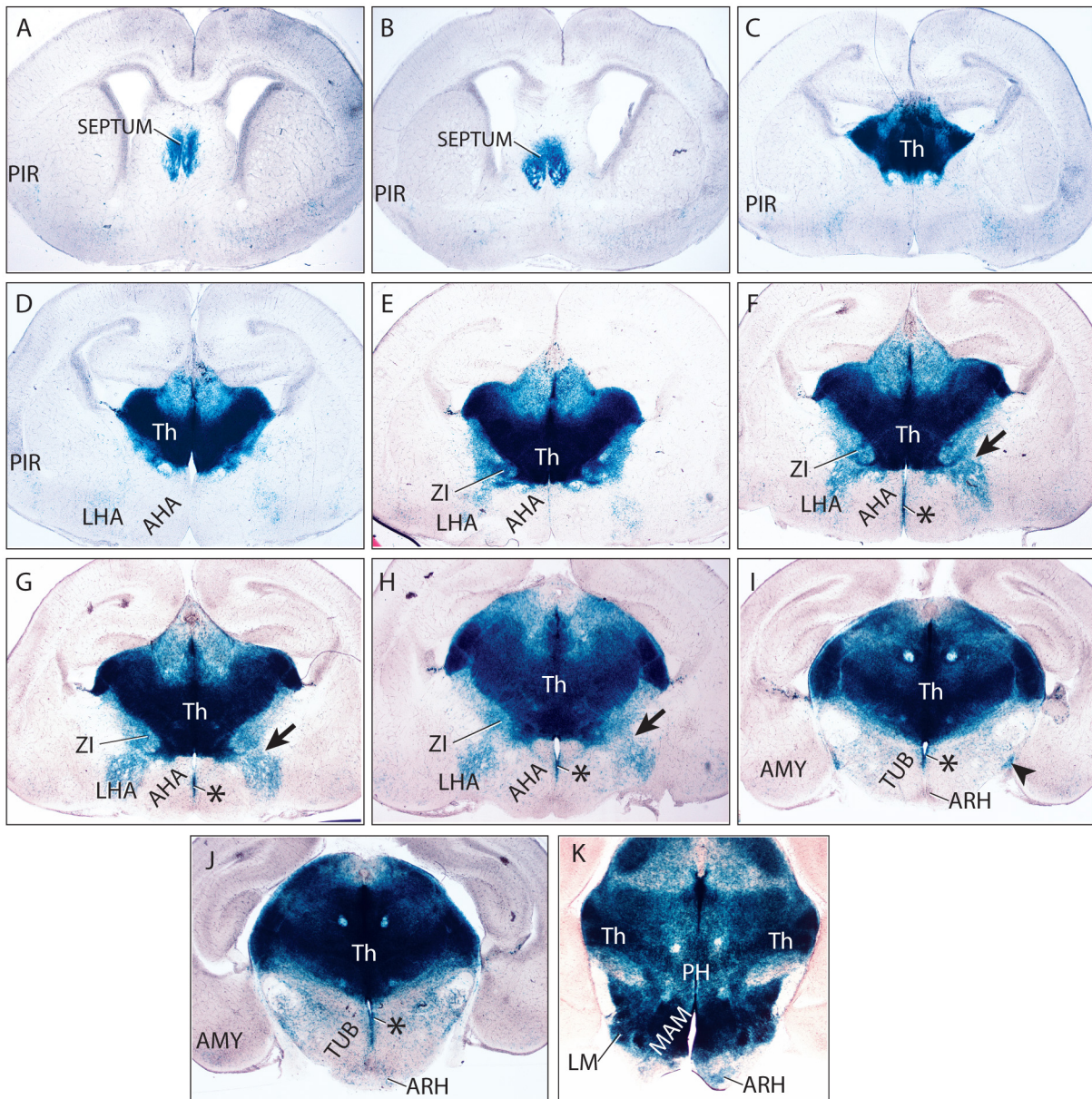
Zhao et al.
Figure 4



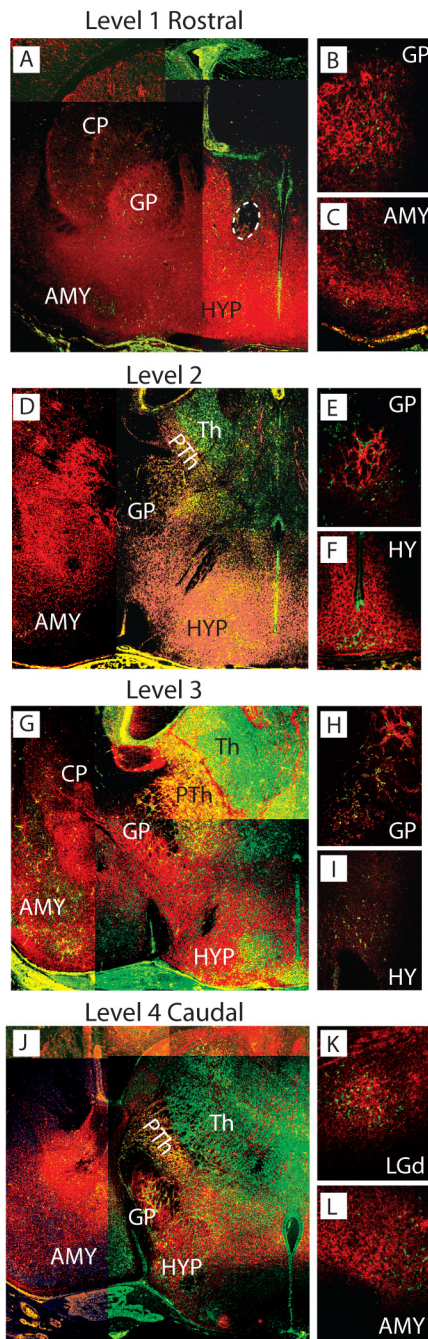
Zhao et al.
Figure 5



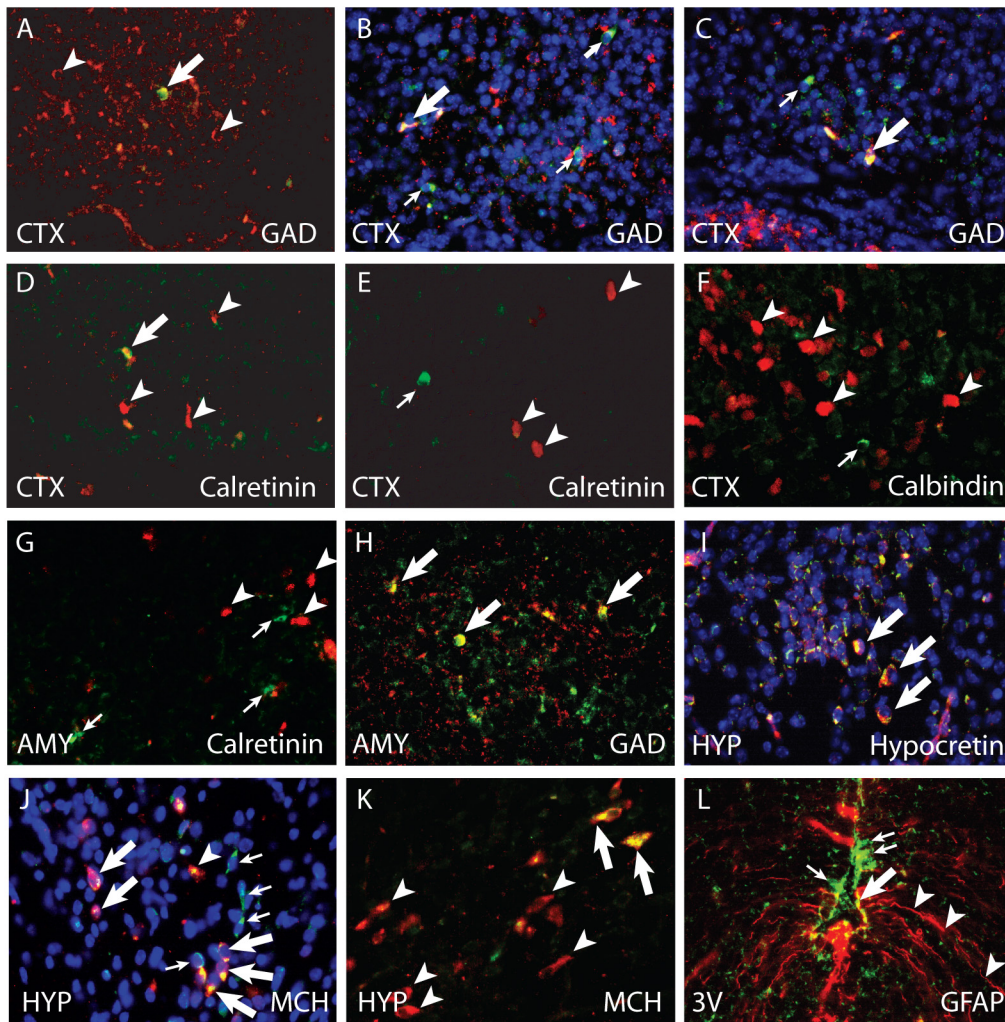
Zhao et al.
Figure 6



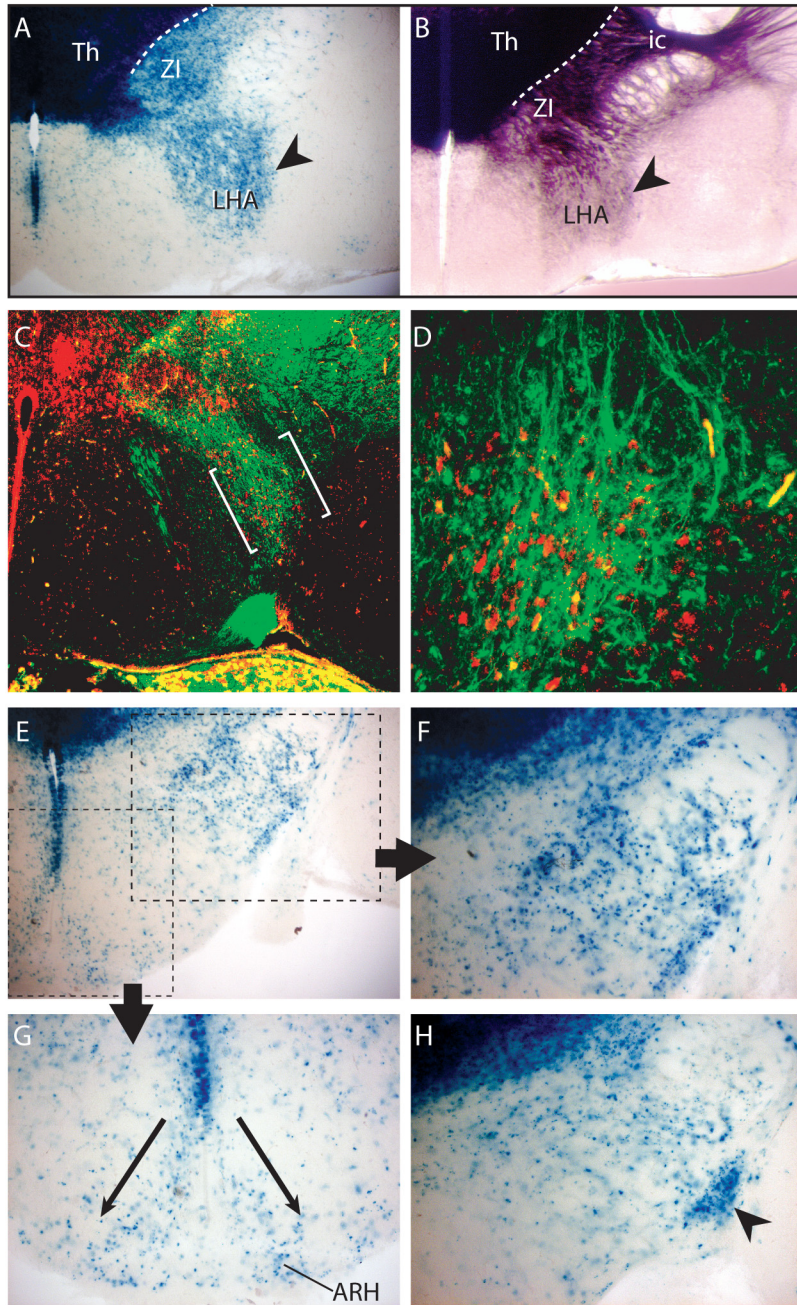
Zhao et al.
Figure 7



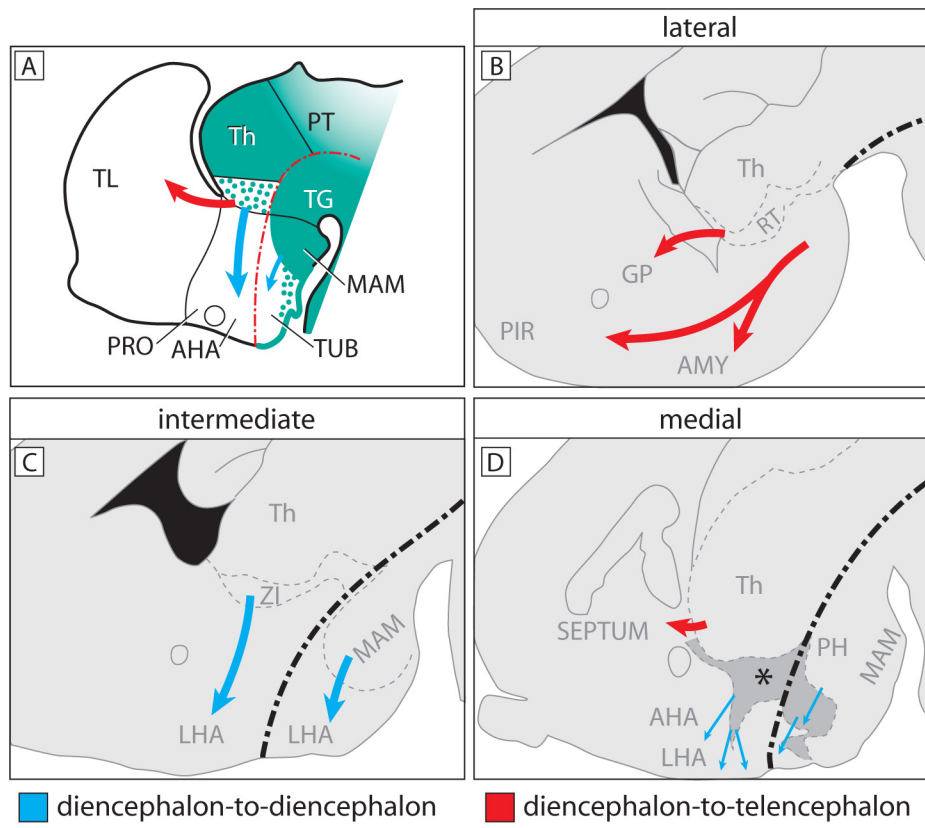
Zhao et al.
Fig.8



Zhao et al.
Figure 9



Zhao et al.
Figure 10



Zhao et al.
Figure 11

Author's contribution - Genetic mapping of Foxb1-cell lineage shows migration from caudal diencephalons to telencephalon and lateral hypothalamus

Maintain the mouse lines used in paper and harvest the appropriate embryos at certain stage. Processing tissues into blocks and cut the block into ready to use sections.

Performed all the Immunohistochemistry work

Performed all the whole mount detection of Beta- galactosidase activity

Performed all the whole mount detection of HPAP activity

DISCUSSION

The underlying aim of this study was to understand the detailed roles of transcription factors *Emx2* and *Foxb1* in mouse embryonic development. Most of the corresponding aspects raised from this work have been discussed in the respective publications. Therefore here I will only address some general questions.

***Emx2* in cortical development**

The cerebral cortex is a layered brain structure found only in mammals, and in which different regions can be distinguished. The largest part corresponds to the neocortex and is located in between the archicortex (hippocampus region) and paleocortex (piriform cortex, also called olfactory cortex). Considered in its radial dimension, the neocortex has 6 layers which are formed during development through an inside-out migratory pattern under the guidance of CR cells (Rice and Curran, 2001).

Considered tangentially, the neocortex is organized into areas with different cytoarchitecture as well as axonal connections. Rostrocaudally, Motor, Auditory, Somatosensory and Visual regions can be recognized (Bishop et al., 2000).

As mentioned before, homeobox transcription factor *Emx2* shows a mediocaudal – laterorostral expression gradient exactly opposed to that of transcription factor *Pax6* (Bishop et al., 2003; Simeone et al., 1992; Stoykova and Gruss, 1994).

These intriguing expression gradients make them candidates to control cortical development. According to previous studies, the contribution of *Emx2* to cortical development goes beyond the control of the development of the CR cells. Indeed, *Emx2* together with *Pax6* are required for normal cortical growth and patterning (Bishop et al., 2003; Bishop et al., 2000). *Emx2* expression in cortex is restricted to cortical ventricular progenitors (cortical stem cells) and previous studies have proved

that *Emx2* can influence proliferation of cortical stem cells to produce more stem cells ("symmetric proliferation") (Heins et al., 2001).

Cortical neurons are highly heterogeneous population, and, in the mouse, more than 20% of the cortical cells are originated in the ventral telencephalon, many of them in the so-called medial ganglionic eminence (MGE) (Nery et al., 2002). In *Emx2*-deficient mice, the migration from ventral telencephalon into neocortex is reduced and in *Emx2/Pax6* double mutant this migration was completely blocked (Muzio et al., 2002).

On the other hand, *Emx2* has been shown to contribute to correct cortical fate determination and arealization together with *Pax6*. Lack of *Emx2* expression in the cortical ventricular zone leads to a shift of the cortical areas from laterorostral to mediocaudal. An areal shift in the opposite direction has been observed in the *Pax6*-deficient mouse (Bishop et al., 2003; Bishop et al., 2000; Muzio and Mallamaci, 2003). Finally, in mouse embryos lacking both *Emx2* and *Pax6*, there is no neocortex at all (Muzio et al., 2002).

Cortical development is extremely complex, and of course there are more transcription factors involved than *Emx2* and *Pax6*. To date, *COUP-TF*, *Sp8* and *Lhx2* have been reported to be expressed in cortical progenitors and have influence on cortical patterning (Monuki et al., 2001; O'Leary and Sahara, 2008). The detailed function of *Emx2* in cortical development is also a complicated question. By placing the *Emx2* coding region under the control of the *Nestin* promoter (*Nestin-Emx2*), *Emx2* can be abnormally overexpressed in cortical progenitors (cortical stem cells). This overexpression results in a size alteration of the entire cortex. This and other related experiments suggests a concentration-dependent regulatory role of transcription factors in controlling the identities of progenitor cell and their progeny (Hamasaki et al., 2004) (Leingartner et al., 2007).

The lineage study of transcription factor through driven Cre recombinase activity provide a new orientation to understand embryonic development beyond the expression

Development of the mouse hypothalamus is a very complicated process primarily patterned by *Shh*, *Nodal* and other still undefined signal molecules from the pituitary and later tightly controlled by a transcriptional network (including *Otp*, *Sim1*, *Arnt2*, *Nkx2.1*, *Sfl*) (Michaud, 2001)(Caqueret et al 2005). Any alteration of this developmental process can be cause of disease. We still do not have a complete description of how the hypothalamus is put together.

Mammals develop inside their mothers, which prevents researchers from direct observation of embryonic processes. Morphological and immunohistological studies have been used to describe population of cells according to their position, morphology and gene expression profile. Those studies are meaningful, but they have limits in determining the relationship between the cell types observed at different stages and their sites of origin and migration routes.

Genetic neuroanatomy tools and methods have been devised in order to avoid these problems. In the second part of this PhD work I have used a knock-in strategy to introduce the DNA for Cre recombinase into the *Foxb1* locus. The mouse Cre line generated in this way is useful to follow the fate of *Foxb1*-lineage cells in the hypothalamus. *Foxb1* is expressed by the progenitors in the developing neural tube with a very specific rostral boundary in the diencephalon: constantly in mammillary body and transiently (E10.5 till E12.5) in the dorsal thalamus (Alvarez-Bolado et al., 2000a; Zhao et al., 2007). This makes my *Foxb1-Cre* line an ideal tool to analyze diencephalic migration.

The *Foxb1*-lineage neurons of the hypothalamus can be classified into 2 groups according to their position: one is the cells migrating from the thalamus into the

anterior part of lateral hypothalamus, the other is formed by the neurons scattered in the ventral part of the hypothalamus (including the ventromedial and arcuate nuclei). These two groups of cells (mostly neurons) (Zhao et al., 2008) follow different strategies upon entering the hypothalamus. The cells migrating from the thalamus into the anterior hypothalamus could form a distinct nucleus with its own, yet unknown, function. The scattered cells probably integrate themselves into pre-existing nuclei and in doing so they contribute to their heterogeneity and complexity.

Tangential migration is a communication between transcription factors

After being born, neurons have to follow certain route to settle down to their final position. There are two major migratory routes, radial and tangential. Radial migration follows radial glial processes towards the pial side (or outer side of the brain). The direction of migration that is oblique or transverse to the radial glial scaffolding, mostly following the trajectory of tangential axons, is called tangential.

Both the migrating stream of *Foxb1*-lineage cells into hypothalamus and the migration of CR cells in the cortex are tangential migrations. Tangential migration is a common phenomenon in telencephalon development and can be found already in reptile forebrain development (Metin et al., 2007). This type of migration helps neurons to cross developmental boundaries (like the pallial-subpallial border) which their progenitor cells normally respect (Fishell et al., 1993). Boundaries are built mostly according to the expression of different transcription factors. Neurons that cross boundaries and settle in novel regions can bring with them novel, distinct functions. Neurons expressing the important hypothalamic hormone GnRH are actually originated in the olfactory bulb but they migrate into hypothalamus (Wray, 2002). In the mouse cortex, all the GABAergic interneurons are from ventral telencephalic medial ganglionic eminence (Anderson et al., 2002) (Marin and Rubenstein, 2003).

Those inherited characters from afar integrate with their local neighbors to shape the final function of a certain region.

Lineage studies require precise Cre recombinase activity and fast responding reporters

To provide a good marker, Cre recombinase activity must precisely duplicate the expression of the driving gene (in my case, *Foxb1*) spatially and temporally. The selection cassette PGK–Neo (a hybrid gene consisting of the phosphoglycerate kinase I promoter driving the neomycin phosphotransferase gene), which is part of the targeting construct, can result in abnormal expression patterns because the PGK promoter is very powerful (Pham et al., 1996) (Olson et al., 1996). Therefore we deleted this cassette by means of an additional crossing step in order to obtain faithful reporter spatiotemporal expression patterns. Our study also showed PGK-Neo deleted mice had higher efficiency comparing to none deleted mice (unpublished data).

There are various reporter mouse lines nowadays for reporting Cre activity. Due to the different cloning strategies and methods, they respond differently to Cre recombinase activity. ROSA26 has the highest efficiency without leakage after comparing several reporter lines. The human alkaline phosphatase reporter enzyme characteristic of the Z/AP mouse line has as unique property the ability to label entire axons.

*Foxb1*Cre-ROSA26 mice permit us to follow the progeny of *Foxb1*-positive precursors through their entire life span from the ventricular zone to their adult location, and thus analyze the cell identity, migration routes and final location of *Foxb1* derived cells. *Foxb1*Cre Z/AP mice help us for precise tracing of axonal projections of *Foxb1*-lineage neurons in an unbiased manner.

REFERENCES

Altman, J. and Bayer, S. A. (1990a). Migration and distribution of two populations of hippocampal granule cell precursors during the perinatal and postnatal periods. *J Comp Neurol* **301**, 365-81.

Altman, J. and Bayer, S. A. (1990b). Mosaic organization of the hippocampal neuroepithelium and the multiple germinal sources of dentate granule cells. *J Comp Neurol* **301**, 325-42.

Alvarez-Bolado, G., Zhou, X., Cecconi, F. and Gruss, P. (2000a). Expression of Foxb1 reveals two strategies for the formation of nuclei in the developing ventral diencephalon. *Dev Neurosci* **22**, 197-206.

Alvarez-Bolado, G., Zhou, X., Voss, A. K., Thomas, T. and Gruss, P. (2000b). Winged helix transcription factor Foxb1 is essential for access of mammillothalamic axons to the thalamus. *Development* **127**, 1029-38.

Amaral, D. G. and Witter, M. P. (1995). Hippocampal Formation. In *The Rat Nervous System*, (ed. G. Paxinos), pp. 443-493. San Diego: Academic Press.

Anderson, S. A., Kaznowski, C. E., Horn, C., Rubenstein, J. L. and McConnell, S. K. (2002). Distinct origins of neocortical projection neurons and interneurons in vivo. *Cereb Cortex* **12**, 702-9.

Angevine, J. B., Jr. and Sidman, R. L. (1961). Autoradiographic study of cell migration during histogenesis of cerebral cortex in the mouse. *Nature* **192**, 766-8.

Babu, M. M., Luscombe, N. M., Aravind, L., Gerstein, M. and Teichmann, S. A. (2004). Structure and evolution of transcriptional regulatory networks. *Curr Opin Struct Biol* **14**, 283-91.

Ball, M. J. (1977). Neuronal loss, neurofibrillary tangles and granulovacuolar degeneration in the hippocampus with ageing and dementia. A quantitative study. *Acta Neuropathol* **37**, 111-8.

Bird, C. M. and Burgess, N. (2008). The hippocampus and memory: insights from spatial processing. *Nat Rev Neurosci* **9**, 182-94.

- Bishop, K. M., Garel, S., Nakagawa, Y., Rubenstein, J. L. and O'Leary, D. D.** (2003). Emx1 and Emx2 cooperate to regulate cortical size, lamination, neuronal differentiation, development of cortical efferents, and thalamocortical pathfinding. *J Comp Neurol* **457**, 345-60.
- Bishop, K. M., Goudreau, G. and O'Leary, D. D.** (2000). Regulation of area identity in the mammalian neocortex by Emx2 and Pax6. *Science* **288**, 344-9.
- Bishop, K. M., Rubenstein, J. L. and O'Leary, D. D.** (2002). Distinct actions of Emx1, Emx2, and Pax6 in regulating the specification of areas in the developing neocortex. *J Neurosci* **22**, 7627-38.
- Boncinelli, E., Mallamaci, A. and Lavorgna, G.** (1994). Vertebrate homeobox genes. *Genetica* **94**, 127-40.
- Breier, G., Albrecht, U., Sterrer, S. and Risau, W.** (1992). Expression of vascular endothelial growth factor during embryonic angiogenesis and endothelial cell differentiation. *Development* **114**, 521-32.
- Caqueret, A., Yang, C., Duplan, S., Boucher, F. and Michaud, J. L.** (2005). Looking for trouble: a search for developmental defects of the hypothalamus. *Horm Res* **64**, 222-30.
- Carmeliet, P., Ferreira, V., Breier, G., Pollefeyt, S., Kieckens, L., Gertsenstein, M., Fahrig, M., Vandenhoeck, A., Harpal, K., Eberhardt, C. et al.** (1996). Abnormal blood vessel development and lethality in embryos lacking a single VEGF allele. *Nature* **380**, 435-9.
- Cecchi, C. and Boncinelli, E.** (2000). Emx homeogenes and mouse brain development. *Trends Neurosci* **23**, 347-52.
- Chen, H., Chedotal, A., He, Z., Goodman, C. S. and Tessier-Lavigne, M.** (1997). Neuropilin-2, a novel member of the neuropilin family, is a high affinity receptor for the semaphorins Sema E and Sema IV but not Sema III. *Neuron* **19**, 547-59.
- D'Arcangelo, G., Miao, G. G., Chen, S. C., Soares, H. D., Morgan, J. I. and Curran, T.** (1995). A protein related to extracellular matrix proteins deleted in the mouse mutant reeler. *Nature* **374**, 719-23.
- Ferrara, N., Carver-Moore, K., Chen, H., Dowd, M., Lu, L., O'Shea, K. S., Powell-Braxton, L., Hillan, K. J. and Moore, M. W.** (1996). Heterozygous embryonic lethality induced by targeted inactivation of the VEGF gene. *Nature* **380**, 439-42.
- Ferrara, N. and Davis-Smyth, T.** (1997). The biology of vascular endothelial growth factor. *Endocr Rev* **18**, 4-25.

- Fishell, G., Mason, C. A. and Hatten, M. E.** (1993). Dispersion of neural progenitors within the germinal zones of the forebrain. *Nature* **362**, 636-8.
- Gaiano, N., Nye, J. S. and Fishell, G.** (2000). Radial glial identity is promoted by Notch1 signaling in the murine forebrain. *Neuron* **26**, 395-404.
- Gleeson, J. G. and Walsh, C. A.** (2000). Neuronal migration disorders: from genetic diseases to developmental mechanisms. *Trends Neurosci* **23**, 352-9.
- Gonzalez, J. L., Russo, C. J., Goldowitz, D., Sweet, H. O., Davisson, M. T. and Walsh, C. A.** (1997). Birthdate and cell marker analysis of scrambler: a novel mutation affecting cortical development with a reeler-like phenotype. *J Neurosci* **17**, 9204-11.
- Grove, E. A., Tole, S., Limon, J., Yip, L. and Ragsdale, C. W.** (1998). The hem of the embryonic cerebral cortex is defined by the expression of multiple Wnt genes and is compromised in Gli3-deficient mice. *Development* **125**, 2315-25.
- Hamasaki, T., Leingartner, A., Ringstedt, T. and O'Leary, D. D.** (2004). EMX2 regulates sizes and positioning of the primary sensory and motor areas in neocortex by direct specification of cortical progenitors. *Neuron* **43**, 359-72.
- Heins, N., Cremisi, F., Malatesta, P., Gangemi, R. M., Corte, G., Price, J., Goudreau, G., Gruss, P. and Gotz, M.** (2001). Emx2 promotes symmetric cell divisions and a multipotential fate in precursors from the cerebral cortex. *Mol Cell Neurosci* **18**, 485-502.
- Heins, N., Malatesta, P., Cecconi, F., Nakafuku, M., Tucker, K. L., Hack, M. A., Chapouton, P., Barde, Y. A. and Gotz, M.** (2002). Glial cells generate neurons: the role of the transcription factor Pax6. *Nat Neurosci* **5**, 308-15.
- Herzig, U., Cadenas, C., Sieckmann, F., Sierralta, W., Thaller, C., Visel, A. and Eichele, G.** (2001). Development of high-throughput tools to unravel the complexity of gene expression patterns in the mammalian brain. *Novartis Found Symp* **239**, 129-46; discussion 146-59.
- Hong, S. M., Liu, Z., Fan, Y., Neumann, M., Won, S. J., Lac, D., Lum, X., Weinstein, P. R. and Liu, J.** (2007). Reduced hippocampal neurogenesis and skill reaching performance in adult Emx1 mutant mice. *Exp Neurol* **206**, 24-32.
- Kuhn, H. G., Dickinson-Anson, H. and Gage, F. H.** (1996). Neurogenesis in the dentate gyrus of the adult rat: age-related decrease of neuronal progenitor proliferation. *J Neurosci* **16**, 2027-33.
- Lehmann, O. J., Sowden, J. C., Carlsson, P., Jordan, T. and Bhattacharya, S. S.** (2003). Fox's in development and disease. *Trends Genet* **19**, 339-44.

- Leingartner, A., Thuret, S., Kroll, T. T., Chou, S. J., Leasure, J. L., Gage, F. H. and O'Leary, D. D.** (2007). Cortical area size dictates performance at modality-specific behaviors. *Proc Natl Acad Sci U S A* **104**, 4153-8.
- Lobe, C. G., Koop, K. E., Kreppner, W., Lomeli, H., Gertsenstein, M. and Nagy, A.** (1999). Z/AP, a double reporter for cre-mediated recombination. *Dev Biol* **208**, 281-92.
- Mallamaci, A., Mercurio, S., Muzio, L., Cecchi, C., Pardini, C. L., Gruss, P. and Boncinelli, E.** (2000). The lack of Emx2 causes impairment of Reelin signaling and defects of neuronal migration in the developing cerebral cortex. *J Neurosci* **20**, 1109-18.
- Marin, O. and Rubenstein, J. L.** (2003). Cell migration in the forebrain. *Annu Rev Neurosci* **26**, 441-83.
- Metin, C., Alvarez, C., Moudoux, D., Vitalis, T., Pieau, C. and Molnar, Z.** (2007). Conserved pattern of tangential neuronal migration during forebrain development. *Development* **134**, 2815-27.
- Michaud, J. L.** (2001). The developmental program of the hypothalamus and its disorders. *Clin Genet* **60**, 255-63.
- Michaud, J. L., Rosenquist, T., May, N. R. and Fan, C. M.** (1998). Development of neuroendocrine lineages requires the bHLH-PAS transcription factor SIM1. *Genes Dev* **12**, 3264-75.
- Monuki, E. S., Porter, F. D. and Walsh, C. A.** (2001). Patterning of the dorsal telencephalon and cerebral cortex by a roof plate-Lhx2 pathway. *Neuron* **32**, 591-604.
- Muzio, L., DiBenedetto, B., Stoykova, A., Boncinelli, E., Gruss, P. and Mallamaci, A.** (2002). Emx2 and Pax6 control regionalization of the pre-neuronogenic cortical primordium. *Cereb Cortex* **12**, 129-39.
- Muzio, L. and Mallamaci, A.** (2003). Emx1, emx2 and pax6 in specification, regionalization and arealization of the cerebral cortex. *Cereb Cortex* **13**, 641-7.
- Myatt, S. S. and Lam, E. W.** (2007). The emerging roles of forkhead box (Fox) proteins in cancer. *Nat Rev Cancer* **7**, 847-59.
- Nery, S., Fishell, G. and Corbin, J. G.** (2002). The caudal ganglionic eminence is a source of distinct cortical and subcortical cell populations. *Nat Neurosci* **5**, 1279-87.
- O'Leary, D. D. and Sahara, S.** (2008). Genetic regulation of arealization of the neocortex. *Curr Opin Neurobiol* **18**, 90-100.

Olson, E. N., Arnold, H. H., Rigby, P. W. and Wold, B. J. (1996). Know your neighbors: three phenotypes in null mutants of the myogenic bHLH gene MRF4. *Cell* **85**, 1-4.

Papez, J. W. (1995). A proposed mechanism of emotion. 1937. *J Neuropsychiatry Clin Neurosci* **7**, 103-12.

Pellegrini, M., Mansouri, A., Simeone, A., Boncinelli, E. and Gruss, P. (1996). Dentate gyrus formation requires Emx2. *Development* **122**, 3893-8.

Pham, C. T., MacIvor, D. M., Hug, B. A., Heusel, J. W. and Ley, T. J. (1996). Long-range disruption of gene expression by a selectable marker cassette. *Proc Natl Acad Sci U S A* **93**, 13090-5.

Radyushkin, K., Anokhin, K., Meyer, B. I., Jiang, Q., Alvarez-Bolado, G. and Gruss, P. (2005). Genetic ablation of the mammillary bodies in the Foxb1 mutant mouse leads to selective deficit of spatial working memory. *Eur J Neurosci* **21**, 219-29.

Rice, D. S. and Curran, T. (2001). Role of the reelin signaling pathway in central nervous system development. *Annu Rev Neurosci* **24**, 1005-39.

Risau, W. (1997). Mechanisms of angiogenesis. *Nature* **386**, 671-4.

Rossant, J. and Howard, L. (2002). Signaling pathways in vascular development. *Annu Rev Cell Dev Biol* **18**, 541-73.

Schlessinger, A. R., Cowan, W. M. and Gottlieb, D. I. (1975). An autoradiographic study of the time of origin and the pattern of granule cell migration in the dentate gyrus of the rat. *J Comp Neurol* **159**, 149-75.

Shimamura, K. and Rubenstein, J. L. (1997). Inductive interactions direct early regionalization of the mouse forebrain. *Development* **124**, 2709-18.

Simeone, A., Gulisano, M., Acampora, D., Stornaiuolo, A., Rambaldi, M. and Boncinelli, E. (1992). Two vertebrate homeobox genes related to the Drosophila empty spiracles gene are expressed in the embryonic cerebral cortex. *Embo J* **11**, 2541-50.

Song, D. L., Chalepakis, G., Gruss, P. and Joyner, A. L. (1996). Two Pax-binding sites are required for early embryonic brain expression of an Engrailed-2 transgene. *Development* **122**, 627-35.

- Soriano, E., Cobas, A. and Fairen, A.** (1989a). Neurogenesis of glutamic acid decarboxylase immunoreactive cells in the hippocampus of the mouse. I: Regio superior and regio inferior. *J Comp Neurol* **281**, 586-602.
- Soriano, E., Cobas, A. and Fairen, A.** (1989b). Neurogenesis of glutamic acid decarboxylase immunoreactive cells in the hippocampus of the mouse. II: Area dentata. *J Comp Neurol* **281**, 603-11.
- Soriano, P.** (1999). Generalized lacZ expression with the ROSA26 Cre reporter strain. *Nat Genet* **21**, 70-1.
- Stern, C. D. and Fraser, S. E.** (2001). Tracing the lineage of tracing cell lineages. *Nat Cell Biol* **3**, E216-8.
- Sternberg, N. and Hamilton, D.** (1981). Bacteriophage P1 site-specific recombination. I. Recombination between loxP sites. *J Mol Biol* **150**, 467-86.
- Sternberg, N., Hamilton, D. and Hoess, R.** (1981). Bacteriophage P1 site-specific recombination. II. Recombination between loxP and the bacterial chromosome. *J Mol Biol* **150**, 487-507.
- Stoykova, A. and Gruss, P.** (1994). Roles of Pax-genes in developing and adult brain as suggested by expression patterns. *J Neurosci* **14**, 1395-412.
- Teyler, T. J. and DiScenna, P.** (1985). The role of hippocampus in memory: a hypothesis. *Neurosci Biobehav Rev* **9**, 377-89.
- Theil, T., Alvarez-Bolado, G., Walter, A. and Ruther, U.** (1999). Gli3 is required for Emx gene expression during dorsal telencephalon development. *Development* **126**, 3561-71.
- Thomas, C., DeVries, P., Hardin, J. and White, J.** (1996). Four-dimensional imaging: computer visualization of 3D movements in living specimens. *Science* **273**, 603-7.
- Tole, S., Goudreau, G., Assimacopoulos, S. and Grove, E. A.** (2000). Emx2 is required for growth of the hippocampus but not for hippocampal field specification. *J Neurosci* **20**, 2618-25.
- Wang, W. and Lufkin, T.** (2000). The murine Otp homeobox gene plays an essential role in the specification of neuronal cell lineages in the developing hypothalamus. *Dev Biol* **227**, 432-49.

Wehr, R., Mansouri, A., de Maeyer, T. and Gruss, P. (1997). Fkh5-deficient mice show dysgenesis in the caudal midbrain and hypothalamic mammillary body. *Development* **124**, 4447-56.

Wray, S. (2002). Development of gonadotropin-releasing hormone-1 neurons. *Front Neuroendocrinol* **23**, 292-316.

Yaylaoglu, M. B., Titmus, A., Visel, A., Alvarez-Bolado, G., Thaller, C. and Eichele, G. (2005). Comprehensive expression atlas of fibroblast growth factors and their receptors generated by a novel robotic in situ hybridization platform. *Dev Dyn* **234**, 371-86.

Yoshida, M., Suda, Y., Matsuo, I., Miyamoto, N., Takeda, N., Kuratani, S. and Aizawa, S. (1997). Emx1 and Emx2 functions in development of dorsal telencephalon. *Development* **124**, 101-11.

Zhao, T., Kraemer, N., Oldekamp, J., Cankaya, M., Szabo, N., Conrad, S., Skutella, T. and Alvarez-Bolado, G. (2006). Emx2 in the developing hippocampal fissure region. *Eur J Neurosci* **23**, 2895-907.

Zhao, T., Zhou, X., Szabo, N., Leites, M. and Alvarez-Bolado, G. (2007). Foxb1-driven Cre expression in somites and the neuroepithelium of diencephalon, brainstem, and spinal cord. *Genesis* **45**, 781-7.

Tianyu Zhao, Nora Szabo, Jun Ma, Lingfei Luo, Xunlei Zhou and Gonzalo Alvarez-Bolado. *Eur J Neurosci* (2008) *in press*

Zinyk, D. L., Mercer, E. H., Harris, E., Anderson, D. J. and Joyner, A. L. (1998). Fate mapping of the mouse midbrain-hindbrain constriction using a site-specific recombination system. *Curr Biol* **8**, 665-8.

Publications:

Zhao, T., Kraemer, N., Oldekamp, J., Cankaya, M., Szabo, N., Conrad, S., Skutella, T. and Alvarez-Bolado, G. (2006). Emx2 in the developing hippocampal fissure region. *Eur J Neurosci* 23, 2895-907.

Zhao, T *, Zhou, X *, Szabo, N., Leitges, M. and Alvarez-Bolado, G. (2007). Foxb1-driven Cre expression in somites and the neuroepithelium of diencephalon, brainstem, and spinal cord. *Genesis* 45, 781-787.

Zhao, T *, Szabo, N *, Ma, J., Luo, L., Zhou, X and Alvarez-Bolado, G. (2008). Genetic mapping of Foxb1-cell lineage shows migration from caudal diencephalon to telencephalon and lateral hypothalamus. *Eur J Neurosci* **Accepted**

Skutella, T*, Conrad, S*, **Zhao, T***, Cankaya, M., Matinez-Hernandez, A and Alvarez-Bolado, G. Gajal-Retzuis neurons that produce Vascular Endothelial Growth Facrtoc have a role in cortical angiogenesis
Submitted

Szabó N, **Zhao T**, Çankaya M, Theil T, Zhou X and Alvarez-Bolado G. Neuroepithelial *Sonic hedgehog* is essential to specify the hypothalamic subregions and to stabilize diencephalic against telencephalic fate
Submitted

Szabó N, **Zhao T**, Zhou X and Alvarez-Bolado G. The role of *Shh* of neural origin in thalamic differentiation in the mouse
Submitted

* Equal contribution

Conference:

Zhao, T ., Zhou, X., Szabo, N., Leitges, M. and Alvarez-Bolado, G. Foxb1-driven Cre expression in somites and the neuroepithelium of diencephalon, brainstem, and spinal cord. Horizon in molecular biology -4th international PhD student symposium, Göttingen.2007.
Abstract and Poster

Curriculum Vitae

Personal information

Name: Tianyu Zhao
Birthdate: 03.July.1976
Place of Birth: Yingkou, P.R. China

Address: Immauel-Kant Str.28
37083, Göttingen

Eudcation:

BS 1995-1999 Nanjing University , Nanjing, P.R. China
Department of Biochemitry.
Thesis: The synthesis of a novel peptides

Msc 2002-2004 Wageningen University, Wageningen, The Netherlands
Thesis title: The influence of the growth factor GA3 on the
elongation of BY2 cells and the arrangement of cortical microtubules

PhD 2004-2008 Max-Planck institute of Expreimental Endocrinology
Hannover, Germany

Max-Planck institute of Biophysical Chemistry
Göttingen, Germany

Working Experience:

1999-2001 Service manager of Tianjin, P.R.China. BSH-Group.

Award:

2002 Delta scholarship from Netherland organization for
international cooperation of higher education (Nuffic)

ACKNOWLEDGEMENTS

First of all I would like to express my gratitude to my PhD adviser Dr. Gonzalo Alvarez-Bolado for accepting me in his group, and for his direction and encouragement. He guided me throughout the difficult process of identifying questions, obtaining data, analyzing results and discussing them. I have benefited enormously from his guidance and insight.

I would like to thank the Department director, Prof. Eichele, for his support and inspiring comments.

I would like to thank Prof. Hildebrandt and Prof. Huchzermeyer for their kindness to agree to be in my PhD committee. Both of them have been very supportive and have graciously spent some of their time to answer my endless questions.

I would like to thank Dr. Xunlei Zhou for her priceless help inside and outside the lab. She contributed to my training in molecular biology, taught me many valuable cloning techniques and was always generous with her time when I went to her with doubts and questions.

My collaboration with Prof. Thomas Skutella as well as with Sabine Conrad, from the University of Tübingen, has been very fruitful and pleasant. To them I acknowledge for their friendship and guidance.

I thank Nora Szabó, another member of Dr. Alvarez-Bolado's group, for her help at the bench as well as her friendship. We had a very good collaboration and she also contributed a lot to obtaining the data for this thesis.

My dear friends Lars Geffers, Murat Cankaya, and Harun Budak provided lots of help and shared with me interesting stories and opinions. Judit Kovac and Axel Visel kindly helped me to settle me down in Hannover. Many other friends and colleagues at the Institute deserve my gratitude for help and support over the years: Jana Husse, Henrik Oster, Murat Yaylaoglu, Silke Kiessling, Gabriela Whelan, Ana Martinez-Hernandez, Brid Bode, Dominic Landgraf and Helena Miletic. The Genepaint team was invaluable in obtaining my "in situ" data: Maren Bürsing, Christin Helbig, Frauke Grabbe, Cornelia Sieverding, Barbara Fischer, Kathrin Schrader, Markus Uhr and Kathryn Koch (...and the Robot!).

Finally, I thank my wife Xiaoling for her unfailing support and for providing the main motivation to finish this thesis.

Erklärung

Hiermit versichere ich, dass ich die vorgelegte Dissertation selbstständig und Zuhilfenahme der angegebenen Hilfsmittel verfasst habe. Ich habe die Dissertation nicht als Diplomarbeit oder ähnliche Arbeit verwendet und abgesehen von den angegebenen Teilveröffentlichungen nicht vorher publiziert.

Göttingen 02.10.2008

Tianyu Zhao